We thank the reviewers for their comments. Our specific response can be found below. The reviewers' comments are in italics and changes made to the manuscript are in quotation marks. All changes made are minor and do not affect the conclusions in the manuscript.

Response to Reviewer 1

1. The authors state (P10484, L14-16) that Budisulistiorini et al. used factor analysis to identify various OA sources, however it is not clear how this specific study shows "the versatility of PMF analysis in OA source apportionment" as the authors state. Please clarify.

Response: We agree with reviewer that the phrase "indicating the versatility of PMF analysis in OA source apportionment" is overstated and have deleted the phrase in the revised manuscript.

2. Why were the organic fractions of NO+ and NO2+ not included in the determination of the elemental ratios, particularly when organic nitrates contributed significantly to the total OA? Would inclusion of the organic fraction of these ions make a significant difference in the O:C or OS values?

Response: We didn't include NO^+ and NO_2^+ in the calculation of elemental ratios for the following two reasons. Firstly, this allows for a more direct comparison with literature values, which typically do not include NO^+ and NO_2^+. Secondly, including NO^+ and NO_2^+ does not affect the O:C or OS values significantly. Take CTR_June as example, where almost all nitrate is estimated to arise from organic nitrate. Including NO^+ and NO_2^+ only increases the O:C value from 0.75 to 0.77.

3. The authors give the RIE values used when analyzing ACSM data (P10488-10489), but not for the AMS data. What values were used for the AMS data?

Response: Default RIE values are used for the AMS data. For ammonium, the average RIE determined from IE calibrations by using ammonium nitrate is 4, which is the default value. We have added the following sentence in the revised manuscript.

"Default RIE values were used for the HR-ToF-AMS data."

4. For the Aethalometer data, black carbon concentrations were determined by averaging the signal determined at all seven wavelengths measured by the instrument. However, absorption at the shorter wavelengths can be enhanced by the presence of organics. Biomass burning in particular emits organics which absorb at the shorter wavelengths. Why was the black carbon concentration determined using an average of all seven wavelengths, as opposed to just using the longer wavelength(s), which theoretically have fewer interferences from non-black carbon material?

Response: The BC concentration calculated using an average of all seven wavelengths is very close to that using just one longer wavelength. Take the GT_Aug site for example, in the figure below, we compare the BC concentration based on 660nm or 950nm with the BC concentration based on average of all wavelengths. The difference is only 4%.

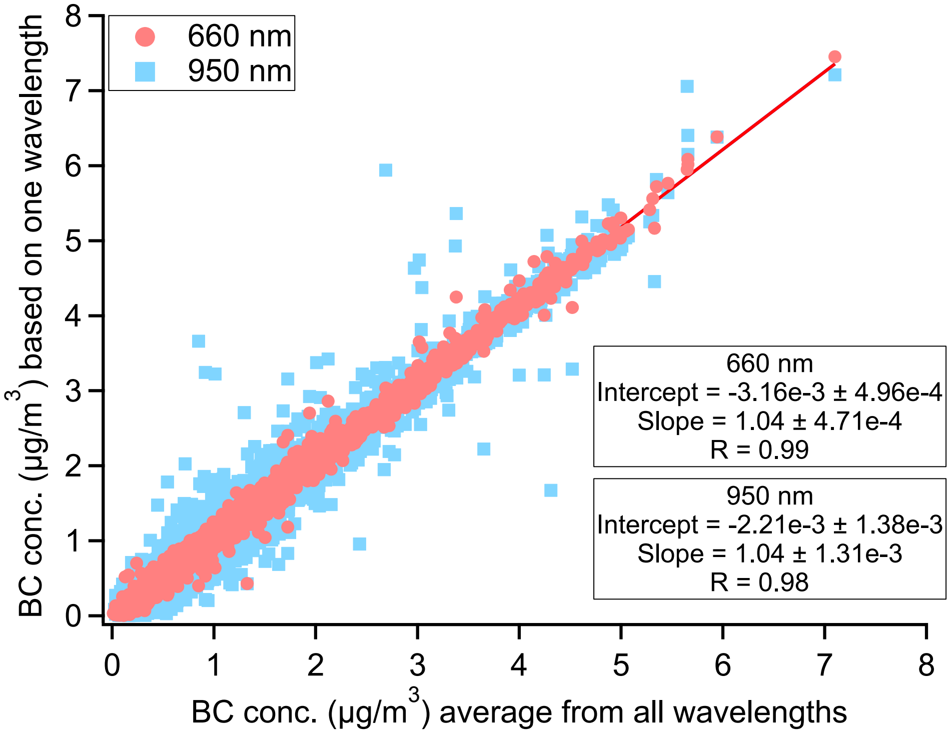

To make things clearer, we will report the BC concentration based on 660nm absorption in the revised manuscript as the reviewer suggested. 660nm is chosen because it is the closest to the MAAP wavelength (i.e., 670 nm), which was deployed at three sites in this study.

5. In addition to isoprene and β-pinene, Bruns et al., 2010 also give Rorg for several other biogenics (i.e., α-pinene, limonene and 3-carene), which have larger Rorg values than for isoprene and β-pinene (although the α-pinene Rorg is only slightly larger than that of β-pinene). Why weren't these other biogenic considered in the determination of the upper and lower values of Rorg in this study? This should be noted in the manuscript.

Response: As stated in the manuscript, "we select organic nitrates formed from isoprene and β-pinene oxidations as representative because of their large abundance in the southeastern US, potential to produce organic nitrates, and that they cover a wide range of R_{ON}/R_{AN} values". The organic nitrate formed from limonene, 3-carene, and α-pinene are not considered due to the following reasons. Firstly, the concentrations of limonene and 3-carene in the southeastern US are much lower than that of isoprene and β-pinene. For example, campaign-averaged nighttime concentration of limonene in CTR_June was only 0.05ppb, while it was 0.31 ppb for β-pinene (Xu et al., 2015). Secondly, while the concentration of α-pinene is similar to that of β-pinene, the SOA yield and organic nitrate of α-pinene is much lower than those of β-pinene (Berndt and Boge, 1997; Boyd et al., 2015; Griffin et al., 1999). Thirdly, as reported in Bruns et al. (2010), the NO^+/NO_2^+ ratios of organic nitrate from α-pinene, limonene, and 3-carene have much larger uncertainties than those of organic nitrate from isoprene and β-pinene. For example, the average + 2 standard deviations are 11 ± 8, 15 ± 8, and 14 ± 12 for α-pinene, limonene, and 3-carene derived organic nitrates, and the values are 10 ± 2 and 5.0 ± 0.7 for β-pinene and isoprene derived organic nitrates.

We have added the following sentence in the revised manuscript.

"The organic nitrates derived from other biogenic VOCs (i.e., α-pinene, limonene, 3-carene, etc) are not considered due to either their lower ambient concentrations in the SE US or lower organic nitrate yields compared to isoprene and β-pinene (Xu et al., 2015)."

6. I have several comments on Figures 3 and 6. Firstly, the authors state that the OA diurnals reach a daily maximum in the early morning and evening (except for YRK_July). Are the authors describing two maximums during the day (one in the early morning and one in the evening), or *one maximum that occurs either during the evening or the early morning? If it is the latter, the peak is in the night/early morning for panel (a, c, f, g, h) in Figure 3. The peak is only in the evening for CTR_June with BLH adjustment. In the conclusions, the authors state that the OA diurnal profiles peak at night in the winter datasets. The description of the diurnal patterns should be clarified. Secondly, there are no error bars given on the diurnals in Figure 3 (or Figure 6), making it difficult to determine if the diurnal trends are significant. For example, are the differences in the GT_Aug OA diurnal, which has little variability, significant? Can error bars be added to the diurnals? Finally, should the units on panel (d) in Figure 3 still be μg m-3, as the concentrations have been multiplied by the planetary boundary layer height?*

Response: Firstly, we are describing that for the summer datasets, the OA shows a slight increase at night and reaches a daily maximum either during the evening or the early morning. The key point of OA diurnal variation is that the OA diurnal trend in summer is relatively flat. The lack of a prominent daytime increase in the OA in summer would at first appear to discount the role of photochemistry-driven secondary OA formation. We interpret the flat OA diurnal trend in summer based on the changes in planetary boundary layer height and changes in contributions to total OA from various sources. When taking the changes in BLH into account, there is net OA production during the day in summer. We have rephrased the description of OA diurnal variation.

"In terms of diurnal variation, the OA diurnal trend is relatively flat in summer and peaks at night in winter (Fig. 3). The diurnal variation of OA is largely influenced by the changes in planetary boundary layer height and changes in contributions to total OA from various sources, which will be discussed in detail in section 4.4.1."

Secondly, we have added the error bars in Figs. 3 and 6 as the reviewer suggested.

Finally, on panel (d) in Fig. 3, the unit of y-axis is indeed μg m^{-2}, instead of μg m^{-3}. The confusion is caused by that the axis labels are not readable in the ACPD version. Once the manuscript gets accepted by ACP, we will request that figure 3 takes up a whole page and we believe the figure will be readable then.

7. In section 4.1.2, the authors describe the COA factor as having a small peak at lunch time and a larger peak at dinner time in all datasets where a COA factor was identified. However, I do not *see a lunch time peak in the JST_Nov data in Figure 6f. Why is there no peak in the COA diurnal during lunch time in JST_Nov?*

Response: For the three out of four datasets where a COA factor is resolved, the COA exhibits a small peak at lunch time and a larger peak at dinner time. The only exception is JST_Nov dataset, where COA starts decreasing since ~6am and reaches daily minimum ~3pm. Although the reason for the lack of a lunch-time peak in JST_Nov is unclear at this moment, the mass spectrum of COA factor in JST_Nov is similar to that of other sites in the current study and it is also similar to the COA mass spectra in the literature, which supports the identification of COA for JST_Nov dataset.

We have amended the text in the revised manuscript for clarity.

"Another feature of COA is its unique diurnal trend. For three out of four datasets (except JST_Nov) where a COA factor is identified, the COA factor exhibits a small peak at lunch time and a large peak at dinner time (Fig. 5)."

8. When discussing the Isoprene-OA factor, the authors state that fC5H6O+ is higher at rural sites than urban sites, which could be explained by advection from rural sites to urban areas, during which time compounds giving rise to C5H6O+ are further transformed. However, the authors conclude based on other evidence that advection is likely not significant. What then is the explanation for the lower fC5H6O+ in urban sites? Could this be an indicator of mixing of the PMF factors in the urban datasets?

Response: In this study, we do not have definite explanations regarding why f_{C5H6O+} is higher at the rural sites than urban sites. Factor mixing in the PMF analysis and the influence of seasonality (as proposed by Reviewer#3 comment#8) are possible explanations. We have added the following discussions in the revised manuscript.

"Another possibility for the lower f_{C5H6O+} at the urban sites is that Isoprene-OA factor from the urban sites may contain isoprene SOA produced via other pathways, in addition to the IEPOX uptake pathway. Isoprene SOA formed via RO_2+NO pathway only has a negligible signal at $C_5H_6O^+$ (Kroll et al., 2006; Xu et al., 2014), so that the mixing of Isoprene SOA via different pathways may lower the f_{C5H6O+} in the Isoprene-OA factor. Moreover, seasonality may also have an influence on the lower f_{C5H6O+} at the urban sites since the sampling periods at the urban sites are May and August, when the isoprene concentration is relatively lower than that during the sampling periods at the rural sites (i.e., June and July)."

9. In section 4.1.4, the authors discuss the degradation of levoglucosan during atmospheric aging and thus loss of BBOA tracer ion signal. However, aging of primary BBOA emissions has also been shown to increase signal of these tracer ions in the AMS. For example, Heringa et al. (2011) showed that aging of BBOA emissions in chamber studies resulted in the formation of SOA which fragmented to give signal at C2H4O2+. This increase in C2H4O2+ from SOA would offset some of the loss of tracer signal due to levoglucosan oxidation. This point could be also be mentioned when discussing the BBOA factor. (Reference: Heringa, M.F., DeCarlo, P.F., Chirico, R., Tritscher, T., Dommen, J., Weingartner, E., Richter, R., Wehrle, G., Prévôt, A.S.H. and Baltensperger, U.: Investigations of primary and secondary particulate matter of different wood combustion appliances with a high-resolution time-of-flight aerosol mass spectrometer, Atmos. Chem. Phys. 11, 5945-5957, 2011)

Response: Thanks for pointing this out and we have amended the text in the revised manuscript.

"These two ions are largely produced by levoglucosan, which is formed from the breakdown of cellulose in biomass burning (Schneider et al., 2006). In addition, Heringa et al. (2011) showed that SOA produced during the aging of primary biomass burning emissions could contribute to these two ions."

However, even if SOA produced during the aging of primary biomass burning emissions could contribute to these two ions, both laboratory studies and ambient measurements show solid evidence that the signals at these two ions decrease rapidly with photochemical aging. We have amended the text in the revised manuscript.

"It is important to note that the BBOA reported in this study likely only represents the relatively fresh OA from biomass burning. For example, laboratory studies revealed that the oxidation of levoglucosan is fast in both the gas and aqueous phases (Zhao et al., 2014; May et al., 2012; Hennigan et al., 2011). The fast oxidation of levoglucosan can result in the rapid decay of signals at $C_2H_4O_2^+$ (*m/z* 60) and $C_3H_5O_2^+$ (*m/z* 73), causing the mass spectrum of BBOA to lose its characteristic signature. In addition, laboratory studies by Hennigan et al. (2011) and Grieshop et al. (2009) showed that the mass spectrum of OA from biomass burning becomes increasingly similar to that of MO-OOA after photochemical aging. Ambient measurements in the eastern Mediterranean by Bougiatioti et al. (2014) showed evidence that BBOA could be rapidly converted to OOA in less than a day. Thus, aged OA from biomass burning could be apportioned to the MO-OOA factor."

10. From Figure 16S, the NO3,org diurnal has a maximum for CTR_Jun and YRK_July in the mid-morning, rather than in the night or early morning. I would expect NO3,org to peak in the night due to organic nitrate formation from nighttime chemistry. Why is the peak shifted to the mid-morning for these two cases? Also, organic nitrates are a significant aspect of the paper, so I suggest to either move Figure 16S to the main text or include the NO3,org diurnal in the main text, perhaps in Figure 6.

Response: The shift of $NO_{3,org}$ diurnal maximum from early morning to mid-morning is likely due to organic nitrate formation from photooxidation of VOCs in the presence of NO (i.e., RO_2+NO pathway) in addition to VOCs+$NO_3^•$ pathway. For the CTR_June dataset, NO concentration increases quickly from ~25ppt to ~275 ppt in early morning (5am to 7am) and decreases quickly back to ~50ppt from 7am to 10am. The relatively high concentration of NO in mid-morning could lead to the formation of organic nitrate when NO reacts with RO_2 radical. This could be supported by that some particle-phase organic nitrate compounds, as measured by a Filter Inlet for Gases and AEROsols Chemical Ionization Mass Spectrometer (FIGAERO-CIMS), show a daily maximum in mid-morning during the SOAS campaign in the SE US (Lee and Thornton, personal communication).

As suggested by the reviewer, we have moved the Fig. S16 to the main text. We also include the following discussion in the revised manuscript.

"Figure 12 shows the diurnal variation of $NO_{3,org}$ based on the NO_x^+ ratio method with an R_{ON} value of 10. For most of the datasets, $NO_{3,org}$ starts increasing after sunset, which is mainly caused by the oxidation of VOCs by nitrate radical at night. The daily maximum of $NO_{3,org}$ appears in mid-morning (i.e., ~8am), which is likely because photooxidation of VOCs in the presence of NO (i.e., RO_2+NO pathway) also contributes to organic nitrate when the NO concentration is highest."

11. The authors state that an FPEAK value of 0 was used in all datasets (P10491), however, in the supplementary information, it is stated that an FPEAK value of 0.2 was used for RS_Jan. This discrepancy should be resolved.

Response: In this study, we performed two types of PMF analysis. One type is PMF analysis on organic mass spectra only (denoted as PMF_{org} in the main text) and the other type is PMF analysis on organic mass spectra together with NO^+ and NO_2^+ ions (denoted as $PMF_{org+NO3}$ in the main text). An FPEAK value of 0 was used in all data sets in PMF_{org}. An FPEAK of value of 0 was also used in all datasets in $PMF_{org+NO3}$, except for RS_Jan, where an FPEAK value of 0.2 was used. As discussed in the SI in detail, an FPEAK value of 0.2 was chosen for RS_Jan after considering the convergence of $PMF_{org+NO3}$ and the correlation between factors from $PMF_{org+NO3}$ and factors from PMF_{org}.

We have modified the sentence for clarity.

"An FPEAK value of 0 is used for all datasets in our PMF analysis on organic mass spectra, ..."

12. TECHNICAL COMMENTS

(1) P10481, L26, P10482, L23, P10483, L28, P10484, L13, P10484, L27, P10486, L2, P10486, L12, P10488, L2-5, P10489, L7, P10489, L10, P10489, L13-14, P10490, L7, P10490, L12, P10490, L13, P10490, L13, P10490, L16, P10490, L16, P10490, L22, P10490, L23, P10494, L5, P10494, L20, P10494, L21, P10497, L4, P10498, L6, P10500, L3, P10502, L10, P10502, L17, P10503, L5, P10504, L13, P10504, L26, P10505, L21, P10505, L22, P10506, L9, P10506, L22, P10509, L20, P10509, L24 and L25, P10510, L21, P10511, L4, P10512, L21-22, P10513, L15, P10513, L19, P10513, L23, P10514, L19, P10515, L6, P10515, L24, P10515, L28, P10516, L1, P10516, L14.

Response: These comments are related to language and we have modified the text accordingly.

(2) Figure 4: Parts (a) and (b) should be same font sizes (e.g., axes).

Response: The changes have been made accordingly.

(3) Figure 5 caption: "Campaign" is misspelled. Figure 11 caption: "Detection" is misspelled.

Response: The changes have been made.

Response to Reviewer 2

1. A main point that should be clarified in the text is the origin and use of boundary layer height (BLH) data. The authors often refer to the BLH diurnal variation as an element that affects the diurnal pattern of the different chemical species observed at the ground. However, very little information is provided on the origin of these BLH data, and on the actual BLH diurnal variation these data show in the region under investigation. More details are definitely needed in the text on this aspect. At least a Figure with the typical BLH diurnal pattern in summer and winter in the region should be included in the supplementary material. This would (possibly) allow the reader to understand the use of the BLH data in generating the results of Figures 3d and 6d. In fact, to my understanding, at present these data are used in an incorrect way. The authors state they multiply the different chemical species loads at the surface (expressed as μg/m3) by the BLH (see e.g. page 10513, line 25), obtaining units of μg/m2. I do not see the physical reason for that. The concept of the BLH dilution effect is that, given a certain load of the chemical component X (expressed in μg), uniformly distributed within a well mixed atmospheric volume V given by [area(m2) x BLH(m)], the concentration of X that is measured at the ground, i.e. X/V, would be higher when BLH is lower (i.e., in the morning/evening), and would be lower when BLH is higher, i.e. at midday. As the authors correctly describe in the text, this effect contributes explaining why, for example, a given component expected to increase in the central part of the day for photochemical processes, can exhibit a flat diurnal cycle (or even be observed to decrease in the central part of the day). So my point is that the authors give the right explanation to justify some of the BLH-driven diurnal patterns observed, but provide the wrong (or insufficiently explained) demonstration for that.

Response: As the reviewer suggested, we have added a figure with the diurnal variation of BLH measured at the CTR_June and added more descriptions of BLH in the revised manuscript.

We agree with the reviewer's interpretation on the effect of BLH on the diurnal variation of a species and it is essentially the same as ours. The interpretation of multiplying the concentration of a compound X (i.e., $\mu g/m^3$) by BLH (i.e., m) is the integrated column concentration of X (i.e., $\mu g/m^2$) from ground to the top of boundary layer over a unit surface area. The value of X*BLH would be conserved if there is no gain or loss of X in the column regardless of the change of BLH. Thus, this value could indicate the net gain or loss of X in the column without the effect of BLH-driven dilution.

We have included the following discussion in the revised manuscript.

"In Centreville, the boundary layer height (BLH) was measured by a ceilometer. The diurnal variation of BLH is shown in Fig. 14. The BLH typically peaks (i.e., 1300m) at 17:00 and exhibits a daily minimum (i.e., 375m) at 07:00. In order to remove the effect of BLH-driven dilution on the diurnal variation of OA, we multiply the OA diurnal profile by BLH. The interpretation of the product of the concentration of OA (i.e., $\mu g\ m^{-3}$) times BLH (i.e., m) is the integrated column concentration of OA (i.e., $\mu g\ m^{-2}$) from ground to the top of boundary layer over a unit surface area, assuming the OA is well-mixed in the boundary layer. The value of OA*BLH would be conserved if there is no gain or loss of OA in the column regardless of the change of BLH. Thus, this value could indicate the net gain or loss of OA in the column without the effect of BLH-driven dilution. As shown in Fig. 3d, the OA*BLH increases rapidly starting at ~7:00 and reaches a daily maximum at ~17:00. The evident peak in the diurnal variation of OA*BLH suggests a substantial OA production in the day, and that the relatively flat OA diurnal variation (i.e., $\mu g\ m^{-3}$) is largely caused by the BLH-driven dilution."

2. The authors often refer to the term 'Brown Carbon' and use 'Brown Carbon' data in the manuscript. As it can be inferred from the text, with this term they refer to the 'Brown-carbon light-absorption' (units m-1). This should be clearly stated in the text and in the relevant Figure showing these data (Figure 7) in order to avoid potential confusion. Additionally, the description of how Brown Carbon Absorption is derived should be improved (Page 10489 lines 11-15). In fact, a) it is not clear how the Black Carbon information from MAAP is combined to the

Aethalometer one to derive the Brown Carbon Absorption, and, b) I doubt that, in the Aethalometer case, 'the measurements under seven wavelengths (i.e., 370, 450, 571, 590, 660, 880, and 950 nm) were averaged to represent the black carbon concentration' as currently stated. Please explain better and give appropriate reference to the methods used to derive the Brown Carbon Absorption data used in the manuscript.

Response: We have replaced "brown carbon" with "brown carbon light absorption" in the revised text and figures. In this study, the brown carbon absorption is measured by a PILS-LWCC-TOC system as described in section 2.3.3. We have clarified the brown carbon measurements in the revised manuscript.

"The PILS-LWCC-TOC system continuously (i.e., 15min resolution) measured the light absorption spectra of water-soluble organic components. The detailed working principle of the PILS-LWCC-TOC system can be found in Hecobian et al. (2010). In brief, water-soluble species are first dissolved in water in a PILS (Weber et al., 2001). The liquid sample from the PILS is then injected into a Liquid Waveguide Capillary Cell, where the absorption spectra are collected over wavelengths of 200 to 800nm. The average light absorption between 360 to 370 nm is used as a measure of brown carbon light absorption."

For the black carbon measurement, please see our response to the comment #4 of reviewer #1.

3. Although the manuscript is generally well written, some parts/sentences could be shortened, improving its readability. Another issue is the quantity and the specific choice of Figures to be included in the main text and in the supplementary material. Some times in the text the authors refer to Figures in the supplementary material as main points of their discussion. This makes the reading not straightforward as it is needed to switch between the main text and the supplementary material several times. To my opinion all the Figures necessary for the main discussion should be in the main text (Figure S14 for example) and the supplement should only provide the material for a deeper investigation/explanation of the results described in the main text.

Response: In the revised manuscript, we have shortened some long sentences and rephrased some sentences to improve readability. As suggested by reviewer #1, we decide to move Fig.

S16 from SI to the main text. We prefer to keep Fig. S14 in the SI since the key point of these plots is the correlation coefficients of species between different sites, which has been shown in Fig. 13.

4. Specific/technical comments

(1) Title. Possibly, given the contents of the manuscript, the title should be modified as 'Aerosol characterization over the southeastern United States using high resolution aerosol mass spectrometry: spatial and seasonal variation of aerosol composition and sources with focus on organic nitrates'

Response: Thanks for the suggestion and we have changed the title as suggested.

(2) Page 10481 Line 6, Page 10490 Line 6, Page 10490 Line 19, Page 10493 Line 1, Page 10496 Line 14, Page 10499 Line 3, Page 10501 Line 29, Page 10502 Line 20, Page 10503 Line 5, Page 10503 Line 8, Page 10505 Line 22, Page 10505 Line 24, Page 10506 Line 3, Page 10506 Line 20, Page 10509 Line 2, Page 10510 Line 2, Page 10510 Line 23, Page 10510 Line 24, Page 10511 Line 14, Page 10512 Line 19, Page 10513 Line 4, Page 10513 line 7-8, Page 10515 Line 28.

Response: These comments are related to language and we have modified the text accordingly.

(3) Page 10481 Line 11: It would be useful to specify in this abstract what 'important' means here, please provide for example data of % contribution of HOA and COA.

Response: We have made the suggested change.

"Hydrocarbon-like OA (HOA) and cooking OA (COA) have important but not dominant contributions to total OA in urban sites (i.e., 21-38% of total OA depending on site and season)."

(4) Page 10488 Line 5: Please, specify the meaning of V mode and W mode

Response: We have made the suggested change.

"We operated the HR-ToF-AMS in two ion optical modes (V and W) with different sensitivity and spectra resolution,…."

(5) Page 10489 Line 5-25: It would be important to know the temporal resolution of the different datasets introduced in this paragraph.

Response: We have added the temporal resolution of all instruments in the revised manuscript.

(6) Page 10494 Line 10-12: It would be useful to know how these averages were obtained (Average of daily averages? Averages of hourly averages? See also my comment above on the temporal resolution of the measurements).

Response: The numbers in Page 10494 Line 10-12 and in table 1 are the campaign-averaged values based on high-temporal resolution data (1 - 60 min depending on instrument). We have added this information in the footnote of table 1 in the revised manuscript.

(7) Page 10494 Line 20-23: BLH also plays a role in the winter-to-summer difference here, not only emissions.

Response: We agree with the reviewer. We have added "or less dispersion". The sentence now reads as "In contrast, at the urban JST site, the NO_x level is elevated in winter compared to summer, indicating more anthropogenic emissions, or less dispersion, in winter at urban sites."

(8) Page 10495 Line 19: Give reference to Fig. 2 here.

Response: We have made the suggested change.

(9) Page 10495 Line 22-23: I'm not convinced entrainment could play a role in this. In fact, it is more likely to act in the first part of the day, when BL grows and intercepts the residual layers aloft (e.g. Curci et al, Atmos. Chem. Phys., 15, 2629-2649, 2015)

Response: Curci et al. (2015) use lidar observations and model simulations to show that the entrainment into the planetary boundary layer (PBL) has significant impacts on the ground-level aerosol concentrations. This supports our hypothesis that entrainment plays a role in the sulfate diurnal variation. We agree with the reviewer that Curci et al. (2015) showed that the entrainment is more likely to act in the first part of the day. However, Curci et al. (2015) studied the effects of entrainment in the Milan urban area, the meteorology and pollutant sources are different from those in the Atlanta area. For example, the Atlanta metropolitan area is surrounded by coal-fired power plants with tall stacks. As suggested by Weber (2003), these tall stacks emit SO_2, which could undergo cloud processing to form sulfate. In the afternoon when the PBL is the highest, sulfate aloft is entrained into the PBL. This hypothesis could be supported by Wagner et al. (2015), who showed evidence of sulfate production above the PBL in the southeastern US in summer time.

(10) Page 10497 Line 15-16: I cannot see this 'clear lunch and dinner feature' here. This is only shown in 3 out of 6 plots and: a) it is not visible in JST_May, b) in RS-Jan the peak is in the morning at 5 a.m. Please explain this point better or rephrase.

Response: We refer the reviewer to the response to comment #7 of reviewer #1.

(11) Page 10498 line 5: Why not referring to Isoprene-OA as IOA as done for all the other categories?

Response: We thank the reviewer for the suggestion. However, there are already a lot of acronyms about OA factors in the literature now. Thus, we prefer to keep the term Isoprene-OA to be more informative.

(12) Page 10498 Line 8: Acronyms should always be introduced first (not all the readers may know IEPOX stands for Isoprene epoxydiols).

Response: We have made the suggested change.

(13) Page 10501 Line 7-14: Could these BBOA differences be also due to the fact that you compare PM1-related data to PM2.5-related ones? Please, comment.

Response: This is one possible explanation and we have included it in the revised manuscript.

(14) Page 10503 Line 11-13: Please, explain better, see also my comment on BLH effect above.

Page 10513 Line 24-26: See my main comment above on this matter. Please give details on how BLH data have been collected, ceilometer instrument used, BLH retrieval. Provide at least a Figure in the supplementary material showing the typical BLH in the region and its seasonality.

Response: We refer the reviewer to the response to your comment #1.

(15) Page 10508 Line 4: Is that from NaNO3 the only possible contamination?

Response: There are other possible contaminations in addition to $NaNO_3$. In this study, we use the concentration of Na as an indicator to show that the potential interference from mineral dust is small. We have modified the sentences for clarity.

"However, due to the transmission efficiency of PM_1 cyclone, PILS-IC measurements might include contributions from particles larger than 1μm (i.e., inorganic NO_3 in mineral dust). Interferences from water-soluble refractory particles (e.g., calcium or sodium nitrate) are likely small given the concentration of sodium measured by the PILS-IC with a PM_1 cyclone, for example, was negligible and mostly below its detection limit (0.07 $\mu g\ m^{-3}$) (Fig. S13)."

(16) Page 10508 Line 27: I just want to highlight here that a variability of 0.11-0.21 means a difference of about 100%!

Response: We thank the review for this note. The large variability is caused by the wide range of R_{ON} values in the estimation.

(17) Page 10509 Line 12: Why do you consider GT_AUG to be in a transition month? Isn't August a summer month (particularly considering that relevant observation started on July 20)?

Response: In this study, all seven datasets are grouped according to the extent of agreement between the NO_x^+ ratio method and PMF method. For summer datasets (CTR_June and YRK_July), the $NO_{3,org}$ estimated from the PMF method falls within the upper and lower bound of the NO_x^+ ratio method. For winter datasets (JST_Nov and YRK_Dec), the PMF method shows good agreement with the NO_x^+ ratio method with an R_{ON} value of 10. For JST_May and GT_Aug, the NO_x^+ ratio method predicts higher $NO_{3,org}$ concentration than the PMF method, which is caused by that PMF method attributes some organic nitrates to the nitrate inorganic aerosol (NIA) factor as discussed in the manuscript. For the convenience of discussion, JST_May and GT_Aug are grouped as "transition month" datasets. To avoid confusion, we have deleted the phrase "the sampling periods of which were between summer and winter".

(18) Page 10511 Line 18-19: Rephrase the sentence to refer to Fig 12 and then address the reader to figure S14 for deeper analysis (if you believe Fig 12 is more 'efficient' than Figure S14 in summarizing the results you are commenting here'....)

Response: We have rephrased the sentence as following.

"Figure 13 shows the correlation coefficients for $NR\text{-}PM_1$ species between ACSM measurements (stationary at the Georgia Tech site) and HR-ToF-AMS measurements (rotating among different sites). Detailed comparisons, in terms of time series and scatter plots, are shown in Fig. S14."

(19) Page 10512 Line 25-27: I cannot see a 'POA' curve in Figure 5

Response: A "POA" line is not included in Fig. 5 because the POA concentration could be easily calculated by subtracting SOA from total OA. In addition, adding a POA curve makes the plot very busy.

5. Figures

(1) Figure 2: it would be useful to also have an additional panel showing the 'absolute' plot (as in Figure 5).

Response: We have included a figure (Fig. 2a in the revised manuscript) to show the concentrations of non-refractory PM_1 species.

(2) Figure 3: Axis Labels and Tick Labels are not readable at all, please increase the character size of all of them. Axis Limits should better be the same in all panels to allow a more direct and straightforward comparison. For Figure 3d see my comments above. I think it can even be removed without losing much of the manuscript significance. Otherwise, carefully describe its content as mentioned.

Response: The axis labels are not readable in the ACPD version. Once the manuscript gets accepted by ACP, we will request that Figs. 3 and 6 take up a whole page and we believe the figures will become readable. We agree with the reviewer that using the same axis limit would allow a more direct comparison. However, the concentrations of species span a wide range for different sites and seasons, so using the same scale would make the diurnal variability less clear. We have addressed your comments regarding figure 3d above (i.e., response to your comment #1).

(3) Figure 5: in the legend Isoprene-OA could conveniently be indicated as IOA for homogeneity. Numbers at the top of panel b are not necessary as also shown in panel a. Possibly you could add error bars on panel a. I cannot see POA line in the Figure.

Response: We prefer to keep Isoprene-OA to be more informative. We have deleted the numbers in panel a as suggested. Adding error bar makes the figure very busy. A “POA” line is not included in Fig. 5 because the POA concentration could be easily calculated by subtracting SOA from total OA.

(4) Figure 6: All the comments for Figure 3 are still valid for this figure.

Response: We refer the reviewer to the response to your comment #5(2).

(5) Figure 7: Please, put labels a) – j) in the plots. Axis Limits should better be the same in all panels to allow a more direct and straightforward comparison (there is no need to reach 70 in the Y axis of panel d, you can leave 'out of scale' values without losing much information. Use 'Brown Carbon Absorption' rather than 'Brown Carbon' in the plot labels (see my comment above).

Response: We have added labels for each sub-panel. We have addressed the comment regarding the axis limit in response to your comment #5(2). In Fig. 7(d), there is actually a split in the left y-axis. We have replaced "brown carbon" with "brown carbon light absorption" throughout the text and figures.

(6) Figure 8: Please, put labels a) – j) in the plots. Axis Limits should better be the same in all panels to allow a more direct and straightforward comparison.

Response: We have addressed similar comments above.

(7) Figure 9: This Figure is not very readable at least in the printed copy I used. Please, try to improve readability/figure resolution. Please, put labels a) – j) in the plots. Axis Limits should better be the same in all panels to allow a more direct and straightforward comparison.

Response: We have addressed similar comments above.

(8) Figure 11: I think the way this Figure is organized is not optimal. You should rather show the AMS-IC value (Y) versus the relevant range coming from the NOX ratio method with the two RON values (e.g. similarly to the vertical lines of Figure 10 but as horizontal lines in the X axis). You can leave info on the two fit lines; correlation R is obviously the same and should not be repeated. The reason of the offset is not clear and should be better explained. Measurement errors are mentioned in the caption but not shown. Please, specify and/or show such errors.

Response: We thank the reviewer for the suggestion. However, we prefer to keep the figure as it is because it already clearly conveys our main points. The 1:1 line is offset by the detection limit of PILS-IC nitrate (i.e., -0.03 μg m^{-3}) for visual clarity. The uncertainty of PILS-IC measurements is about 10% according to Weber et al. (2001). We have added the information in the figure 11 caption.

(9) Figure 12: In the caption it should be 'values are plotted versus the relevant distance of the measurement site from the GT one, where the…'

Response: We have made the suggested change.

<u>Response to Reviewer 3</u>

1. Page 10481, line 14: So far only the AMS and ACSM are mentioned. Therefore, it seems as if brown carbon was measured by one of these instruments. Give the instruments used to measure brown carbon.

Response: The brown carbon light absorption is measured by a PILS-LWCC-TOC system as described in section 2.3.3.

2. Page 10490, line 4: Only AMS publications are listed, but the aerosol community is much bigger. Could the authors list non-AMS publications presenting PMF results (or similar statistical analysis), since it is supposed to be widely applied in the aerosol community?

Response: We have added the following references.

(1) Positive Matrix Factorization (PMF) Analysis of Molecular Marker Measurements to Quantify the Sources of Organic Aerosols. Jaeckels et al. 2007 ES&T.

(2) Receptor modelling of both particle composition and size distribution from a background site in London, UK. Beddows et al. 2015 ACPD.

(3) Advanced source apportionment of size-resolved trace elements at multiple sites in London during winter. Visser et al. 2015 ACPD.

3. Page 10493, line 20: The authors might reconsider the wording. "Nitrate inorganic aerosol particles" would be solely consisting of inorganic compounds including nitrate but especially in the presented case, the aerosol particles consist of inorganic nitrate and organic compounds at *the same time. How about hyphenating to clarify the word associations: Inorganic-nitrate aerosol particles in contrast to organic-nitrate aerosol particles?*

Response: We thank the reviewer for the suggestion. The terminology "nitrate inorganic aerosol (NIA)" is adapted from Sun et al. (2012b). In order to be consistent with literature and avoid confusion, we prefer to keep it as is.

4. Page 10495 line 9: General comment to ALL figures not just Fig. 3: Error bars are missing, which are of specific importance for the interpretation of diurnal profiles. The axes labeling and legend text is rather small. Please try to use the same scaling (or multiplication) for multiple panels in one figure to support easy comparability.

Response: We refer the reviewer to the response to comment #6 of reviewer #1. The figures will become readable in the ACP version.

5. Page 10496, line 6: Many readers might be more familiar with low-volatility (LV-) and semi-volatile (SV-) oxygenated organic aerosol (OOA). Please move the introduction of more-oxidized (MO-) and less-oxidized (LO-) OOA from page 10502 to here.

Response: We have made the suggested change.

6. Page 10498, line 1: This reference might be obsolete. It seems as if the impact of the lower resolution on the number/type of PMF factors was discussed in this publication, but this is not the case. The authors of the cited publication rather recombine two separate OOA factors and proceed with a 2 factor solution (HOA and OOA) for an easier comparison to PMF results of a collocated HR-AMS instrument.

Response: We have deleted the reference as suggested.

7. Page 10498, line 8: What are IEPOX? The authors should give a brief description as well as an explanation of the acronym since not all readers are chemists.

Response: IEPOX stands for Isoprene epoxydiols. We have made the suggested change.

8. Page 10498, line 25ff: Is the difference in fC5H6O+ solely due to rural vs. urban? Could there be an influence from the seasonality in terms of transient (May, August) vs. summer (June/July) months?

Response: We refer the reviewer to the response to comment #8 of reviewer #1.

9. Page 10502, line 26: The ranges given for LO- and MO-OOA are specific to this publication. Taking the cited references into account, it seems to be hard to generate a generality in the range of values. A short discussion on this might be helpful for nonfamiliar readers.

Response: In this study, the O:C ratios are determined by following the latest procedures as recommended by Canagaratna et al. (2015) (i.e., denoted as “Canagaratna method”). Canagaratna et al. (2015) improved the estimation from Aiken et al. (2008) (i.e., denoted as “Aiken method”), which has been widely used in the literature. The Canagaratna method has only been published very recently. Currently, there are only few studies that calculated O:C ratio using Canagaratna method, thus we don’t have many literature values to compare with. The O:C ranges of MO-OOA and LO-OOA for multiple ambient measurements in the northern hemisphere calculated using the Aiken method have been reported in Ng et al. (2010) and Jimenez et al. (2009). If we were to calculate the O:C values of the MO-OOA and LO-OOA reported in our study using the Aiken method, our values are consistent with literature values (Ng et al., 2010; Jimenez et al., 2009).

10. Page 10503, line 8: I suspect the authors consider the identification of specific sources of MO-OOA to be challenging but not the identification of the factor itself. In that case, please rephrase the sentence.

Response: The reviewer is correct. We mean the identification of specific sources of MO-OOA to be challenging. We have rephrased the sentence.

11. Page 10505, line 21: As a general comment, please check on your significant figures (digits) throughout the text and in all figures! The text in figure 9 is hard to read! Please reduce to/highlight the most important information (R values). Take the appropriate detection limits into consideration. Include a zero line to guide the eye of the reader. Give the color coding in the figure caption as well, especially, since the legends are hard to read.

Response: We have used two significant digits in figure 9 and increased the text font in the revised manuscript. The correlation coefficients, which are the most important information, are already listed in table 2. Zero line has been added and the figure captions are color coded as suggested.

12. Page 10506, line 4: The authors mention inorganic nitrates other than ammonium nitrate but do not discuss possible compounds and sources. A short discussion maybe taking the results of Alfarra(http://cires1.colorado.edu/jimenez/Papers/Alfarra_PhD%20Thesis_4Chapter4_Labwork.pdf) into account would be very informative.

Response: We thank the reviewer for the suggestion. The Alfarra's thesis shows the NO^+/NO_2^+ of $Mg(NO_3)_2$, $NaNO_3$, and $Ca(NO_3)_2$, which are mainly from mineral dust. However, these species are negligible in PM_1 in the SE US. In addition, the main reason for smaller R_{meas} than R_{AN} is due to variations in instrument performance. Thus, we decide to delete the phrase "contribution from inorganic nitrates other than ammonium nitrate or". The sentence now reads as: "The negative values are a result of smaller R_{meas} than R_{AN}, at times (see Eqn 1), which is likely caused by variations in instrument performance (Farmer et al., 2010; Rollins et al., 2010)."

13. Comment on figures in supplemental material: Please check on readability of figure legends and axes labeling. Please extend the information in the figure captions. Most probably, figures as Fig. S5 are not as self explanatory to a broader community as the short figure caption suggests. Please check on readability of the figures themselves. E.g. the readability of Fig S8 could be improved significantly when multiple panels were used each displaying only a subset of the lines.

Response: We have made the suggested changes for the SI figures. The major changes are listed below.

(1) Extend the information in the figure captions, especially for figure S5.

(2) Increase the font of axis and legends of some figures.

(3) Check the significant digits.

(4) Divide Fig. S8 into multiple panels

14. Technical comments

(1) Page 10483, line 3, Page 10484, line 19, Page 10490 line 7, Page 10498, line 14, Page 10485, line 21, Page 10498, line 20, Page 10499, line 3, Page 10502, line 15, Page 10504, line 12, Page 10504, line 27, Page 10505, line 25, Page 10507, line 11, Page 10509, line 2, Page 10512, line 18, Page 10512, line 21, Page 10519 line 11

Response: These comments are related to language and we have modified the text accordingly.

(2) Page 10498, line 18: Is this a different "R" than the one mentioned on Page 10499, line 15? If not, please move definition of it to first appearance.

Response: We only used Pearson's R in the manuscript. We have made the suggested change.

Additional Corrections

1. We replace the citation
"Guo, H., Xu, L., Bougiatioti, A., Cerully, K. M., Capps, S. L., Hite, J. R., Carlton, A. G., Lee, S. H., Bergin, M. H., Ng, N. L., Nenes, A., and Weber, R. J.: Particle water and pH in the southeastern United States, Atmos. Chem. Phys. Discuss., 14, 27143-27193, 10.5194/acpd-14-27143-2014, 2014."
With
"Guo, H., Xu, L., Bougiatioti, A., Cerully, K. M., Capps, S. L., Hite Jr, J. R., Carlton, A. G., Lee, S. H., Bergin, M. H., Ng, N. L., Nenes, A., and Weber, R. J.: Fine-particle water and pH in the

southeastern United States, Atmos. Chem. Phys., 15, 5211-5228, 10.5194/acp-15-5211-2015, 2015."

Reference

Aiken, A. C., Decarlo, P. F., Kroll, J. H., Worsnop, D. R., Huffman, J. A., Docherty, K. S., Ulbrich, I. M., Mohr, C., Kimmel, J. R., Sueper, D., Sun, Y., Zhang, Q., Trimborn, A., Northway, M., Ziemann, P. J., Canagaratna, M. R., Onasch, T. B., Alfarra, M. R., Prevot, A. S. H., Dommen, J., Duplissy, J., Metzger, A., Baltensperger, U., and Jimenez, J. L.: O/C and OM/OC ratios of primary, secondary, and ambient organic aerosols with high-resolution time-of-flight aerosol mass spectrometry, Environ Sci Technol, 42, 4478-4485, Doi 10.1021/Es703009q, 2008.

Berndt, T., and Boge, O.: Products and mechanism of the gas-phase reaction of NO3 radicals with [small alpha]-pinene, Journal of the Chemical Society, Faraday Transactions, 93, 3021-3027, 10.1039/A702364B, 1997.

Boyd, C. M., Sanchez, J., Xu, L., Eugene, A. J., Nah, T., Tuet, W. Y., Guzman, M. I., and Ng, N. L.: Secondary Organic Aerosol (SOA) formation from the β-pinene + NO3 system: effect of humidity and peroxy radical fate, Atmos. Chem. Phys. Discuss., 15, 2679-2744, 10.5194/acpd-15-2679-2015, 2015.

Bruns, E. A., Perraud, V., Zelenyuk, A., Ezell, M. J., Johnson, S. N., Yu, Y., Imre, D., Finlayson-Pitts, B. J., and Alexander, M. L.: Comparison of FTIR and Particle Mass Spectrometry for the Measurement of Particulate Organic Nitrates, Environ Sci Technol, 44, 1056-1061, 10.1021/es9029864, 2010.

Canagaratna, M. R., Jimenez, J. L., Kroll, J. H., Chen, Q., Kessler, S. H., Massoli, P., Hildebrandt Ruiz, L., Fortner, E., Williams, L. R., Wilson, K. R., Surratt, J. D., Donahue, N. M., Jayne, J. T., and Worsnop, D. R.: Elemental ratio measurements of organic compounds using aerosol mass spectrometry: characterization, improved calibration, and implications, Atmos. Chem. Phys., 15, 253-272, 10.5194/acp-15-253-2015, 2015.

Curci, G., Ferrero, L., Tuccella, P., Barnaba, F., Angelini, F., Bolzacchini, E., Carbone, C., Denier van der Gon, H. A. C., Facchini, M. C., Gobbi, G. P., Kuenen, J. P. P., Landi, T. C., Perrino, C., Perrone, M. G., Sangiorgi, G., and Stocchi, P.: How much is particulate matter near the ground influenced by upper-level processes within and above the PBL? A summertime case study in Milan (Italy) evidences the distinctive role of nitrate, Atmos. Chem. Phys., 15, 2629-2649, 10.5194/acp-15-2629-2015, 2015.

Griffin, R. J., Cocker, D. R., Flagan, R. C., and Seinfeld, J. H.: Organic aerosol formation from the oxidation of biogenic hydrocarbons, J Geophys Res-Atmos, 104, 3555-3567, Doi 10.1029/1998jd100049, 1999.

Jimenez, J. L., Canagaratna, M. R., Donahue, N. M., Prevot, A. S. H., Zhang, Q., Kroll, J. H., DeCarlo, P. F., Allan, J. D., Coe, H., Ng, N. L., Aiken, A. C., Docherty, K. S., Ulbrich, I. M., Grieshop, A. P., Robinson, A. L., Duplissy, J., Smith, J. D., Wilson, K. R., Lanz, V. A., Hueglin, C., Sun, Y. L., Tian, J., Laaksonen, A., Raatikainen, T., Rautiainen, J., Vaattovaara, P., Ehn, M., Kulmala, M., Tomlinson, J. M., Collins, D. R., Cubison, M. J., Dunlea, E. J., Huffman, J. A., Onasch, T. B., Alfarra, M. R., Williams, P. I., Bower, K., Kondo, Y., Schneider, J., Drewnick, F., Borrmann, S., Weimer, S., Demerjian, K., Salcedo, D., Cottrell, L., Griffin, R., Takami, A., Miyoshi, T., Hatakeyama, S., Shimono, A., Sun, J. Y., Zhang, Y. M., Dzepina, K., Kimmel, J. R., Sueper, D., Jayne, J. T., Herndon, S. C., Trimborn, A. M., Williams, L. R., Wood, E. C., Middlebrook, A. M., Kolb, C. E., Baltensperger, U., and Worsnop, D. R.: Evolution of Organic Aerosols in the Atmosphere, Science, 326, 1525-1529, DOI 10.1126/science.1180353, 2009.

Ng, N. L., Canagaratna, M. R., Zhang, Q., Jimenez, J. L., Tian, J., Ulbrich, I. M., Kroll, J. H., Docherty, K. S., Chhabra, P. S., Bahreini, R., Murphy, S. M., Seinfeld, J. H., Hildebrandt, L., Donahue, N. M., DeCarlo, P. F., Lanz, V. A., Prevot, A. S. H., Dinar, E., Rudich, Y., and Worsnop, D. R.: Organic aerosol components observed in Northern Hemispheric datasets from Aerosol Mass Spectrometry, Atmos Chem Phys, 10, 4625-4641, DOI 10.5194/acp-10-4625-2010, 2010.

Wagner, N. L., Brock, C. A., Angevine, W. M., Beyersdorf, A., Campuzano-Jost, P., Day, D. A., de Gouw, J. A., Diskin, G. S., Gordon, T. D., Graus, M. G., Huey, G., Jimenez, J. L., Lack, D. A., Liao, J., Liu, X., Markovic, M. Z., Middlebrook, A. M., Mikoviny, T., Peischl, J., Perring, A. E., Richardson, M. S., Ryerson, T. B., Schwarz, J. P., Warneke, C., Welti, A., Wisthaler, A., Ziemba, L. D., and Murphy, D. M.: In situ vertical profiles of aerosol extinction, mass, and composition over the southeast United States during SENEX and SEAC4RS: observations of a modest aerosol enhancement aloft, Atmos. Chem. Phys. Discuss., 15, 3127-3172, 10.5194/acpd-15-3127-2015, 2015.

Weber, R.: Short-Term Temporal Variation in PM2.5 Mass and Chemical Composition during the Atlanta Supersite Experiment, 1999, J Air Waste Manage, 53, 84-91, 10.1080/10473289.2003.10466123, 2003.

Weber, R. J., Orsini, D., Daun, Y., Lee, Y. N., Klotz, P. J., and Brechtel, F.: A particle-into-liquid collector for rapid measurement of aerosol bulk chemical composition, Aerosol Sci Tech, 35, 718-727, Doi 10.1080/02786820152546761, 2001.

Xu, L., Guo, H., Boyd, C. M., Klein, M., Bougiatioti, A., Cerully, K. M., Hite, J. R., Isaacman-VanWertz, G., Kreisberg, N. M., Knote, C., Olson, K., Koss, A., Goldstein, A. H., Hering, S. V., de Gouw, J., Baumann, K., Lee, S.-H., Nenes, A., Weber, R. J., and Ng, N. L.: Effects of anthropogenic emissions on aerosol formation from isoprene and monoterpenes in the southeastern United States, Proceedings of the National Academy of Sciences, 112, 37-42, 10.1073/pnas.1417609112, 2015.

Aerosol Characterization over the Southeastern United States Using High Resolution Aerosol Mass Spectrometry: Spatial and Seasonal Variation of Aerosol Composition~~,~~ and Sources~~, and~~ with a Focus on Organic Nitrates

Lu Xu[1], Sriram Suresh[1,*], Hongyu Guo[2], Rodney J. Weber[2], Nga Lee Ng[1,2]

[1]School of Chemical and Biomolecular Engineering, Georgia Institute of Technology, Atlanta, GA, USA

[2]School of Earth and Atmospheric Sciences, Georgia Institute of Technology, Atlanta, GA, USA

[*]now at: ExxonMoBil, Omaha, NE, USA

Correspondence to: N. L. Ng (ng@chbe.gatech.edu)

Abstract

We deployed a High-Resolution Time-of-Flight Aerosol Mass Spectrometer (HR-ToF-AMS) and an Aerosol Chemical Speciation Monitor (ACSM) to characterize the chemical composition of submicron non-refractory particles (NR-PM$_1$) in the southeastern US. Measurements were performed in both rural and urban sites in the greater Atlanta area, Georgia (GA), and Centreville, Alabama (AL) for approximately one year, as part of Southeastern Center ~~of~~for Air Pollution and Epidemiology study (SCAPE) and Southern Oxidant and Aerosol Study (SOAS). Organic aerosol (OA) accounts for more than half of NR-PM$_1$ mass concentration regardless of sampling sites and seasons. Positive matrix factorization (PMF) analysis of HR-ToF-AMS measurements identified various OA sources, depending on location and season. Hydrocarbon-like OA (HOA) and cooking OA (COA) have important, but not dominant, contributions to total OA in urban sites~~.~~ (i.e., 21-38% of total OA depending on site and season). Biomass burning OA (BBOA) concentration shows a distinct seasonal variation with a larger enhancement in winter than summer. We find a good correlation between BBOA and brown carbon, indicating biomass burning is an important source for brown carbon, although an additional, unidentified brown carbon source is likely present at the rural Yorkville site. Isoprene-derived OA (Isoprene-OA) is only deconvolved in warmer months and contributes 18-36% of total OA. The presence of Isoprene-OA factor in urban sites is more likely from local production in the presence of NO$_x$ than transport from rural sites. More-oxidized and less-oxidized oxygenated organic aerosol (MO-OOA and LO-OOA, respectively) are dominant fractions (47-79%) of OA in all sites. MO-OOA correlates well with ozone in summer, but not in winter, indicating MO-OOA sources may vary with seasons. LO-OOA, which reaches a daily maximum at night, correlates better with estimated nitrate functionality from organic nitrates than total nitrates.

Based on the HR-ToF-AMS measurements, we estimate that the nitrate functionality from organic nitrates contributes 63-100% ~~of~~to the total measured nitrates in summer. Further, the contribution of organic nitrates to total OA is estimated to be 5-12% in summer, suggesting that organic nitrates are important components in the ambient aerosol in the southeastern US. The spatial distribution of OA is investigated by comparing simultaneous HR-ToF-AMS measurements with ACSM measurements at two different sampling sites. OA is found to be

spatially homogeneous in summer, possibly due to stagnant air mass and a dominant amount of regional secondary organic aerosol (SOA) in the southeastern US. The homogeneity is less in winter, which is likely due to spatial variation of primary emissions.

We observed that the seasonality of OA concentration shows a clear urban/rural contrast. While OA exhibits weak seasonal variation in the urban sites, its concentration is higher in summer than winter for rural sites. This observation from our year-long measurements is consistent with 14 years of organic carbon (OC) data from the SouthEastern Aerosol Research and Characterization (SEARCH) network. The comparison between short-term measurements with advanced instruments and long-term measurements of basic air quality indicators not only tests the robustness of the short-term measurements, but also provides insights in interpreting long-term measurements. We find that OA factors resolved from PMF analysis on HR-ToF-AMS measurements have distinctly different diurnal variations. The compensation of OA factors with different diurnal trends is one possible reason for the repeatedly observed, relatively flat OA diurnal profile in the southeastern US. In addition, analysis of long-term measurements shows that the correlation between OC and sulfate is substantially ~~higher~~stronger in summer than winter. This seasonality could be partly due to the effects of sulfate on isoprene SOA formation as revealed by the short-term, intensive measurements.

1. Introduction

The southeastern US ~~has been~~is an ~~interesting~~intriguing region to study aerosol formation. Firstly, the fine particulate matter ($PM_{2.5}$) concentration is generally high and often exceeds the National Ambient Air Quality Standards (NAAQS) (Cohan et al., 2007; Blanchard et al., 2013). Secondly, the southeastern US is characterized by large emissions from both biogenic and anthropogenic sources, which makes it an ideal region to study the effects of interactions between biogenic/anthropogenic ~~interactions~~emissions on organic aerosol formation and air quality. Roughly, half of the land in the southeastern US is covered by forests, which emit large amounts of biogenic volatile organic compounds (VOCs) that are precursors for secondary organic aerosol (SOA) formation (Geron et al., 2000; Guenther et al., 2006). Based on radiocarbon analysis, Schichtel et al. (2008) showed that about 90% of total carbon is biogenic in a rural site in Tennessee. Similarly, Weber et al. (2007) found that 70-80% of the carbon in water-soluble organic carbon (WSOC, a surrogate for SOA) is of biogenic origin in Atlanta, GA. However, recent studies revealed that the formation of SOA from biogenic VOCs is largely controlled by anthropogenic emissions in the southeastern US (Weber et al., 2007; Xu et al., 2015). Thirdly, a wide range of air quality data has been routinely collected by the SEARCH (SouthEastern Aerosol Research and Characterization) network, including multiple rural and urban sites in the southeastern US from 1999 to 2013 (Edgerton et al., 2005; Hansen et al., 2003; Hidy et al., 2014). Combining short-term field campaigns and long-term measurements is useful because short-term field campaigns with state-of-the-art instruments can better characterize atmospheric processes and provide insights in interpreting the long-term observations. In turn, long-term measurements ~~with~~of basic ~~variables of~~ air quality parameters are helpful ~~to test~~when testing the robustness of short-term field campaign results (Hidy et al., 2014).

A number of field studies have been conducted to understand the sources of OA in the southeastern US. Lim and Turpin (2002) showed that ~50% of OC is secondary in urban Atlanta by using an EC tracer method. ~~Blanchard et al. (2008)~~Blanchard et al. (2008) applied three different empirical models and estimated that the fraction of secondary OC (SOC) in OC is ~20-60% in the southeastern US, which ~~is~~was higher ~~in~~at rural sites ~~and~~ compared to urban sites and higher in summer compared to ~~urban sites and~~ winter~~, respectively~~. The authors also showed that the estimated SOC/OC ratio highly depends on the estimation methods. By using WSOC as a surrogate for SOC, Weber et al. (2007) showed that SOC accounts for roughly 75% of OC in Yorkville, a rural site in GA, while the contribution of SOC to OC decreases to about 65% in Georgia Institute of Technology, an urban site. However, these studies were based on bulk properties, such as OC and WSOC, which makes it challenging for OC source apportionment beyond separating it into primary and secondary OC. Attempts have been made to apportion OC into different sources based on molecular makers. For example, by using~~ a~~ molecular maker-based chemical mass balance modeling (CMB-MM), Zheng et al. (2006) attributed OC into various primary emission sources such as wood combustion and gasoline engine exhaust. However, limited by the number of molecular markers included in the model, the CMB-MM method is insufficient to resolve SOC and often results in high percentages of unexplained OC (Zheng et al., 2002). Also, filter samples collected on a daily basis ~~were~~have been used in most previous studies, which ~~limit~~limits the temporal resolution and could introduce uncertainty due to filter sampling artifacts. The Aerodyne Aerosol Mass Spectrometer (AMS) has been widely used to characterize the chemical composition of submicron non-refractory species with high temporal resolution (Canagaratna et al., 2007; Jayne et al., 2000). Budisulistiorini et al. (2013) deployed an Aerosol Chemical Speciation Monitor (ACSM) (Ng et al., 2011) at the SEARCH Jefferson Street site in downtown Atlanta, GA. Various OA sources were identified by factor analysis in Budisulistiorini et al. (2013), including one source related to isoprene oxidation~~,~~ ~~indicating the versatility of PMF analysis in OA source apportionment.~~. However, due to the lower resolving power of ACSM, PMF analysis on ACSM data ~~might~~can have difficulty in separating different primary sources such as cooking and vehicle emission, which have similar mass ~~spectrum~~spectra (Crippa et al., 2014; Mohr et al., 2009). In addition, measurements at both rural and urban sites are needed in order to investigate the spatial distribution of aerosol and various OA subtypes.

Organic nitrates are important atmospheric species~~ in the atmosphere~~ as their fate could affect the nitrogen cycle and ozone production (Perring et al., 2013; Mao et al., 2012). Organic nitrates, which are primarily formed from VOCs oxidation by nitrate radicals, or by ozone and hydroxyl radical in the presence of NO_x, have been shown to be an important component of organic aerosol. For example, Rollins et al. (2012) observed that organic nitrates contribute about 27-40% ~~of~~to the OA growth at night in Bakersfield, CA, by using ~~the~~a Thermal-Dissociation Laser-Induced-Fluorescence technique (TD-LIF) (Day et al., 2002). Multiple approaches have also been proposed to estimate organic nitrates from indirect measurements. For example, Farmer et al. (2010) proposed that the concentration of the nitrate functionality (i.e., $-ONO_2$) in organic nitrates could be estimated based on the nitrate functionality fragmentation pattern in the AMS, or the differences between AMS and ion-chromatography (IC) measurements.

In this study, we performed measurements by a suite of instrumentation in multiple sites in the greater Atlanta, GA, area,~~ GA~~ and Centerville, AL, with a focus on a high-resolution time-of-flight aerosol mass spectrometer (HR-ToF-AMS). Positive matrix factorization analysis is performed on HR-ToF-AMS data to identify distinct OA sources. The contribution of organic nitrates to total OA is estimated by different methods based on HR-ToF-AMS measurements. Measurements were performed in both rural and urban sites to investigate the spatial distribution of aerosol in the southeastern US. In addition, measurements spanning over a year allow us to evaluate the seasonal variation of aerosol composition. ~~Our~~These results are ~~not only~~ supported by ~~the available~~ long-term measurements from the SEARCH network~~, but also~~ and provide further insights into interpreting historic measurements.

2. Method

Measurements were conducted at the following sites as part of two field campaigns:

2.1 Southern Oxidant and Aerosol Study (SOAS)

The Southern Oxidant and Aerosol Study (SOAS, http://soas2013.rutgers.edu/) is a collaborative field campaign that took place from 1 June ~~1st~~ to 15 July ~~15th,~~ 2013. The sampling site (32.94˚N, 87.18˚W) is a SEARCH network site near Centreville, in rural Alabama, as shown in Fig. 1. The site is located in a forested area away from large urban cities (55km SE of Tuscaloosa and 84 km SW of Birmingham, AL). Detailed meteorological conditions of the sampling site can be found in Hidy et al. (2014). In brief, the sampling period was characterized by high relative humidity (>50% all the time), warm temperatures (daily maximum 28.6 °C at 15:00 local time), and light winds (Xu et al., 2015).

2.2 Southeastern Center ~~of~~for Air Pollution and Epidemiology study (SCAPE)

This extensive field study was part of the Southeastern Center for Air Pollution and Epidemiology (SCAPE, http://scape.gatech.edu/), which is an EPA-funded joint research center between Georgia Tech and Emory University, focusing on the study of air quality and the health effects of air pollutants (Verma et al., 2014; Winquist et al., 2014; Russell et al., 2014). Four sampling sites in both rural and urban areas are selected, as shown in Fig. 1. Detailed description of each sampling site can be found in Verma et al. (2014) and Hansen et al. (2003). Briefly,

- Roadside site (RS site) is on the Georgia Tech campus and adjacent (within 5 m) to the Interstate 75/85 (8 ~~lines~~lanes each direction). According to Georgia Department of Transportation, about 95% of the traffic fleet on the Interstate 75/85 is light-duty gasoline vehicles.

- Georgia Tech site (GT site) is also on the Georgia Tech campus, but 840 m away from the roadside site. The GT site is located on the top floor of the Ford Environmental Science & Technology Building, which is 30-40 m above ground.
- Jefferson Street site (JST site) is a central SEARCH network site, which is about 2 km west of the Georgia Tech site. This site is situated in Atlanta's urban area and surrounded by a mixed residential and commercial neighborhood and is considered representative of ~~the ~~urban Atlanta.
- Yorkville site (YRK site) is the SEARCH rural pair to the JST site~~ and~~ located approximately 80 km northwest of ~~the ~~JST~~ site~~. This site is situated in a mixed forested – agricultural area and immediately surrounded by pastures for cattle grazing.

We outfitted a trailer with a large suite of instrumentation (described in section 2.3) and conducted measurements from May 2012 to February 2013, with roughly one month at each site, and repeated it in different seasons. The sampling periods are listed in Table 1.

While the trailer was rotated between multiple sites, we also deployed an Aerosol Chemical Speciation Monitor (ACSM, described in section 2.3.2) (Ng et al., 2011) at the Georgia Tech site from May 2012 to February 2013. The paired and simultaneous measurements using an ACSM at the Georgia Tech site and a High Resolution Time-of-Flight Aerosol Mass Spectrometer (HR-ToF-AMS, described in section 2.3.1) rotating among four different sites allow for ~~the investigation of the~~investigating spatial ~~distribution~~distributions of aerosol loading and composition in the greater Atlanta area. It is noted that from 20 July ~~20th ~~to 4 September~~ 4th,~~ 2012, both the HR-ToF-AMS and the ACSM were deployed at the Georgia Tech site for instrument inter-comparison.

2.3 Instrumentation

2.3.1 High Resolution Time-of-Flight Aerosol Mass Spectrometer (HR-ToF-AMS)

An Aerodyne High-Resolution Time-of-Flight Aerosol Mass Spectrometer (HR-ToF-AMS) was rotated among different sites in this study to characterize the composition of ambient submicron non-refractory particulate matter (NR-PM_1). A detailed description of the HR-ToF-AMS can be found in the literature (Canagaratna et al., 2007; DeCarlo et al., 2006). In brief, the HR-ToF-AMS focuses ambient particles with vacuum aerodynamic diameter smaller than 1μm into a narrow beam ~~by using~~via an aerodynamic lens. The submicron particles are then impacted on a hot tungsten surface (~600°C), where non-refractory species are flash ~~evaporated~~vaporized. The resultant vapors are ionized using 70eV electron impact ionization and analyzed by a time-of-flight mass spectrometer. During sampling, a PM_1 cyclone was used to remove coarse particles. A nafion-dryer was placed upstream of the HR-ToF-AMS to dry the particles (relative humidity <20%) in order to eliminate the potential influence of relative humidity on particle collection efficiency (CE) at the vaporizer (Matthew et al., 2008). Gas-phase interference was eliminated by subtracting the signals when the HR-ToF-AMS sampled through a HEPA filter, which was performed regularly on a daily basis at different times of the day. Ionization efficiency (IE) ~~calibration by using~~calibrations were performed with 300nm ammonium nitrate particles~~ was performed ,~~, on a weekly basis~~ and the~~. The composition-dependent CE was applied to the data based on Middlebrook et al. (2012). We operated the HR-ToF-AMS in ~~both V mode and W mode~~two ion optical modes (V and W) with different sensitivity and spectra resolution, but only V mode data are reported in this study considering the low intensity of W mode data. The average sampling time was set at two minutes. The data analysis was performed using the standard AMS analysis toolkits SQUIRREL v1.53 and PIKA v1.12 in Igor Pro 6.34 (WaveMetrics Inc.). Default RIE values were used for the HR-ToF-AMS data. Elemental ratios, such as atomic oxygen-to-carbon ratio (O:C), hydrogen-to-carbon ratio (H:C), and organic mass-to-organic carbon ratio (OM:OC), are determined by following the latest procedures ~~as~~ recommended by Canagaratna et al. (2015). Canagaratna et al. (2015) improved the estimation from Aiken et al. (2008), which has been widely used in the literature to estimate elemental ratios, by including composition-dependent correction factors. Caution is required when comparing the elemental ratios in this study with values reported in the literature, which typically used the Aiken estimation. Nitrate signals (NO^+ and NO_2^+) and sulfate signals (SO^+, SO_2^+, etc) are not included in the elemental ~~ratios calculation.~~ratio calculations. Oxidation state (OS) is calculated as 2*O:C – H:C (Kroll et al., 2011).

2.3.2 Aerosol Chemical Speciation Monitor (ACSM)

An Aerosol Chemical Speciation Monitor (ACSM) was stationary at the Georgia Tech site from 10 May ~~10th,~~ 2012 to 28 February ~~28th~~ 2013. Similar to the HR-ToF-AMS, the ACSM also provides continuous, quantitative measurements of $NR\text{-}PM_1$ (Ng et al., 2011). The mass resolving power of ACSM (~200) is lower than that of the HR-ToF-AMS (~2000 in V mode) due to ~~the~~ use of a low cost residual gas analyzer (RGA) quadrupole mass spectrometer in ACSM (Ng et al., 2011). In addition, the time resolution of ACSM (~30min) is longer than that of HR-ToF-AMS (~2min). The response factor (RF) of the ACSM was also determined by using 300nm ammonium nitrate particles (Ng et al., 2011). The relative ionization efficiency (RIE) values used for organics, nitrate, and chloride are 1.4, 1.1, and 1.3, respectively. RIE values of 4.18 and 0.59 were used for ammonium and sulfate, which were determined from IE calibrations by using ammonium nitrate and ammonium sulfate particles.

2.3.3 Co-located Instruments

In addition to the HR-ToF-AMS, we deployed various instruments in the trailer while performing measurements at multiple sites (Verma et al., 2014). Instruments of interest to this study ~~includes~~include a PILS-LWCC-TOC system (Particle Into Liquid Sampler - Liquid Waveguide Capillary Cell - Total Organic Carbon analyzer), ~~which was deployed to measure~~a seven-wavelength Aethalometer and a multi-angle absorption photometer (MAAP). The PILS-LWCC-TOC system continuously (i.e., 15min resolution) measured the light absorption spectra of water-soluble organic components. ~~Detailed~~The detailed working principle of the PILS-LWCC-TOC system can be found in Hecobian et al. (2010). ~~The average light absorption between 360 to 370 nm is used as a measure of brown carbon.~~In brief, water-soluble species are first dissolved in water in a PILS (Weber et al., 2001). The liquid sample from the PILS is then injected into a Liquid Waveguide Capillary Cell, where the absorption spectra are collected over wavelengths of 200 to 800nm. The average light absorption between 360 to 370 nm is used as a measure of brown carbon light absorption. Black carbon concentration was measured by either a seven-wavelength Aethalometer or a multi-angle absorption photometer (MAAP). For the Aethalometer, ~~the~~ measurements ~~under seven wavelengths (i.e., 370, 450, 571, 590, 660, 880, and 950nm)~~at 660nm were ~~averaged~~chosen to represent the black carbon concentration, because 660nm is closest to the wavelength utilized by the MAAP. The measured data were corrected for loading effects (Virkkula et al., 2007). The temporal resolutions are 2 min and 1 min for Aethalometer and MAAP, respectively.

At the Jefferson Street ~~site~~ (JST) and Yorkville ~~site~~ (YRK~~),~~) sites, a suite of instruments was operated by the SEARCH Network. Detailed ~~description~~descriptions about the collocated instruments can be found in Hansen et al. (2003) and Edgerton et al. (2005). In brief, O_3 concentration was measured by a UV-absorption analyzer~~.~~ with a temporal resolution of 1min. NO and NO_x were measured by a chemilumnescence analyzer~~,~~ (1min temporal resolution), where the NO_2 concentration was calculated by subtracting NO from the total NO_x. $PM_{2.5}$ sulfate and OC were continuously measured by a Fe reduction/UV-fluorescence analyzer and an oxidative combustion (R&P 5400) analyzer, respectively. The temporal resolution is 5min and 60min for $PM_{2.5}$ sulfate and OC, respectively. Meteorological conditions, such as temperature, relative humidity (RH), solar radiation, and wind speed were also recorded.

2.4 Positive Matrix Factorization (PMF) Analysis

Positive Matrix Factorization (PMF) is a mathematical technique to solve bilinear unmixing problems (Paatero, 1997; Paatero and Tapper, 1994). PMF analysis has been widely applied in the aerosol community for source apportionment (Ulbrich et al., 2009; Jimenez et al., 2009; Zhang et al., 2010; Lanz et al., 2007; Ng et al., 2010; Beddows et al., 2015; Jaeckels et al., 2007; Visser et al., 2015). For the data measured by AMS, PMF analysis represents the observed data matrix as a linear combination of various factors with constant mass ~~spectrum~~spectra but varying concentrations across the dataset (Ulbrich et al., 2009; Zhang et al., 2011). To determine the sources of organic aerosol, PMF analysis was performed on the high-resolution organic mass spectra (*m/z* 12 - 200) obtained by the HR-ToF-AMS for each sampling dataset. We generated the organic data matrix and error matrix from PIKA v1.12 and pretreated the error matrix by using PMF Evaluation Toolkit (PET) software ~~and~~ following the procedure described in Ulbrich et al. (2009). Variables (i.e., *m/z*'s) with a signal-to-noise ~~smaller~~ratio less than 0.2 are removed and ~~*m/z*'s~~variables with a signal-to-noise ratio ranging between 0.2 and 2 are downweighted by a factor of 2. We downweighted the errors of O^+, HO^+, H_2O^+, and CO^+, which are related to CO_2^+ ~~organic ions~~signal, to avoid excessive weighting of CO_2^+. In addition, for four datasets (JST_May, CTR_June, YRK_July, and GT_Aug), the error of CHO^+ is downweighted by a factor of 4. This is because that PIKA v1.12 appears to underestimate CHO^+ error, ~~which is~~ possibly caused by ~~that~~ the overlap of the CHO^+ (*m/z* 29.0027) ion with its adjacent N_2 isotope ion (j15NN, *m/z* 29.0032). For the other three datasets (JST_Nov, YRK_Dec, and RS_Jan), CHO^+ is not included in the PMF analysis due to its ~~occasionally~~occasional negative ~~signals~~signal, which is likely caused by a low CHO^+ signal in winter. At times, the CHO^+

concentration is near the detection limit, so ~~that~~ a shift in threshold might cause the CHO^+ signal to be treated as noise. PMF solutions were carefully evaluated according to the procedure outlined in Zhang et al. (2011). For each dataset, the optimal solution was determined after examining the residuals of PMF fits, interpretability of factor's diurnal trend, factor correlation with external tracers, and characteristic ~~signature in~~ signatures of factor mass spectrum. The rotational ambiguity of solutions ~~were~~was examined by changing the parameter FPEAK and the robustness of solutions were evaluated by starting PMF with different initial conditions (parameter SEED). The key diagnostic plots for all datasets are shown in Fig. S1. An FPEAK value of 0 is used for all datasets in our PMF analysis on organic mass spectra, because the use of FPEAK values that are different from 0 do not improve the correlations between PMF factors with external tracers.

2.5 Estimation of organic nitrates contribution to ambient OA

As direct measurements of organic nitrates are not available, we estimate the concentration of particle-phase organic nitrates at each site based on HR-ToF-AMS measurements in this study. It is important to note that total nitrates measured by the HR-ToF-AMS (denoted as $NO_{3,meas}$) is the nitrate functionality ($-ONO_2$~~)~~), which could arise from both inorganic and organic nitrates. Here, we apply two independent methods in separating the measured total nitrates into nitrate functionality from inorganic and organic nitrates. In the following discussion, we use the subscripts $_{meas,\ inorg,}$ and $_{org}$ to denote nitrate functionality ($-ONO_2$) or fragments (NO^+ and NO_2^+) from total nitrates (measured), inorganic nitrates (calculated), and organic nitrates (calculated), respectively.

The first method is based on the NO^+/NO_2^+ ratio (denoted as NO_x^+ ratio method for discussions hereafter) in the AMS mass spectra (Farmer et al., 2010). Due to the extensive fragmentation caused by 70eV electron ionization in the HR-ToF-AMS, the nitrate functionality ($-ONO_2$) fragments to produce NO^+ and NO_2^+ ions. Previous laboratory studies have shown that the NO^+/NO_2^+ ratio in the aerosol mass spectrum is substantially higher for organic nitrates than ammonium nitrate (AN) (Bruns et al., 2010; Fry et al., 2009; Sato et al., 2010; Farmer et al., 2010; Boyd et al., 2015), which is the major source of PM_1 inorganic nitrates in the southeast US that can be detected by the AMS (Guo et al., ~~2014~~2015; Allan et al., 2004). For example, while the NO^+/NO_2^+ ratio is about 2.4 for ammonium nitrate, the ratio ranges from 5 to 10 for SOA derived from isoprene+$NO_3^{\bullet}$ and β-pinene+$NO_3^{\bullet}$ reactions, respectively (Bruns et al., 2010; Boyd et al., 2015). In addition to organic nitrates produced from biogenic VOC oxidation, ~~Sato et al. (2010)~~Sato et al. (2010) showed that the NO_x^+ ratio of organic nitrates from the photooxidation of aromatic hydrocarbons is also clearly higher than that of ammonium nitrate (3.8-5.8 vs 1.1-2.8). Based on the differences in NO_x^+ ratio between organic and inorganic nitrates, Farmer et al. (2010) proposed that the concentrations of NO_{org} and $NO_{2,org}$ can be estimated from NO_{meas} and $NO_{2,meas}$ by ~~Eqn~~Eq. 1 and 2.

~~$NO_{2,org}=\frac{NO_{2,meas}\times(R_{meas}-R_{AN})}{R_{ON}-R_{AN}}$ Eqn 1~~

~~$NO_{org}=R_{ON}\times NO_{2,org}$ Eqn 2~~

$$NO_{2,org}=\frac{NO_{2,meas}\times(R_{meas}-R_{AN})}{R_{ON}-R_{AN}} \qquad \text{Eq. 1}$$

$$NO_{org}=R_{ON}\times NO_{2,org} \qquad \text{Eq. 2}$$

R_{meas} is the NO_x^+ ratio from observation. R_{AN} is the NO_x^+ ratio for pure ammonium nitrate (AN), which has been reported to depend on instrument performance and vary between different instruments (Farmer et al., 2010; Rollins et al., 2010). In this study, we determine the R_{AN} of each dataset from Ionization Efficiency (IE) calibrations using 300nm ammonium nitrate particles. We find that R_{AN} varies between 1.73 and 2.93 (Table 2), which is within the range (1.1 – 3.5) reported in the literature (Sato et al., 2010; Farmer et al., 2010; Sun et al., 2012b; Fry et al., 2013). R_{ON} is the NO_x^+ ratio for organic nitrates. Similar to R_{AN}, R_{ON} also varies between instruments (Boyd et al., 2015; Bruns et al., 2010; Fry et al., 2009). Thus, the R_{ON} values reported in the literature cannot be directly applied in our datasets. In order to circumvent this issue, Fry et al. (2013) assumed that the R_{ON}/R_{AN} value is instrument independent. The authors further obtained R_{ON} by multiplying R_{AN} determined from in-field IE calibrations with R_{ON}/R_{AN} determined from six organic nitrate standards (average value = 2.25) . However, the reported R_{ON}/R_{AN} values in the literature vary for different organic nitrates. For example, while the average R_{ON}/R_{AN} value is 2.25 for the organic nitrate standards in Farmer et al. (2010), the R_{ON}/R_{AN} ranges from 3.70 to 4.17 for organic nitrates produced from β-pinene oxidation by nitrate radicals (Boyd et al., 2015; Bruns et al., 2010; Fry et al., 2009). Considering the large variations in R_{ON}/R_{AN} values and unknown contributions from different organic nitrates, we apply the NO_x^+ ratio method to obtain an estimation range by using extreme R_{ON} values. We select organic nitrates formed from isoprene and ~~monoterpene oxidations~~β-pinene oxidation as representative because of their large abundance in the southeastern US, potential to produce organic nitrates, and because that they cover a wide range of R_{ON}/R_{AN} values (i.e., 2.08 for isoprene and 3.70-4.17 for β-pinene) (Boyd et al., 2015; Bruns et al., 2010; Fry et al., 2009). ~~Though the photooxidation of aromatic VOCs could also produce organic nitrates, their R_{ON}/R_{AN} ratio is close to that of isoprene organic nitrates~~ The organic nitrates derived from other biogenic VOCs (i.e., α-pinene, limonene, 3-carene, etc) are not considered due to either their lower ambient concentrations in the SE US or lower organic nitrate yields compared to isoprene and β-pinene (Xu et al., 2015). Though the photooxidation of aromatic VOCs could also produce organic nitrates, their R_{ON}/R_{AN} ratio is close to that of isoprene organic nitrates ~~(Sato et al., 2010)~~(Sato et al., 2010). Multiplying the average R_{AN} (i.e., 2.28±0.40) of all datasets in this study by the average R_{ON}/R_{AN} ratio of isoprene (i.e., 2.08) and β-pinene organic nitrates (i.e., 3.99±0.25) in the literature (Boyd et al., 2015; Bruns et al., 2010; Fry et al., 2009), within one standard deviation we selected 5 (i.e., 4.74±0.83) and 10 (i.e., 9.10±1.69) as the lower and upper values of R_{ON}. It is important to note that R_{ON} values of 5 and 10 likely correspond to upper and lower bounds of the $NO_{3,org}$ concentrations estimated by the NO_x^+ ratio method. The assumption that R_{ON}/R_{AN} is instrument independent warrants further study.

The second method is based on PMF analysis (denoted as PMF method). In addition to PMF analysis on organic mass spectra (denoted as PMF_{org}), we have also performed PMF analysis on organic mass spectra together with NO^+ and NO_2^+ ions (denoted as $PMF_{org+NO3}$). Such analysis could provide useful insights regarding the relative contributions of organic and inorganic nitrates. For instance, Sun et al. (2012b) and Hao et al. (2014) performed PMF analysis on merged mass spectra with both organic and inorganic signals from HR-ToF-AMS measurements. The authors showed that the NO^+ and NO_2^+ fragments are distributed among a nitrate inorganic aerosol (NIA) factor and other organic aerosol factors.

In this study, the selection of optimal solutions for PMF analysis on the merged mass spectra (i.e~~.~~., $PMF_{org+NO3}$) is discussed in detail in the Supplement. In brief, in addition to examining the typical diagnostic plots (Fig. S3), the optimal solutions are selected by comparing the time series (Fig. S5), mass spectrum (Fig. S5), and mass concentration (Fig. S6) with results from PMF_{org}. After determining the optimal solution of $PMF_{org+NO3}$, the concentrations of “nitrate functionality from organic nitrates” (i.e., $NO_{3,org}$) are calculated by summing up the nitrate signals (i.e., NO^+ and NO_2^+) from all OA factors by the following equations.

~~$[NO^+_{org}]=\sum([\text{OA factor}]_i \times f\_NO_i)$ Eqn 3~~

~~$[NO^+_{2,org}]=\sum([\text{OA factor}]_i \times f\_NO_{2,i})$ Eqn 4~~

$$[NO^+_{org}]=\sum([\text{OA factor}]_i \times f\_NO_i) \quad \text{Eq. 3}$$

$$[NO^+_{2,org}]=\sum([\text{OA factor}]_i \times f\_NO_{2,i}) \quad \text{Eq. 4}$$

where $[\text{OA factor}]_i$ is the mass concentration of the *i*th OA factor, f_NO_i and $f\_NO_{2,i}$ are the mass fraction of NO^+ and NO_2^+, respectively, in the *i*th OA factor. For both the NO_x^+ ratio method and PMF method, we calculate the concentration of $NO_{3,inorg}$ (i.e., nitrate functionality from inorganic nitrates) by subtracting $NO_{3,org}$ (i.e., nitrate functionality from organic nitrates) from $NO_{3,meas}$ (i.e., total measured nitrates).

3. Results

Table 1 lists the meteorology parameters (temperature, relative humidity, and wind speed), gas-phase concentrations of NO, NO_2, and O_3, and aerosol ~~compositions~~composition of the seven datasets reported in this study. The average RH is above 60% for all the datasets, with little seasonal variation, which is consistent with previous observations (Ford and Heald, 2013). The high RH in the southeastern US has direct impacts on particle water content and particle acidity. Recently, ~~Guo et al. (2014)~~Guo et al. (2015) showed that particle water and acidity are mainly driven by the variability of RH, although particle composition also plays a role. The average wind speed is relatively constant (1.3–3.4 m s^{-1}) throughout the year at all sites. NO_x (NO and NO_2) and black carbon (BC), which are tracers for anthropogenic emissions, are lower in the rural Yorkville (YRK) site than the urban Jefferson Street (JST) site. In YRK, the NO_x level is low (i.e., average concentration < 0.3 ppb) in all seasons. In contrast, at the urban JST site, the NO_x level is elevated in winter compared to summer, indicating more anthropogenic emissions, or less dispersion, in winter at urban sites.

Fig. 2 shows the composition of non-refractory submicron particulate matter (NR-PM$_1$) ~~of~~for all datasets. Organics are the dominant components, which account for more than 50% of NR-PM$_1$ mass at all sites throughout the year. Although dominant, the concentration of organic aerosol varies substantially among sites and seasons. The seasonal variation of OA mass concentration is small for the urban JST site (9.1 µg m^{-3} in May vs 7.9 µg m^{-3} in November); however, the OA concentration is about 4 times higher in summer than winter for the rural YRK site (11.2 µg m^{-3} in July vs 3.2 µg m^{-3} in December). The difference in seasonality of OA between urban and rural sites is likely due to the varying strength of different OA sources, which will be discussed in detail in section 4.4.2. In terms of diurnal variation, the OA ~~reaches daily maximum~~diurnal trend is relatively flat in ~~the early morning~~summer and ~~evening for most datasets (except YRK_July)~~peaks at night in winter (Fig. 3). ~~This~~The diurnal variation ~~in~~of OA is ~~likely caused~~largely influenced by the changes in planetary boundary layer height and changes in contributions to total OA from various sources, which will be discussed in detail in section 4.4.1. The campaign-average mass spectra of OA from all datasets are similar, as shown in Fig. S7. In order to assess the degree of oxidation of OA, average f_{44} (the ratio of m/z 44 to total OA signal) and f_{43} (the ratio of m/z 43 to total OA signal) of each dataset is plotted in the triangular space as defined by Ng et al. (2010) in Fig. 4. The OA from all datasets locate in the middle part of the triangle, indicating they are moderately oxidized and have a similar degree of oxidation.

Following organics, sulfate (SO_4) has the second largest contribution to total NR-PM$_1$ mass at all sites~~.~~ (Fig. 2). Average SO_4 concentration varies between 3.0 to 4.0 µg m^{-3} at different sites in summer and decreases to 1.4~1.7 µg m^{-3} in winter. The SO_4 concentration at most sites (except JST_Nov and RS_Jan) reaches a daily maximum in the afternoon (Fig. 3), which is likely caused by the strong photooxidation of SO_2 or sulfate entrainment from aloft when the boundary layer height is the highest in the afternoon (Weber, 2003). In contrast to SO_4, where the concentration is higher in summer, total nitrate concentration is elevated in winter. While the average concentration of total nitrates is 0.3-0.4 µg m^{-3} (2-3% of total NR-PM$_1$, Fig. 2) in summer, it almost triples in winter (0.8-1.4 µg m^{-3}) with elevated mass fraction in total NR-

PM_1 (10-16%). The reason for the seasonal variation of the total nitrates will be discussed in section 4.2.2.

4. Discussion

4.1 OA source apportionment

In this section, we focus on the OA source apportionment based on results from PMF analysis on organic mass spectra only (i.e., PMF_{org}). We resolved various factors, including hydrocarbon-like OA (HOA), cooking OA (COA), biomass burning OA (BBOA), isoprene-derived OA (Isoprene-OA), more-oxidized oxygenated OA (MO-OOA), and less-oxidized oxygenated OA (LO-OOA) at multiple sites in different seasons.

Based on the inferred volatility from O:C ratios, the two oxygenated OA factors (i.e., MO-OOA and LO-OOA) are typically named as low-volatility OOA (higher O:C and lower volatility) and semi-volatile OOA (lower O:C and higher volatility) (Ng et al., 2010; Jimenez et al., 2009). However, recent studies showed that O:C ratios are not always well-correlated with aerosol volatility (Hildebrandt et al., 2010; Xu et al., 2014). Thus, in this study, we use the terms “more-oxidized OOA” (MO-OOA, O:C ranges between 0.66 and 1.05, with an average of 0.87) and “less-oxidized OOA” (LO-OOA, O:C ranges between 0.44 and 0.62, with an average of 0.54) (Fig. S10). This terminology has been used in several previous studies (Setyan et al., 2012; Xu et al., 2015).

4.1.1 HOA

Hydrocarbon-like organic aerosol (HOA) is a surrogate of primary OA from vehicle emissions. Among all the OA factors, HOA is the least oxidized with oxidation state (OS) ranging from -1.86 to -1.39 (Fig. 4). The mass spectrum of HOA is characterized by hydrocarbon-like ions (C_xH_y family) as shown in Fig. S2, which is similar to the mass spectrum of freshly emitted traffic aerosol (Zhang et al., 2005). HOA is only identified ~~in~~at urban sites with evident morning and evening rush hour peaks (Fig. ~~6~~5). HOA also shows good correlation with black carbon (R ranges from 0.70 to 0.83) (Fig. S2), further supporting the primary nature of this OA subtype.

For the sites where HOA is identified, HOA accounts for 9-15% (daily average) of total OA (Fig. ~~5~~6). Even for the roadside (RS) site, which is within 5 meter ~~to~~of the Interstate 75/85, HOA only contributes 15% of total OA. Low contributions of HOA to total OA near highways have been observed in several prior studies (Sun et al., 2012a; DeWitt et al., 2014). For example, DeWitt et al. (2014) found that HOA only comprised 20% of total OA based on HR-ToF-AMS measurements in a high diesel environment (near a highway) in Paris, France. The small contribution of HOA could arise from the types of vehicles on road, the rapid dilution of vehicle emissions, or the high level of regional background OA. Firstly, roughly 95% of the traffic fleet on I75/85 is light-duty gasoline vehicles, according to Georgia Department of Transportation. Unlike diesel vehicles which have large emissions of POA and BC, gasoline vehicles have a larger emission of VOCs (e.g., toluene and benzene) (Platt et al., 2013). Secondly, in addition to vehicle type, the evaporation of POA emitted from vehicles would further decrease its mass concentration. Robinson et al. (2007) showed that POA from vehicle ~~emission~~emissions is indeed semi-volatile, which would evaporate substantially upon dilution from tailpipe to ambient conditions (a dilution ratio of 10^3 to 10^4). Thirdly, HOA tends to contribute a small fraction of OA because of the high level of regional background OA in the greater Atlanta area. For example, OOA factors (i.e., LO-OOA and MO-OOA) compromise 47-79% of OA as shown in Fig. ~~5~~6. The effect of wind direction on HOA concentration is expected to be small considering the close proximity of the roadside sampling site to the highway.

4.1.2 COA

The mass spectrum of cooking organic aerosol (COA) is characterized by prominent ~~signal~~signals at ~~ion~~ions $C_3H_5^+$ (*m/z* 41) and $C_4H_7^+$ (*m/z* 55) (Fig. S2), which could arise from the heating of seed oil (Allan et al., 2010). Another feature of COA is its ~~clear and~~ unique diurnal trend~~, which~~. For three out of four datasets (except JST_Nov) where a COA factor is identified, the COA factor exhibits a small peak at lunch time and a large peak at dinner time (Fig. ~~6~~5). The COA factor is identified in urban sites (JST~~ site~~, GT~~ site~~, and RS~~ site~~) throughout the year, with the average mass fraction varying from 12-20%. A prior study by Zheng et al. (2002) estimated that meat cooking accounts for 5-12% of $PM_{2.5}$ organic carbon in the southeastern US by using a chemical mass balance receptor model. The range reported by Zheng et al. (2002) is similar to our study, considering the differences in sampling periods, particle size range, and estimation method. The COA factor has also been detected in many megacities around the world (Huang et al., 2010; Allan et al., 2010; Slowik et al., 2010; Mohr et al., 2012; Crippa et al., 2013), indicating cooking is an important OA source in megacities.

We note that the COA factor was not resolved in Budisulistiorini et al. (2013), in which the authors performed PMF analysis on the data collected by an Aerosol Chemical Speciation Monitor (ACSM) at the JST site in 2011 summer and fall. The lack of a COA factor in the analysis by Budisulistiorini et al. (2013) could be a result of the lower resolution (unit mass resolution) of the ACSM compared to HR-ToF-AMS~~ (Ng et al., 2011).~~. Previous studies have suggested that COA is not easily differentiated from HOA due to the similarity of their mass spectra in unit mass resolution data (Crippa et al., 2014; Mohr et al., 2009).

4.1.3 Isoprene-OA

The Isoprene-OA factor is characterized by prominent signals at ~~ion~~ $C_4H_5^+$ (*m/z* 53) and $C_5H_6O^+$ (*m/z* 82) in its mass spectrum (Fig. S2), which resembles that of isoprene SOA formed via isoprene epoxydiols (i.e., IEPOX) uptake in the presence of hydrated sulfate in laboratory experiments (Lin et al., 2012; Budisulistiorini et al., 2013; Nguyen et al., 2014; Liu et al., 2015). For our datasets, Isoprene-OA is only identified in warmer months (May - August) and accounts for 18-36% of total OA (Fig. ~~5~~6). The seasonal variation of Isoprene-OA factor is consistent with that of isoprene emissions, which are high in summer and nearly zero in winter (Guenther et al., 2006). The identification of the Isoprene-OA factor ~~could be~~is further supported by its correlation with ~~methytetrols~~methyltetrols, which are products formed from isoprene oxidation and likely via IEPOX uptake. For the Centreville dataset where methyltetrols were continuously measured by a semi-volatile thermal desorption aerosol gas chromatograph (SV-TAG) (Isaacman et al., 2014), the correlation coefficient (Pearson's R) between the Isoprene-OA factor and methyltetrols is found to be 0.68 (Xu et al., 2015).

The f_{C5H6O+} (the ratio of $C_5H_6O^+$ to total signal~~ of~~) in isoprene-OA factor,~~ f_{C5H6O+},~~ which is used as a characteristic marker for SOA formed via IEPOX uptake in the literature, ranges from 0.9% - 2.3% in this study. This range is similar to the values from other ambient data (Budisulistiorini et al., 2013; Chen et al., 2014; Robinson et al., 2011a; Slowik et al., 2011), but lower than that from laboratory-generated fresh SOA from IEPOX uptake (3.6% from Liu et al.

(2015)). We note that the f_{C5H6O+} is higher at rural sites (1.9% for YRK_July and 2.3% for CTR_June) than urban sites (0.9% for JST_May and 1.4% for GT_Aug). Similarly, Liu et al. (2015) observed that the mass spectrum of laboratory-generated SOA from IEPOX uptake has a stronger correlation with that of Isoprene-OA factor from remote regions (Amazon and Borneo) than urban regions (Atlanta, US). The identification of an Isoprene-OA factor at urban sites in the current study has interesting implications. The compound IEPOX is thought to be an oxidation product of isoprene where the organic peroxy radicals react with hydroperoxy radicals (Paulot et al., 2009). In urban areas, one would expect the majority of organic peroxy radicals to react with NO_x, considering the relatively high NO_x level (~15.4 ppb for JST_May in Table 1). However, a recent laboratory study by Jacobs et al. (2014) found that the oxidation of isoprene-derived hydroxynitrates in the presence of NO_x could also produce IEPOX. Thus, Isoprene-OA observed in urban sites could be locally produced. Another possible source for Isoprene-OA at urban sites is advection from rural sites. This could explain the lower f_{C5H6O+} in the Isoprene-OA factor in urban sites, because the compounds which give rise to the $C_5H_6O^+$ signal can be further oxidized during transport. However, the lifetime of the Isoprene-OA factor and the changes in its mass spectral features with chemical aging are largely uncertain. The contribution of advection is probably small as it is unlikely that advection would result in a consistent diurnal profile of Isoprene-OA, which reaches a daily maximum in the afternoon observed not only in this study (Fig. ~~6~~5), but also in other regions, such as Amazon (Chen et al., 2014) and Borneo forest (Janssen et al., 2013; Robinson et al., 2011a). In addition, Robinson et al. (2011a) only observed the Isoprene-OA factor in data obtained from afternoon flights, but not in morning flights through airborne measurements in the Borneo forest, implying that the Isoprene-OA formation is rapid and local. Another possibility for the lower f_{C5H6O+} at the urban sites is that Isoprene-OA factor from the urban sites may contain isoprene SOA produced via other pathways, in addition to the IEPOX uptake pathway. Isoprene SOA formed via RO_2+NO pathway only has a negligible signal at $C_5H_6O^+$ (Kroll et al., 2006; Xu et al., 2014), so that the mixing of Isoprene SOA via different pathways may lower the f_{C5H6O+} in the Isoprene-OA factor. Moreover, seasonality may also have an influence on the lower f_{C5H6O+} at the urban sites since the sampling periods at the urban sites are May and August, when the isoprene concentration is relatively lower than that during the sampling periods at the rural sites (i.e., June and July).

For all the sites where an Isoprene-OA factor is resolved, the Isoprene-OA factor is found to be well-correlated with sulfate (R ranging from 0.73 to 0.88, Fig. S2). Xu et al. (2015) showed that the formation of isoprene-OA in the southeastern US is largely controlled by the abundance of sulfate, instead of the particle water content and/or particle acidity. While many prior laboratory studies show that particle acidity plays an important role in IEPOX uptake (Gaston et al., 2014; Surratt et al., 2007), results from ambient observations suggest that particle acidity is critical, but not the limiting factor in isoprene OA formation in the southeastern US, which is likely due to the consistently high particle acidity in the southeastern US (Guo et al., ~~2014~~2015; Xu et al., 2015)~~. Guo et al. (2014)~~. Guo et al. (2015) showed that the daily average particle pH throughout the southeastern US ranges between 1.1 and 1.3 in summer time. In the afternoon, when the isoprene mixing ratio is highest and photochemistry is strongest, the particle pH is even lower, ranging between 0 and 0.75~~.~~ due to lower particle water content. A recent chamber study (Gaston et al., 2014) showed that decreasing pH from 4.63 to 0.5 could greatly enhance IEPOX uptake by up to 150 times, but the enhancement is much weaker (a factor of 2) when furthering decreasing the pH from 0.5 to -0.27, the range of which is relevant to ambient particle pH (0-0.75) in the summer afternoon in the southeastern US ~~(Guo et al., 2014).~~(Guo et al., 2015). Similarly, another laboratory study also showed that the effect of particle acidity on IEPOX uptake is minor when the particle pH is low (Nguyen et al., 2014). By comparing the reactive uptake of IEPOX by using wet $(NH_4)_2SO_4$ seed (pH ~3.5) and wet $MgSO_4$+H_2SO_4 mixture seed (pH~0-1 with large uncertainty), Nguyen et al. (2014) found that the ~~reaction~~reactive partitioning coefficient of IEPOX increases by only 1.5 times as pH decreases from 3.5 to 1 ($H^+_{(aq)}$ increases by two or three orders of magnitude). Taken together, laboratory studies revealed that while increasing particle acidity could greatly enhance IEPOX uptake when pH is high, the sensitivity of IEPOX uptake to particle acidity is minor when pH is low. This is likely caused by isoprene OA formation from IEPOX uptake being limited by nucleophiles instead of catalyst activity under low pH (Eddingsaas et al., 2010; Piletic et al., 2013), although a low pH is needed to enhance these reactions. We also note that the co-variation between particle acidity and sulfate is not considered in previous laboratory studies (Gaston et al., 2014; Surratt et al., 2007), so the effect of particle acidity could possibly be confounded with the effect of sulfate and warrants further investigation.

4.1.4 BBOA

The mass spectrum of biomass burning organic aerosol (BBOA) is characterized by prominent signals at ion $C_2H_4O_2^+$ (m/z 60) and $C_3H_5O_2^+$ (m/z 73). These two ions are ~~known to be~~largely produced by levoglucosan, which is formed from the breakdown of cellulose in biomass burning ~~(Schneider et al., 2006). In the greater Atlanta area, the~~(Schneider et al., 2006). In addition, Heringa et al. (2011) showed that SOA produced during the aging of primary biomass burning emissions could contribute to these two ions. In this study, BBOA accounts for 9-22% of the OA (Fig. 6). The BBOA factor is mainly resolved in winter datasets, which is consistent with the EPA reported Georgia fire season in late winter (January – March) (Hidy et al., 2014) and the large enhancement in levoglucosan concentrations in winter compared to summer in Georgia (Zhang et al., 2010). BBOA is also identified in JST_May, which may arise from residential wood burning near JST site.

~~BBOA accounts for 9-22% of the OA at the sites where BBOA is identified (Fig. 5), which is~~The contribution of BBOA to total OA is slightly smaller than the values reported in other studies. Zhang et al. (2010) estimated that biomass burning accounted for 27% of $PM_{2.5}$ mass in winter over the southeastern US by performing PMF analysis on 10 species extracted from filter samples. The~~ cause for the~~ differences in biomass burning contribution to OA between this study and Zhang et al. (2010) ~~is unclear at this point, but~~are likely ~~a result of~~due to different estimation methods~~ and~~, sampling years~~.~~ (i.e., 2012-2013 vs. 2007), and sample size cut (i.e., PM_1 vs. $PM_{2.5}$).

It is important to note that the BBOA reported in this study likely only represents the relatively fresh OA from biomass burning. ~~Recent~~For example, laboratory studies revealed that the oxidation of levoglucosan is fast in both the gas ~~phase~~ and aqueous ~~phase~~phases (Zhao et al., 2014; May et al., 2012; Hennigan et al., 2011). The fast oxidation of levoglucosan can result in the rapid decay of signals at $C_2H_4O_2^+$ (m/z 60) and $C_3H_5O_2^+$ (m/z 73), causing the mass spectrum of BBOA to lose its characteristic signature~~ (Cubison et al., 2011).~~. In addition, laboratory studies by Hennigan et al. (2011) and Grieshop et al. (2009) showed that the mass spectrum of OA from biomass burning becomes increasingly similar to that of MO-OOA after ~~aging by photooxidation. Thus, the aged OA from biomass burning could be apportioned to the MO-OOA factor (Bougiatioti et al., 2014) and the mass fraction of the BBOA factor likely serves as a lower~~

~~bound of OA from biomass burning. The extent to which aged BBOA contributes to the MO-OOA factor warrants further investigation~~photochemical aging. Ambient measurements in the eastern Mediterranean by Bougiatioti et al. (2014) showed evidence that BBOA could be rapidly converted to OOA in less than a day. Thus, aged OA from biomass burning could be apportioned to the MO-OOA factor.

Recent studies have revealed that OA from biomass burning is an important source for brown carbon (Washenfelder et al., 2015; Andreae and Gelencsér, 2006; Zhang et al., 2010; Lack et al., 2013), which has important impacts on climate (Feng et al., 2013; Liu et al., 2014). For ~~the~~ four (out of five) datasets where BBOA is resolved by PMF analysis in this study, the Pearson's correlation coefficient (R) between BBOA and brown carbon is greater than 0.69, with the best correlation observed at JST_Nov (R=0.90) (Fig. 7). The correlation coefficient between BBOA and brown carbon is only 0.47 for YRK_Dec, which is likely caused by other brown carbon sources at the YRK site. This hypothesis ~~could be~~is supported by ~~the~~ summer measurements ~~in~~at YRK. In YRK_July, we observed a large abundance of brown carbon, which ~~reaches~~reached a daily maximum at around 2pm (Fig. S8); however, a BBOA factor is not resolved for YRK_July, indicating that brown carbon, in this case, could arise from sources other than biomass burning. Hecobian et al. (2010) suggested that SOA from aqueous phase reactions may be an important source for brown carbon in summer based on analysis ~~on~~of ~900 filters collected in 2007 in the southeastern US. A recent laboratory study showed that SOA from IEPOX reactive uptake could be light-absorbing and potentially an important source for brown carbon (Lin et al., 2014). However, Isoprene-OA factor, which is related to the IEPOX uptake pathway studied in Lin et al. (2014), only shows weak correlation (R ranges from 0.22 to 0.50) with brown carbon, as shown in Fig. S9. As suggested by Washenfelder et al. (2015), the difference between ambient observation and laboratory studies ~~might be due to~~is possibly caused by the fact that the IEPOX-derived absorbing chromophores do not dominate the Isoprene-OA mass. However, further studies are warranted to resolve this difference.

4.1.5 MO-OOA

Two oxygenated OA factors (MO-OOA and LO-OOA) with high, but differing O:C ratios, were identified in both rural and urban sites throughout the year. ~~Based on their inferred volatility from O:C ratios, OOA factors are typically named as low-volatility OOA (higher O:C~~

~~and lower volatility) and semi-volatile OOA (lower O:C and higher volatility) (Ng et al., 2010; Jimenez et al., 2009). However, recent studies showed that O:C ratios are not always well-correlated with aerosol volatility (Hildebrandt et al., 2010; Xu et al., 2014). Thus, in this study, we use the terms "more-oxidized OOA" (MO-OOA, O:C ranges between 0.66 and 1.05, with an average of 0.87) and "less-oxidized OOA" (LO-OOA, O:C ranges between 0.44 and 0.62, with an average of 0.54) (Fig. S10). This terminology has been used in several previous studies (Setyan et al., 2012; Xu et al., 2015).~~

MO-OOA contributes 24-49% of total OA mass (Fig. ~~5~~6). This factor has the highest O:C ratio, indicating that it is highly oxidized. It has been shown that as OA ages in the ~~atmospheric~~atmosphere, the mass spectra of OA from different sources become increasingly similar to each other and resemble that of MO-OOA (Jimenez et al., 2009; Ng et al., 2010). Thus, MO-OOA likely represents a highly aged organic aerosol from multiple sources, which causes the identification of specific sources of MO-OOA to be challenging. In addition to a high degree of oxidation, other notable features of MO-OOA are its diurnal profile and ubiquitous presence. As shown in Fig. ~~6~~5, in most datasets except RS_Jan, the diurnal profile of MO-OOA reaches a daily maximum in the afternoon. The daytime increase in MO-OOA would become more prominent after considering the dilution caused by boundary layer height expansion during the day. The similar diurnal profile has also been observed in a number of studies (Aiken et al., 2009; DeWitt et al., 2014; Hildebrandt et al., 2010; Huang et al., 2010; Setyan et al., 2012). Moreover, not only in this study in which MO-OOA is identified in different sites and seasons, MO-OOA (or the OOA factor in general) was also identified in datasets obtained at multiple sites around the world, pointing to the ubiquitous nature of this OA subtype (Jimenez et al., 2009; Ng et al., 2010).

Possible sources of this factor have been proposed in the literature. Firstly, a number of studies proposed that the source for MO-OOA is long-range transport (Li et al., 2015; Hayes et al., 2013; Robinson et al., 2011b; Raatikainen et al., 2010). This proposed mechanism could explain the high degree of oxidation of MO-OOA because the aerosol gets progressively more oxidized during advection, but it is unlikely to explain the well-defined diurnal profile of MO-OOA (peaks in the afternoon). Secondly, humic-like substances (HULIS) are proposed to be ~~a source of~~synonymous with MO-OOA because the mass spectrum and the degree of oxidation of

HULIS resembles those of MO-OOA (Ng et al., 2010; El Haddad et al., 2013). A recent study by Paglione et al. (2014) performed factor analysis on NMR measurements of water-soluble organic carbon extracted from filters collected in the Netherlands and resolved a factor with mass spectral features that are similar to HULIS. Further, the authors showed that this HUILS factor correlates with the most-oxidized OOA factor (O:C = 0.98) resolved from PMF analysis of their HR-ToF-AMS measurements, providing a linkage between HULIS and MO-OOA. Thirdly, the oxidation of vehicle emission or fuel combustion in general might also contribute to MO-OOA mass, but such contribution is uncertain. On one hand, multiple studies have shown that the photooxidation of gas-phase species from direct vehicle emissions or POA evaporation could rapidly produce secondary OA, which resembles the mass spectrum of oxygenated OA factors and could be 1-2 orders of magnitude higher than the primary OA emissions (Nordin et al., 2013; Presto et al., 2014; Jathar et al., 2014; Platt et al., 2013). In addition, a previous study by Liu et al. (2011) showed that the carboxylic acids measured by ~~FT-IR~~FTIR are exclusively associated with fossil fuel combustion and correlate with the PMF resolved OOA factor from HR-ToF-AMS measurements in coastal California. On the other hand, Zotter et al. (2014) showed that >69% of MO-OOA originated from non-fossil sources in LA basin based on a combination of radiocarbon analysis and AMS PMF analysis. By using the same method, DeWitt et al. (2014) showed that the majority of carbon in OOA is non-fossil even in an environment heavily influenced by traffic emissions, suggesting the source of MO-OOA is not vehicle emissions. ~~At last~~Lastly, aged biomass burning is also a possible source for MO-OOA as discussed above in section 4.1.4.

One interesting observation in this study is that MO-OOA is well-correlated with ozone in summer (R = 0.73 for JST_May and YRK_July), but not in winter (R = -0.059 and -0.27 for JST_Nov and YRK_Dec, respectively) (Fig. 8), implying that the sources of MO-OOA may vary with seasons. Considering the large biogenic VOC emissions in summer, the summer MO-OOA may be related to the oxidation of biogenic VOCs. Recently, Ehn et al. (2014) for the first time observed that ~~monoterpenes~~monoterpene oxidation could produce large ~~amounts~~quantities of compounds with extremely low~~-volatility vapors~~ vapor pressure. As these compounds have very high O:C (~0.7), it is possible that they serve as an important source for MO-OOA. The identification of the sources of winter MO-OOA could be aided by the radiocarbon analysis. For example, if the majority of MO-OOA in winter has non-fossil sources, it could suggest that aged

OA from biomass burning is an important source for MO-OOA, because biomass burning is enhanced and the emissions of biogenic VOCs are low in winter.

4.1.6 LO-OOA

Similar to MO-OOA, less-oxidized oxygenated organic aerosol (LO-OOA) is also observed in both rural and urban sites throughout the year. LO-OOA comprises 19-34% of total OA (Fig. ~~5~~6). A key feature of LO-OOA is that it consistently exhibits a daily maximum at early morning and at night, in all datasets (Fig. ~~6~~5). The similar diurnal variation of LO-OOA has also been observed in previous field measurements and thought to be primarily driven by the semi-volatile nature of LO-OOA. The LO-OOA factor identified in multiple prior field measurements has been observed to correlate with ammonium nitrate, a semi-volatile species which mainly partitions into the particle phase at night when the temperature is relatively low (Jimenez et al., 2009; Sun et al., 2012a; Zhang et al., 2011; Ulbrich et al., 2009). However, in this study, LO-OOA only shows moderate correlation with total NO_3 (i.e., $NO_{3,meas}$) measured by the HR-ToF-AMS in summer datasets (R ranges between 0.56 and 0.76) and ~~no correlation~~is not correlated in winter datasets (R ranges between 0.14 and 0.46) (Fig. 9 and Table 2).

While LO-OOA is only moderately, or sometimes poorly ~~correlates~~correlated, with $NO_{3,meas}$ in this study, we find improved correlation between LO-OOA and "nitrate functionality from organic nitrates" (i.e., $NO_{3,org}$) (Fig. 9 and Table 2). $NO_{3,org}$ is estimated by using the NO_x^+ ratio method, as described in section 2.5. ~~A~~An R_{ON} value of 10 is applied in this case since different R_{ON} values would only affect the estimated concentration of $NO_{3,org}$, but not the correlation between LO-OOA and $NO_{3,org}$~~, because estimated $NO_{3,org}$ has a linear relationship with R_{ON}.~~. For most datasets, LO-OOA correlates better with $NO_{3,org}$ than total nitrates. The biggest improvement is seen in JST_Nov, where the correlation ~~R~~coefficient increases from 0.14 to 0.63. However, we also note that the correlation becomes worse for YRK_Dec and RS_Jan, which is likely caused by the small contribution of organic nitrates to total nitrates, resulting in a larger uncertainty in the NO_x^+ ratio method (Bruns et al., 2010). In addition, the correlations between LO-OOA and $NO_{3,org}$ for YRK_Dec and RS_Jan are weakened by the negative $NO_{3,org}$ concentration estimated from ~~estimation~~the NO_x^+ ratio method (Fig. 9~~), which is~~). The negative values are a result of smaller R_{meas} than R_{AN}, at times (see ~~Eqn~~Eq. 1), which is likely caused by

~~contribution from inorganic nitrates other than ammonium nitrate or variation~~variations in instrument performance (Farmer et al., 2010; Rollins et al., 2010).

4.2 Nitrates source apportionment

4.2.1 Estimation of organic nitrates

The NO_x^+ ratio method and PMF method are applied to estimate the concentration of "nitrate functionality from organic nitrates" (i.e., $NO_{3,org}$) at different sites. The concentration of $NO_{3,org}$ and the mass fraction of $NO_{3,org}$ in total measured NO_3 (i.e., $NO_{3,meas}$) estimated from both methods are shown in Fig. 10. Both the NO_x^+ ratio method and the PMF method show a similar seasonality ~~of~~in the contribution of $NO_{3,org}$ to $NO_{3,meas}$ (denoted as $NO_{3,org}/NO_{3,meas}$), which is higher in summer than winter. However, we observe noticeable differences between the two methods. In the following~~ discussion~~, we first discuss the uncertainties associated with NO_x^+ ratio method and PMF method. Then, we discuss how the uncertainties affect the comparison between the two methods, and provide a "best estimate" range of $NO_{3,org}$ based on the two methods. Lastly, we use the "best estimate" range of $NO_{3,org}$ to calculate the contribution of organic nitrates to OA by assuming the molecular weight (MW) of organic nitrates.

For the PMF method, the uncertainty is mainly associated with the identification of a nitrate inorganic aerosol (NIA) factor. The NIA factor is resolved ~~from~~in most datasets, except CTR_June and YRK_July. The mass spectrum of the NIA factor is similar to the corresponding factor in Sun et al. (2012b) (Fig. S4). Specifically, it is dominated by NO^+ and contains some organic signals such as CO_2^+ and $C_2H_3O^+$, indicating the NIA factor has a potential interference from organics. The mass fraction of organic signals in the NIA factor varies across sites, with a higher value in warmer months (~70% in JST_May and GT_Aug) than colder months (16%-38% in JST_Nov, YRK_Dec, and RS_Jan) (Fig. S11). The fact that the NO^+/NO_2^+ ratio of the NIA factor resolved from warmer months is higher than that of pure ammonium nitrate (Fig. S12) is also indicative of organic nitrate interference in the NIA factor. Conversely, the NO^+/NO_2^+ ratio of the NIA factor resolved from colder months is closer to that of pure ammonium nitrate, suggesting less interference from organics. Thus, for the sites where a NIA factor is identified, the presence of organic nitrates in the NIA factor would result in an underestimation of $NO_{3,org}$, and the underestimation is larger for warmer months (i.e., JST_May and GT_Aug). For

CTR_June and YRK_July, the NIA factor is not resolved from $PMF_{org+NO3}$ analysis, likely due to a small concentration of inorganic nitrates. For example, the concentrations of organics and total nitrates (i.e., $NO_{3,meas}$) are 5.0 and 0.1 µg m^{-3}, respectively, for CTR_June. Even if one assumes that all the measured nitrates arise from inorganic nitrates, the nitrates/organics ratios is only 2%, making it difficult for PMF to retrieve the NIA factor accurately (Ulbrich et al., 2009). Thus, for CTR_June and YRK_July, the small amount of $NO_{3,inorg}$, which is not retrievable by PMF, was attributed ~~into~~to OA factors so that the PMF method would slightly overestimate $NO_{3,org}$.

For the NO_x^+ ratio method, considering the large variation in NO_x^+ ratio for different organic nitrates, the largest uncertainty is associated with the value of R_{ON}. Ideally, the time-dependent R_{ON} values should be applied. However, this is challenging because the determination of time-dependent R_{ON} requires measurements of every ambient organic nitrate species, which are not available. ~~With~~Knowing this, we apply R_{ON} values of 5 and 10 in our analysis to provide the upper and lower bounds of the estimated $NO_{3,org}$ concentration for the NO_x^+ ratio method as discussed in section 2.5. It is noted that for Centreville, we applied a third method to calculate the concentration of $NO_{3,org}$, which is based on the differences between HR-ToF-AMS measurements (NO_3 from both organic and inorganic species) and PILS-IC measurements (NO_3 from inorganic species only) (Xu et al., 2015; Bae et al., 2007; Orsini et al., 2003). This method, denoted as AMS-IC method, is only applied for Centreville because the PILS-IC was not deployed in the SCAPE study. In order to match the HR-ToF-AMS particle cut size (i.e., PM_1), a PM_1 cyclone was deployed at the inlet of PILS-IC. However, due to the transmission efficiency of PM_1 cyclone, PILS-IC measurements might ~~have interferences~~include contributions from particles larger than 1µm (i.e., ~~$NaNO_3$~~inorganic NO_3 in mineral dust). ~~The interferences~~Interferences from water-soluble refractory particles (e.g., calcium or sodium nitrate) are ~~expected to be~~likely small ~~because~~given the ~~sodium~~ concentration of sodium measured by the PILS-IC with a PM_1 cyclone ~~is~~, for example, was negligible and mostly below its detection limit (0.07 µg m^{-3}) (Fig. S13). As shown in Fig. 11, The $NO_{3,org}$ estimated by the AMS-IC method falls within the range of NO_x^+ ratio method, which is defined by R_{ON} values of 5 and 10, indicating the feasibility ~~to use~~of using these two values as the upper and lower bounds to estimate $NO_{3,org}$ for the NO_x^+ ratio method.

Based on the uncertainties of the PMF method and the NO_x^+ ratio method, we could explain the differences between the two methods and further combine them in order to narrow the estimation range. According to the extent of agreement between the two methods, all seven datasets are grouped into three categories: summer months (CTR_June and YRK_July), transition months (JST_May and GT_Aug), and winter months (JST_Nov, YRK_Dec, and RS_Jan).

For winter months, the PMF method shows good agreement with the NO_x^+ ratio method with a R_{ON} value of 10 for JST_Nov and YRK_Dec. This is consistent with the observations that the interference of organic nitrates in the NIA factor is small in winter datasets (Figs. S11 and S12) and isoprene emission is negligible in winter (Guenther et al., 2006). Thus, results from the NO_x^+ ratio method with R_{ON} = 5 (i.e., isoprene organic nitrates) are likely unrealistic. With this in mind, we combine the results from the PMF method and the NO_x^+ ratio method with R_{ON} = 10 as the "best estimate" range of organic nitrates for JST_Nov and YRK_Dec. For RS_Jan, the NO_x^+ ratio method predicts negative $NO_{3,org}$ due to R_{meas} being smaller than R_{AN} at times (~~Eqn~~Eq. 1). In this case, the PMF method is selected as the "best estimate". Taken together, the mass fraction of organic nitrates (i.e., $NO_{3,org}/NO_{3,meas}$) is 0.19-0.21, 0.11-0.21, and ~0.10 for JST_Nov, YRK_Dec, and RS_Jan, respectively.

For summer months, the PMF method predicts that all the measured nitrates are from organic nitrates (i.e., $NO_{3,org}/NO_{3,meas}$ = 1, Fig. 10), because a NIA factor is not resolved from PMF analysis and ~~that~~ all the measured NO_3 are distributed in the OA factors. The $NO_{3,org}$ estimated from the PMF method falls within the upper (i.e., R_{ON} = 5) and lower bound (i.e., R_{ON} = 10) of the NO_x^+ ratio method (Fig. 10). For CTR_June, the NO_x^+ ratio method with R_{ON} value of 5 predicts a $NO_{3,org}/NO_{3,meas}$ ratio that is greater than 1, which results from the assumed R_{ON} value (i.e., 5) being smaller than R_{meas}, at times (~~Eqn~~Eq. 1). Thus, the PMF method and the NO_x^+ ratio method with R_{ON} = 10 define the upper and lower bound, respectively. Accordingly, the "best estimate" range of $NO_{3,org}/NO_{3,meas}$ is 0.80-1 and 0.63-1 for CTR_June and YRK_July, respectively.

For transition months (i.e., JST_May and GT_Aug~~, the sampling periods of which were between summer and winter~~), the PMF method and the NO_x^+ ratio method show large discrepancies. Compared to the PMF method, the NO_x^+ ratio method predicts 1.5–2.5 times higher $NO_{3,org}$ concentration depending on the site and R_{ON} value. This is likely caused by the PMF method under-predicting $NO_{3,org}$, owing to the attribution of some organic nitrates to the NIA factor. Thus, we select the NO_x^+ ratio method with R_{ON} values of 5 and 10 as the "best estimate" range. Accordingly, $NO_{3,org}/NO_{3,meas}$ ranges 0.55-0.76 and 0.64-0.99 for JST_May and GT_Aug, respectively.

~~Further, we~~ We also calculate the contribution of organic nitrate molecules to OA from the "best-estimate" range of nitrate functionality (i.e., $NO_{3,org}$). We assume that particle-phase organic nitrates have an average molecule weight of 200 and 300 g mol^{-1} (Rollins et al., 2012), which provides an lower and upper bound for ~~estimated concentration~~estimating concentrations of organic nitrates. As shown in Fig. 10, organic nitrates contribute about 5-12% ~~of~~to total OA for summer datasets (CTR_June and YRK_July) and 9-25% ~~of~~to total OA for winter datasets (JST_Nov, YRK_Dec, and RS_Jan), suggesting that organic nitrates are important components of total OA in the southeastern US.

Figure 12 shows the diurnal variation of $NO_{3,org}$ based on the NO_x^+ ratio method with an R_{ON} value of 10. For most of the datasets, $NO_{3,org}$ starts increasing after sunset, which is mainly caused by the oxidation of VOCs by nitrate radical at night. The daily maximum of $NO_{3,org}$ appears in mid-morning (i.e., ~8am), which is likely because photooxidation of VOCs in the presence of NO (i.e., RO_2+NO pathway) also contributes to organic nitrate when the NO concentration is highest.

4.2.2 Nitrate seasonal variation

As shown in table 1 and Fig. 2, the total nitrate concentration is higher in winter (0.8-1.4 μg m^{-3}, 10-16% of total NR-PM_1) than in summer (0.3-0.4 μg m^{-3}, 2-3% of total NR-PM_1). Based on the NO_x^+ ratio method, $NO_{3,inorg}$ is greatly enhanced in winter relative to summer. For example, the concentration of $NO_{3,inorg}$ increases from 0.22 μg m^{-3} (average of upper and lower bound of the NO_x^+ ratio method) in May to 1.6 μg m^{-3} in November for the JST site. Similarly, $NO_{3,inorg}$ shows a 10-fold increase for YRK_Dec compared to YRK_July.

The seasonal variation of inorganic nitrates could possibly be caused by its semi-volatile nature and varying NO_x emissions. Based on volatility measurements by a thermal denuder, Huffman et al. (2009) showed that ammonium nitrate is very volatile and its gas/particle partitioning is largely affected by temperature. The average temperature in summer is about 15 °C higher than that in winter (Table 1). According to laboratory measurements of ammonium nitrate volatility, a 15°C increase in temperature would lead to the evaporation of 60% of nitrate mass (Huffman et al., 2009). In addition to volatility, the winter enhancement of inorganic nitrates is related to higher NO_x ~~level~~levels, which is the major source for inorganic nitrates and largely elevated in winter in the southeastern US (Blanchard et al., 2013). For example, as shown in Table 1, the NO_x concentration in JST_Nov (50.5 ppb) is 3.5 times higher than that in JST_May (14.4 ppb). Thus, the lower temperature and higher NO_x ~~level~~levels in winter than summer likely compensate for the weaker photooxidation and result in the increase in inorganic nitrates. Interestingly, we observe a rush hour peak (around 9am) in the diurnal trend of total nitrates at urban sites in winter (JST_Nov and RS_Jan). This rush hour peak is primarily from inorganic nitrates supported by the following evidence: 1) the R_{meas} is close to R_{AN} during the rush hour period (Fig. S15); 2) the rush hour peak only exists in the diurnal profile of $NO_{3,inorg}$ (Fig. ~~S16~~12); and 3) the coincident peak in the diurnal trend of NH_4 (Fig. 3). Early morning peaks in inorganic nitrates were also consistently seen by a variety of online instruments as part of the Atlanta Supersite Experiment at the JST site (Weber et al., 2003). In Mexico City, Hennigan et al. (2008) attributed the fast production of inorganic nitrates mainly to secondary formation from photooxidation of NO_x and subsequent partitioning of HNO_3. The rush hour peak of inorganic nitrates ~~disappear~~disappears rapidly, which is likely caused by evaporation and dilution as the planetary boundary layer height increases (Hennigan et al., 2008).

The concentration of $NO_{3,org}$ is slightly higher in summer, but its seasonal variation is not as strong as $NO_{3,inorg}$ (Table 2 and Fig. 10). This is likely due to the compensating effects of source strength and gas/particle partitioning. The organic nitrates mainly originate from ~~VOCs~~VOC oxidation by the nitrate radical and/or photooxidation in the presence of NO_x. The VOC concentrations are higher in summer due to stronger biogenic emissions, which would provide sources for organic nitrates. However, the temperature is higher in summer than winter, which would hinder the partitioning of organic nitrates into the ~~aerosol~~particle phase.

4.3 Aerosol Spatial ~~Distribution~~Variability

The spatial ~~distribution~~variability of organics, sulfate, ammonium, and total nitrate in the greater Atlanta area is investigated by comparing ACSM measurements (stationary at the Georgia Tech site) with HR-ToF-AMS measurements (rotating among different sites). ~~The HR-ToF-AMS and~~ Figure 13 shows the correlation coefficients for NR-PM_1 species between ACSM measurements ~~between~~ (stationary at the Georgia Tech site) and HR-ToF-AMS measurements (rotating among different sites~~ are shown~~). Detailed comparisons, in ~~Fig. S14~~terms of time series and ~~the correlations (Pearson's R) of the four species~~ scatter plots, are shown in Fig. ~~12~~S14. The ACSM and HR-ToF-AMS are compared side-by-side at the Georgia Tech (GT) site from 20 July ~~20th~~ to 4 September~~ 4th~~, 2012 and the time series of the species measured by the two instruments are well correlated (R=0.95, 0.93, 0.82, 0.85 for organics, sulfate, ammonium, and total nitrate, respectively) and agree within instrument uncertainty (i.e., 20-35%) (Bahreini et al., 2009).

As expected, the correlation gets weaker as the distance between the GT site and other sampling sites increases. Surprisingly, the organic correlation coefficient in July is 0.92 between GT and YRK sites, which have considerable spatial separation (i.e., 70 km), indicating that the organics are uniformly distributed in the greater Atlanta area in summer time. In contrast, the organic correlation coefficient between GT and YRK decreases to 0.66 in winter. Unlike organics, the correlation in SO_4 between GT and YRK is similarly good in both summer and winter (R=0.7 and 0.85 for summer and winter, respectively). Our observation is generally consistent with the previous study by Zhang et al. (2012), who showed that WSOC, and to a less extent SO_4, are spatially homogeneous in the southeastern US based on results from daily-average filter measurements (one filter in every six days) in 2007. The authors attributed the uniform distribution of WSOC and SO_4 largely to stagnant air masses in southeastern US during summer time and both long-lived secondary WSOC and SO_4 eventually spread across the region~~.~~, although somewhat higher WSOC spatial correlations compared to sulfate were thought to be due to widely distributed SOA precursor emissions compared to point sources for SO_2. Hidy et al. (2014) also showed that secondary species, like SO_4, have weaker rural and urban contrast in the southeastern US, though only yearly average data were considered in that study.

Although meteorology plays an important role in the spatial ~~distribution~~variability of aerosol, it alone cannot explain the ~~seasonal variation~~seasonality of the OA spatial

~~distribution~~variability. For example, meteorology should have the same effect on the regional ~~distribution~~variability of SO_4 and OA. However, while SO_4 is uniformly distributed in both summer and winter, OA is more uniform in summer than winter, suggesting other factors also influence the spatial ~~distribution~~variability of OA. The seasonality of OA spatial ~~distribution~~variability (i.e., ~~highly~~more spatially homogeneous in summer ~~than~~compared to winter) is probably affected by the seasonal variation of OA sources in addition to meteorology. As shown in Fig. ~~5~~6, SOA is the dominant source for total OA (69-100% of OA) in summer for both rural and urban sites. This likely arises from the fact that biogenic VOCs, which are important precursors for SOA, are abundant and widely distributed in the southeastern US during summer time (Guenther et al., 2006). Thus, SOA is regional and the dominant component of OA, leading to the uniform distribution of OA. In contrast, POA concentration varies greatly between urban and rural sites. In winter, while the SOA still dominates total OA at rural sites, the POA is comparable with SOA at urban sites (Fig. ~~5~~6). This is because that the concentration of regional SOA decreases due to weaker photochemical activity and lower biogenic VOCs emissions in winter, but the concentration of POA (HOA+BBOA+COA) is relatively constant, or even increases. This is likely due to elevated emission from biomass burning and reduced evaporation and ~~dilution~~dispersion, which are associated with lower temperatures in winter (Fig. ~~5~~6). Thus, the ~~fact~~facts that POA is not uniformly distributed and that the concentration of POA is comparable to SOA possibly lead to the spatial non-uniformity of OA in winter.

4.4 Interpretation of long-term measurements

In this section, we compare our observations from short-term ~~and extensive~~detailed aerosol chemical measurements with those from long-term and more basic measurements to test the ~~robustness~~validity of our conclusions. Further, based on our extensive measurements, we attempt to provide insights ~~in~~into interpreting long-term observations.

4.4.1 OA Diurnal Variation

By investigating the diurnal pattern of organic carbon (OC) from 1 June ~~1 –~~– 15 July~~ 15~~ of each year (from 2000 to 2013) in Centreville, rural Alabama, Hidy et al. (2014) observed that OC shows consistently weak diurnal variability. Similarly, Zhang et al. (2012) observed that water-soluble organic carbon (WSOC), which is a surrogate for SOA~~,~~ (in summer), only shows a moderate increase in the daytime in Jefferson Street and Yorkville, GA, during 2008 summer. In this study, we find that OA shows little diurnal variability in summer datasets (Fig. 3), which is consistent with long-term observations and previous studies~~ in literature~~.

The lack of a prominent daytime increase in the OA in summer could appear to discount the role of photochemistry-driven secondary OA formation. However, a number of factors need to be considered, such as the changes in planetary boundary layer height, contribution of various sources to OA, and temperature-dependent gas/particle partitioning. ~~Firstly, the rapid expansion of boundary layer during the day may dilute the OA concentration. In Centreville, we observed that OA exhibits a distinct increase starting at noon after multiplying its diurnal profile by boundary layer height (Fig. 3d), which was measured by a ceilometer.~~Firstly, the rapid expansion of the boundary layer during the day may dilute the OA concentration. In Centreville, the boundary layer height (BLH) was measured by a ceilometer. The diurnal variation of BLH is shown in Fig. 14. The BLH typically peaks (i.e., 1300m) at 17:00 and exhibits a daily minimum (i.e., 375m) at 07:00. In order to remove the effect of BLH-driven dilution on the diurnal variation of OA, we multiply the OA diurnal profile by BLH. The interpretation of the product of the concentration of OA (i.e., $\mu g\ m^{-3}$) times BLH (i.e., m) is the integrated column concentration of OA (i.e., $\mu g\ m^{-2}$) from ground to the top of boundary layer over a unit surface area, assuming the OA is well-mixed in the boundary layer. The value of OA*BLH would be conserved if there is no gain or loss of OA in the column regardless of the change of BLH. Thus, this value could indicate the net gain or loss of OA in the column without the effect of BLH-driven dilution. As shown in Fig. 3d, the OA*BLH increases rapidly starting at ~7:00 and reaches a daily maximum at ~17:00. The evident peak in the diurnal variation of OA*BLH suggests a substantial OA production in the day, and that the relatively flat OA diurnal variation (i.e., $\mu g\ m^{-3}$) is largely caused by the BLH-driven dilution. For the cases where boundary layer height data are not available, normalizing OA by CO is often utilized in the literature to minimize the effect of dilution, considering CO as an inert species. By using this method, Blanchard et al. (2011) and Zhang et al. (2012) showed that OC/CO and WSOC/CO exhibit pronounced daytime increase, suggesting that the expansion of boundary layer would weaken the OA diurnal variation. The fact that both OC/CO and WSOC/CO peaks in the day implies that photochemistry-driven SOA production is an important source of OA.

Secondly, the time-dependent contributions of various sources to total OA could also affect its diurnal profile. As shown in Fig. ~~6~~5, the various OA sources resolved by PMF analysis have distinctly different diurnal trends, indicating that their contributions to total OA vary throughout the day. Primary sources, such as HOA and COA, peak during rush hours and meal--time, respectively. The contributions of Isoprene-OA and MO-OOA to total OA are largest in the afternoon and decrease after sunset. In contrast, another SOA source, LO-OOA, peaks in the early morning and at night, as the formation of LO-OOA is proposed to mainly correspond to nocturnal nitrate radical oxidation of biogenic VOCs in summer (Xu et al., 2015). Therefore, different diurnal trends of various OA sources compensate each other, which possibly results in the weak diurnal variation of total OA.

Specifically, LO-OOA, which exhibits a daily maximum at night, compensates for the decrease of other OA sources after sunset and results in the relatively flat total OA diurnal profile. This has important implication in interpreting non-speciated OC measurements. For example, Hennigan et al. (2009) observed a substantial nocturnal increase of gas-phase WSOC, but not an accompanied increase in particle-phase WSOC in Atlanta during summer. The authors hypothesized that the differences between gas-phase and particle-phase WSOC are caused by the oxidation of α-pinene and isoprene by $NO_3^{\bullet}$ radical producing substantial amount of gas-phase WSOC but little particle-phase WSOC. Though it is plausible that α-pinene+$NO_3^{\bullet}$ and isoprene+$NO_3^{\bullet}$ reactions produce more volatile products than low-volatility products, our study shows that there is indeed substantial nocturnal SOA production (i.e., LO-OOA), which likely corresponds to the nocturnal increase in gas-phase WSOC in Hennigan et al. (2009), but not clearly discernible in particle-phase WSOC due to the compensation by the decreasing concentrations of other OA sources at night.

In addition, temperature-dependent gas/particle partitioning also plays a role in OA diurnal variation. As the temperature is higher during day, the gas/particle partitioning would favor the gas-phase and hence lower the particle-phase concentration. Taken together, the weak diurnal variation of OA in summer is likely caused by changes in boundary layer height and the varying contribution of various OA sources throughout the day, which does not contradict the importance of photochemistry-driven SOA production. Especially, LO-OOA, which is likely related to $NO_3^{\bullet}$ chemistry, peaks at night and compensates the nocturnal decrease of other SOA sources. In fact, the importance of photochemistry can be gained by comparing OA diurnal profile of summer and winter. As the photochemistry is relatively weaker in winter, daytime SOA production is suppressed, which results ~~that~~in OA ~~reaches~~reaching a daily minimum during daytime in winter datasets (Fig. 3).

4.4.2 Urban and rural contrast of OA seasonality

In this study, we observed that the seasonality of OA behaves differently between urban and rural sites. For example, while the OA concentration is relatively constant between summer and winter for the urban JST site (9.1 µg m^{-3} in May vs 7.9 µg m^{-3} in November), the OA concentration is ~4 times higher in summer than winter for the rural YRK site (11.2 µg m^{-3} in July vs 3.2 µg m^{-3} in December). Our observations are consistent with the long~~-~~-term measurements from the SEARCH network. Fig. ~~13~~15 shows the seasonal average OC concentration measured in JST and YRK ~~sites~~ from 1999 to 2013. Despite ~~of~~ the decreasing trend of OC in the past 14 years, which has been noted and discussed extensively in Hidy et al. (2014), we note that the OC concentration is similar between summer and winter at the JST site, but OC is elevated in summer compared to winter for the YRK site. The urban and rural contrast of OA seasonality is likely caused by the fact that OA sources are different at urban and rural sites. As shown by PMF analysis on our short-term measurements, the total OA ~~in~~at the rural YRK site is dominant by SOA in both summer and winter (SOA/OA = 100% and 78% for summer and winter, respectively, Fig. ~~5~~6), but the concentration of SOA is lower in winter when the SOA formation is depressed due to low biogenic VOCs emissions and weak photochemical activity. For the urban JST site, in contrast, POA accounts for a large fraction of total OA (30-48%, depending on the month). Though the SOA formation is also depressed in winter at urban sites, the decrease in SOA concentration is compensated by the increase in POA concentration from vehicles and cooking (Fig. ~~5). Thus, the OA in JST is relatively constant between summer and winter.~~6). Thus, the OA at JST is relatively constant between summer and winter. The changing composition of the OA also implies differing aerosol toxicity and health impacts, not discernible from measurements of total OA (or OC) (Verma et al., 2015). The fairly flat seasonal trend in OA or OC at urban sites has not been captured by current models. All 31 models reviewed in a recent study by Tsigaridis et al. (2014) predicted higher OC concentration in summer than winter for urban monitoring sites in Georgia. One possible reason is that the anthropogenic emission inventories applied in current models do not take seasonal variation into account, resulting in an under-prediction of the pollution levels in urban area.

4.4.3 Correlation between OC and sulfate

Based on the OC and sulfate measurements (2005 – 2010) from three SEARCH network sites (Centreville, Jefferson Street, and Yorkville), we find that regardless of the sampling sites, the correlation between OC and sulfate has a distinct seasonal variation, with the best correlation in summer (R ranging 0.47-0.69) and worst in winter (R ranging 0.01-0.33) (Fig. ~~14~~16). Since sulfate is mostly secondary in the southeastern US, one possible explanation for the seasonality of the correlation between OC and sulfate is that the majority of OC is secondary in summer, but not in winter, which is supported by the OA source apportionment in this study. It is also likely that sulfate is directly involved in the OA production in summer. Specifically, Xu et al. (2015) found that sulfate directly and largely mediates the formation of isoprene OA (18-36% of total OA in summer) in the southeastern US, instead of particle water content and/or particle acidity, as previous studies have suggested.

5. Conclusion

Nearly one-year of measurements were performed across multiple sites in the southeastern US with a variety of online instruments, with the focus on HR-ToF-AMS data in this study. We find that organics are the dominant components of the NR-PM_1 at both rural and urban sites throughout the year. The OA diurnal profile shows little variation in summer and peaks at night in winter datasets. The lack of midday enhancement in OA diurnal profile is likely caused by the expansion of boundary layer in the day and compensating effects of various OA factors. The OA measured at different sampling sites and seasons has a similar degree of oxidation. Sulfate contributes the second highest to NR-PM_1. Sulfate concentration is higher in summer (3.0 to 4.0 µg m^{-3}) than winter (1.4 to 1.7 µg m^{-3}), probably due to stronger photochemistry in summer. In contrast to sulfate, the inorganic nitrate concentration is estimated to be ~~tripled~~three times higher in winter than summer. This is likely caused by higher NO_x levels in winter, which serves as the source for inorganic nitrates and the semi-volatile nature of inorganic nitrates, which tend to partitions into the particle phase when the temperature is low.

Positive Matrix Factorization (PMF) analysis revealed that the organic aerosol has various sources in the southeastern US, which changes between seasons and sampling sites (rural vs urban). Hydrocarbon-like organic aerosol (HOA) and cooking organic aerosol (COA), which arise from primary vehicle emissions and cooking, respectively, are important but not dominant OA sources for urban sites. Biomass burning OA (BBOA) concentrations shows clear enhancements in winter compared to summer. In addition, biomass burning is found to be an important, but not exclusive, source for brown carbon in the southeastern US. Isoprene-derived OA (Isoprene-OA), which is from the reactive uptake of isoprene epoxides in the presence of hydrated sulfate, only exists in warmer months (May-August) when ~~the~~ isoprene ~~emission is~~emissions are substantial. In addition to rural sites, Isoprene-OA is resolved from urban sites where the majority of peroxy radicals are believed to react with NO_x. We note that f_{C5H6O+}, which has been used as a marker for Isoprene-OA, ranges from 0.9-2.3% and is higher in the Isoprene-OA factor from rural sites than urban sites. One possible source of Isoprene-OA in urban sites is transport. However, transport would ~~unlikely~~not likely result in the reproducible diurnal profile of Isoprene-OA, which peaks in early afternoon. Instead, Isoprene-OA in urban sites more likely comes from local production, as a recent study showed that IEPOX could be produced in the presence of NO_x (Jacobs et al., 2014). Less-oxidized oxygenated OA (LO-OOA) and more-oxidized oxygenated OA (MO-OOA) are resolved from both rural and urban sites throughout the year. LO-OOA shows improved correlation with estimated "nitrate functionality from organic nitrates" (i.e., $NO_{3,org}$) than total nitrates. In addition, both LO-OOA and estimated $NO_{3,org}$ peaks at night (~~Fig. 6~~Figs. 5 and 12~~Fig. S16~~), implying that LO-OOA could arise from nighttime oxidation of biogenic VOCs by nitrate radicals. Unlike isoprene, monoterpene ~~emission is~~emissions occur year-around and ~~continues~~continue into the ~~nights~~night. The ~~prevalent presence~~prevalence of the LO-OOA factor at all sites year-around points to the important contribution of monoterpene SOA to the total OA budget in the southeastern US. As the most oxidized OA factor, MO-OOA reaches a daily maximum in the afternoon and likely contains aged OA from various sources, such as vehicle emission, biomass burning, and aged OA from biogenic VOCs. We find that the correlation between MO-OOA and ozone is substantially better in summer than winter, suggesting that the sources of MO-OOA might vary with season.

In order to estimate the organic nitrate contribution to OA, we applied and evaluated three methods, i.e, NO_x^+ ratio method, PMF method, and AMS-IC method. Despite the uncertainty of the NO_x^+ ratio method (i.e., the values of R_{ON} and R_{AN}) and the PMF method (i.e., the separation of pure NIA factor), both methods provide reasonable results in separating the measured total nitrates into nitrate functionality from inorganic and organic nitrates. The "nitrate functionality from organic nitrates" (i.e., $NO_{3,org}$) accounts for about 63–100% and 10-20% of total measured nitrate (i.e., $NO_{3,meas}$) in summer and winter, respectively. Further, we estimate the contribution of organic nitrates to total OA based on estimated $NO_{3,org}$ and assumed ~~MW~~molecular weigth of bulk organic nitrates. Depending on location, season and estimation method, organic nitrates account for about 5-25% of total OA, which indicates that organic nitrates are important components in the ambient aerosol.

The spatial distribution of OA is investigated by comparing ACSM measurements (stationary at the Georgia Tech site) and HR-ToF-AMS measurements (rotating among different sites). In summer, OA is spatially homogeneous as suggested by the good correlation (R=0.92) in July between the GT and YRK sites, which are 70km apart. The spatial homogeneity of OA in summer is likely caused by SOA being the dominant source of OA for both urban and rural sites. The parameters such as temperature, solar radiation, and precursor VOCs, which have great influences on SOA formation, are similar between urban and rural sites. Compared to summer, the OA is less spatially homogenous in winter. The correlation coefficient of OA between GT and YRK decreases to 0.66 in winter. This is likely due to the elevated contribution from POA to total OA in winter and the spatially inhomogeneous distribution of POA. Meteorology also plays a role in the OA spatial distribution, but alone is unlikely to explain the observation.

We show that short-term and extensive measurements can help interpret long-term basic measurements. For example, consistent with long-term (1999 – 2013) OC measurements from the SEARCH network, we also observed that the seasonal variation of OA has some urban and rural contrasts. While the OA concentration is similar between summer and winter for the urban JST site, it increases ~~4 times~~by a factor of 4 from winter to summer for the rural YRK site, according to our year-long ~~observation~~observations. PMF analysis suggests that the different OA seasonality between urban and rural sites is likely due to the varying strength of OA sources. For rural sites, SOA represents the dominant fraction of OA in both summer and winter, but SOA concentration is much lower in winter. For urban sites, in contrast, the decrease in SOA concentration in winter is compensated by the increase in POA concentration due to less dispersion from lower boundary layer heights, leading to a relatively constant total OA concentration compared to summer. In addition, analysis of long-term OC and sulfate ~~measurement~~measurements from the SEARCH network shows that the correlation between OC and sulfate is substantially better in summer than winter, consistent with our source apportionment results that show the majority of OA is secondary in summer. The better correlation of OC and sulfate in summer also supports that sulfate directly mediates the formation of isoprene SOA (Xu et al., 2015), which is only present in warmer months.

Acknowledgement

~~The SCAPE Clean Air Center~~This publication was made possible ~~through~~by US EPA grant R834799. ~~The~~This publication's contents ~~of this publication~~ are solely the responsibility of the grantee and do not necessarily represent the official views of the US EPA. Further, US EPA does not endorse the purchase of any commercial products or services mentioned in the publication. Measurements in SOAS are supported by the NSF under grant number 1242258. S.S. acknowledges support from the Air Products Undergraduate Research Program and the President's Undergraduate Research Award (PURA) at Georgia Tech. The authors thank the SEARCH personnel for their many contributions. Without their support this work would not have been possible.

Reference

Aiken, A. C., Decarlo, P. F., Kroll, J. H., Worsnop, D. R., Huffman, J. A., Docherty, K. S., Ulbrich, I. M., Mohr, C., Kimmel, J. R., Sueper, D., Sun, Y., Zhang, Q., Trimborn, A., Northway, M., Ziemann, P. J., Canagaratna, M. R., Onasch, T. B., Alfarra, M. R., Prevot, A. S. H., Dommen, J., Duplissy, J., Metzger, A., Baltensperger, U., and Jimenez, J. L.: O/C and OM/OC ratios of primary, secondary, and ambient organic aerosols with high-resolution time-of-flight aerosol mass spectrometry, Environ Sci Technol, 42, 4478-4485, Doi 10.1021/Es703009q, 2008.

Aiken, A. C., Salcedo, D., Cubison, M. J., Huffman, J. A., DeCarlo, P. F., Ulbrich, I. M., Docherty, K. S., Sueper, D., Kimmel, J. R., Worsnop, D. R., Trimborn, A., Northway, M., Stone, E. A., Schauer, J. J., Volkamer, R. M., Fortner, E., de Foy, B., Wang, J., Laskin, A., Shutthanandan, V., Zheng, J., Zhang, R., Gaffney, J., Marley, N. A., Paredes-Miranda, G., Arnott, W. P., Molina, L. T., Sosa, G., and Jimenez, J. L.: Mexico City aerosol analysis during MILAGRO using high resolution aerosol mass spectrometry at the urban supersite (T0) – Part 1: Fine particle composition and organic source apportionment, Atmos. Chem. Phys., 9, 6633-6653, 10.5194/acp-9-6633-2009, 2009.

Allan, J. D., Bower, K. N., Coe, H., Boudries, H., Jayne, J. T., Canagaratna, M. R., Millet, D. B., Goldstein, A. H., Quinn, P. K., Weber, R. J., and Worsnop, D. R.: Submicron aerosol composition at Trinidad Head, California, during ITCT 2K2: Its relationship with gas phase volatile organic carbon and assessment of instrument performance, Journal of Geophysical Research: Atmospheres, 109, D23S24, 10.1029/2003JD004208, 2004.

Allan, J. D., Williams, P. I., Morgan, W. T., Martin, C. L., Flynn, M. J., Lee, J., Nemitz, E., Phillips, G. J., Gallagher, M. W., and Coe, H.: Contributions from transport, solid fuel burning and cooking to primary organic aerosols in two UK cities, Atmos. Chem. Phys., 10, 647-668, 10.5194/acp-10-647-2010, 2010.

Andreae, M. O., and Gelencsér, A.: Black carbon or brown carbon? The nature of light-absorbing carbonaceous aerosols, Atmos. Chem. Phys., 6, 3131-3148, 10.5194/acp-6-3131-2006, 2006.

Bae, M. S., Schwab, J. J., Zhang, Q., Hogrefe, O., Demerjian, K. L., Weimer, S., Rhoads, K., Orsini, D., Venkatachari, P., and Hopke, P. K.: Interference of organic signals in highly time resolved nitrate measurements by low mass resolution aerosol mass spectrometry, J Geophys Res-Atmos, 112, Artn D22305 Doi 10.1029/2007jd008614, 2007.

Bahreini, R., Ervens, B., Middlebrook, A. M., Warneke, C., de Gouw, J. A., DeCarlo, P. F., Jimenez, J. L., Brock, C. A., Neuman, J. A., Ryerson, T. B., Stark, H., Atlas, E., Brioude, J., Fried, A., Holloway, J. S., Peischl, J., Richter, D., Walega, J., Weibring, P., Wollny, A. G., and Fehsenfeld, F. C.: Organic aerosol formation in urban and industrial plumes near Houston and Dallas, Texas, Journal of Geophysical Research: Atmospheres, 114, D00F16, 10.1029/2008JD011493, 2009.

Beddows, D. C. S., Harrison, R. M., Green, D. C., and Fuller, G. W.: Receptor modelling of both particle composition and size distribution from a background site in London, UK, Atmos. Chem. Phys. Discuss., 15, 10123-10162, 10.5194/acpd-15-10123-2015, 2015.

Blanchard, C. L., Hidy, G. M., Tanenbaum, S., Edgerton, E., Hartsell, B., and Jansen, J.: Carbon in southeastern U.S. aerosol particles: Empirical estimates of secondary organic aerosol formation, Atmospheric Environment, 42, 6710-6720, ~~http://dx.doi.org/10.1016/j.atmosenv.2008.04.011,~~dx.doi.org/10.1016/j.atmosenv.2008.04.011, 2008.

Blanchard, C. L., Hidy, G. M., Tanenbaum, S., and Edgerton, E. S.: NMOC, ozone, and organic aerosol in the southeastern United States, 1999-2007: 3. Origins of organic aerosol in Atlanta, Georgia, and surrounding areas, Atmospheric Environment, 45, 1291-1302, DOI 10.1016/j.atmosenv.2010.12.004, 2011.

Blanchard, C. L., Hidy, G. M., Tanenbaum, S., Edgerton, E. S., and Hartsell, B. E.: The Southeastern Aerosol Research and Characterization (SEARCH) study: Spatial variations and chemical climatology, 1999–2010, J Air Waste Manage, 63, 260-275, 10.1080/10962247.2012.749816, 2013.

Bougiatioti, A., Stavroulas, I., Kostenidou, E., Zarmpas, P., Theodosi, C., Kouvarakis, G., Canonaco, F., Prévôt, A. S. H., Nenes, A., Pandis, S. N., and Mihalopoulos, N.: Processing of biomass-burning aerosol in the eastern Mediterranean during summertime, Atmos. Chem. Phys., 14, 4793-4807, 10.5194/acp-14-4793-2014, 2014.

Boyd, C. M., Sanchez, J., Xu, L., Eugene, A. J., Nah, T., Tuet, W. Y., Guzman, M. I., and Ng, N. L.: Secondary Organic Aerosol (SOA) formation from the β-pinene + NO3 system: effect of humidity and peroxy radical fate, Atmos. Chem. Phys. Discuss., 15, 2679-2744, 10.5194/acpd-15-2679-2015, 2015.

Bruns, E. A., Perraud, V., Zelenyuk, A., Ezell, M. J., Johnson, S. N., Yu, Y., Imre, D., Finlayson-Pitts, B. J., and Alexander, M. L.: Comparison of FTIR and Particle Mass Spectrometry for the Measurement of Particulate Organic Nitrates, Environ Sci Technol, 44, 1056-1061, 10.1021/es9029864, 2010.

Budisulistiorini, S. H., Canagaratna, M. R., Croteau, P. L., Marth, W. J., Baumann, K., Edgerton, E. S., Shaw, S. L., Knipping, E. M., Worsnop, D. R., Jayne, J. T., Gold, A., and Surratt, J. D.: Real-Time Continuous Characterization of Secondary Organic Aerosol Derived from Isoprene Epoxydiols in Downtown Atlanta, Georgia, Using the Aerodyne Aerosol Chemical Speciation Monitor, Environ~~.~~ Sci~~.~~ Technol~~.,~~, 47, 5686-5694, Doi 10.1021/~~es400023n~~Es400023n, 2013.

Canagaratna, M. R., Jayne, J. T., Jimenez, J. L., Allan, J. D., Alfarra, M. R., Zhang, Q., Onasch, T. B., Drewnick, F., Coe, H., Middlebrook, A., Delia, A., Williams, L. R., Trimborn, A. M., Northway, M. J., DeCarlo, P. F., Kolb, C. E., Davidovits, P., and Worsnop, D. R.: Chemical and microphysical characterization of ambient aerosols with the aerodyne aerosol mass spectrometer, Mass Spectrometry Reviews, 26, 185-222, 10.1002/mas.20115, 2007.

Canagaratna, M. R., Jimenez, J. L., Kroll, J. H., Chen, Q., Kessler, S. H., Massoli, P., Hildebrandt Ruiz, L., Fortner, E., Williams, L. R., Wilson, K. R., Surratt, J. D., Donahue, N. M., Jayne, J. T., and Worsnop, D. R.: Elemental ratio measurements of organic compounds using aerosol mass spectrometry: characterization, improved calibration, and implications, Atmos. Chem. Phys., 15, 253-272, 10.5194/acp-15-253-2015, 2015.

Chen, Q., Farmer, D. K., Rizzo, L. V., Pauliquevis, T., Kuwata, M., Karl, T. G., Guenther, A., Allan, J. D., Coe, H., Andreae, M. O., Pöschl, U., Jimenez, J. L., Artaxo, P., and Martin, S. T.: Fine-mode organic mass concentrations and sources in the Amazonian wet season (AMAZE-08), Atmos. Chem. Phys. Discuss., 14, 16151-16186, 10.5194/acpd-14-16151-2014, 2014.

Cohan, D., Boylan, J., Marmur, A., and Khan, M.: An Integrated Framework for Multipollutant Air Quality Management and Its Application in Georgia, Environmental Management, 40, 545-554, 10.1007/s00267-006-0228-4, 2007.

Crippa, M., DeCarlo, P. F., Slowik, J. G., Mohr, C., Heringa, M. F., Chirico, R., Poulain, L., Freutel, F., Sciare, J., Cozic, J., Di Marco, C. F., Elsasser, M., Nicolas, J. B., Marchand, N., Abidi, E., Wiedensohler, A., Drewnick, F., Schneider, J., Borrmann, S., Nemitz, E., Zimmermann, R., Jaffrezo, J. L., Prévôt, A. S. H., and Baltensperger, U.: Wintertime aerosol chemical composition and source apportionment of the organic fraction in the metropolitan area of Paris, Atmos. Chem. Phys., 13, 961-981, 10.5194/acp-13-961-2013, 2013.

Crippa, M., Canonaco, F., Lanz, V. A., Äijälä, M., Allan, J. D., Carbone, S., Capes, G., Ceburnis, D., Dall'Osto, M., Day, D. A., DeCarlo, P. F., Ehn, M., Eriksson, A., Freney, E., Hildebrandt Ruiz, L., Hillamo, R., Jimenez, J. L., Junninen, H., Kiendler-Scharr, A., Kortelainen, A. M., Kulmala, M., Laaksonen, A., Mensah, A. A., Mohr, C., Nemitz, E., O'Dowd, C., Ovadnevaite, J., Pandis, S. N., Petäjä, T., Poulain, L., Saarikoski, S., Sellegri, K., Swietlicki, E., Tiitta, P., Worsnop, D. R., Baltensperger, U., and Prévôt, A. S. H.: Organic aerosol components derived from 25 AMS data sets across Europe using a consistent ME-2 based source apportionment approach, Atmos. Chem. Phys., 14, 6159-6176, 10.5194/acp-14-6159-2014, 2014.

~~Cubison, M. J., Ortega, A. M., Hayes, P. L., Farmer, D. K., Day, D., Lechner, M. J., Brune, W. H., Apel, E., Diskin, G. S., Fisher, J. A., Fuelberg, H. E., Hecobian, A., Knapp, D. J., Mikoviny, T., Riemer, D., Sachse, G. W., Sessions, W., Weber, R. J., Weinheimer, A. J., Wisthaler, A., and Jimenez, J. L.: Effects of aging on organic aerosol from open biomass burning smoke in aircraft and laboratory studies, Atmos. Chem. Phys., 11, 12049-12064, 10.5194/acp-11-12049-2011, 2011.~~

Day, D. A., Wooldridge, P. J., Dillon, M. B., Thornton, J. A., and Cohen, R. C.: A thermal dissociation laser-induced fluorescence instrument for in situ detection of NO2, peroxy nitrates, alkyl nitrates, and HNO3, Journal of Geophysical Research: Atmospheres, 107, ACH 4-1-ACH 4-14, 10.1029/2001JD000779, 2002.

DeCarlo, P. F., Kimmel, J. R., Trimborn, A., Northway, M. J., Jayne, J. T., Aiken, A. C., Gonin, M., Fuhrer, K., Horvath, T., Docherty, K. S., Worsnop, D. R., and Jimenez, J. L.: Field-Deployable, High-Resolution, Time-of-Flight Aerosol Mass Spectrometer, Anal Chem, 78, 8281-8289, 10.1021/ac061249n, 2006.

DeWitt, H. L., Hellebust, S., Temime-Roussel, B., Ravier, S., Polo, L., Jacob, V., Buisson, C., Charron, A., André, M., Pasquier, A., Besombes, J. L., Jaffrezo, J. L., Wortham, H., and Marchand, N.: Direct measurements of near-highway emissions in a high diesel environment, Atmos. Chem. Phys. Discuss., 14, 27373-27424, 10.5194/acpd-14-27373-2014, 2014.

Eddingsaas, N. C., VanderVelde, D. G., and Wennberg, P. O.: Kinetics and Products of the Acid-Catalyzed Ring-Opening of Atmospherically Relevant Butyl Epoxy Alcohols, J Phys Chem A, 114, 8106-8113, Doi 10.1021/Jp103907c, 2010.

Edgerton, E. S., Hartsell, B. E., Saylor, R. D., Jansen, J. J., Hansen, D. A., and Hidy, G. M.: The southeastern aerosol research and characterization study: Part II. Filter-based measurements of fine and coarse particulate matter mass and composition, J Air Waste Manage, 55, 1527-1542, 2005.

Ehn, M., Thornton, J. A., Kleist, E., Sipila, M., Junninen, H., Pullinen, I., Springer, M., Rubach, F., Tillmann, R., Lee, B., Lopez-Hilfiker, F., Andres, S., Acir, I.-H., Rissanen, M., Jokinen, T., Schobesberger, S., Kangasluoma, J., Kontkanen, J., Nieminen, T., Kurten, T., Nielsen, L. B., Jorgensen, S., Kjaergaard, H. G., Canagaratna, M., Maso, M. D., Berndt, T., Petaja, T., Wahner, A., Kerminen, V.-M., Kulmala, M., Worsnop, D. R., Wildt, J., and Mentel, T. F.: A large source of low-volatility secondary organic aerosol, Nature, 506, 476-479, 10.1038/nature13032, 2014.

El Haddad, I., D'Anna, B., Temime-Roussel, B., Nicolas, M., Boreave, A., Favez, O., Voisin, D., Sciare, J., George, C., Jaffrezo, J. L., Wortham, H., and Marchand, N.: Towards a better understanding of the origins, chemical composition and aging of oxygenated organic aerosols: case study of a Mediterranean industrialized environment, Marseille, Atmos. Chem. Phys., 13, 7875-7894, 10.5194/acp-13-7875-2013, 2013.

Farmer, D. K., Matsunaga, A., Docherty, K. S., Surratt, J. D., Seinfeld, J. H., Ziemann, P. J., and Jimenez, J. L.: Response of an aerosol mass spectrometer to organonitrates and organosulfates and implications for atmospheric chemistry, Proceedings of the National Academy of Sciences, 107, 6670-6675, 10.1073/pnas.0912340107, 2010.

Feng, Y., Ramanathan, V., and Kotamarthi, V. R.: Brown carbon: a significant atmospheric absorber of solar radiation?, Atmos. Chem. Phys., 13, 8607-8621, 10.5194/acp-13-8607-2013, 2013.

Ford, B., and Heald, C. L.: Aerosol loading in the Southeastern United States: reconciling surface and satellite observations, Atmos Chem Phys, 13, 9269-9283, DOI 10.5194/acp-13-9269-2013, 2013.

Fry, J. L., Kiendler-Scharr, A., Rollins, A. W., Wooldridge, P. J., Brown, S. S., Fuchs, H., Dube, W., Mensah, A., dal Maso, M., Tillmann, R., Dorn, H. P., Brauers, T., and Cohen, R. C.: Organic nitrate and secondary organic aerosol yield from NO3 oxidation of beta-pinene evaluated using a gas-phase kinetics/aerosol partitioning model, Atmos~~.~~ Chem~~.~~ Phys~~.,~~, 9, 1431-1449, 2009.

Fry, J. L., Draper, D. C., Zarzana, K. J., Campuzano-Jost, P., Day, D. A., Jimenez, J. L., Brown, S. S., Cohen, R. C., Kaser, L., Hansel, A., Cappellin, L., Karl, T., Roux, A. H., Turnipseed, A., Cantrell, C., Lefer, B. L., and Grossberg, N.: Observations of gas- and aerosol-phase organic nitrates at BEACHON-RoMBAS 2011, Atmos Chem Phys, 13, 8585-8605, DOI 10.5194/acp-13-8585-2013, 2013.

Gaston, C. J., Riedel, T. P., Zhang, Z., Gold, A., Surratt, J. D., and Thornton, J. A.: Reactive Uptake of an Isoprene-Derived Epoxydiol to Submicron Aerosol Particles, Environ Sci Technol, 48, 11178-11186, 10.1021/es5034266, 2014.

Geron, C., Rasmussen, R., Arnts, R. R., and Guenther, A.: A review and synthesis of monoterpene speciation from forests in the United States, Atmospheric Environment, 34, 1761-1781, Doi 10.1016/S1352-2310(99)00364-7, 2000.

Grieshop, A. P., Donahue, N. M., and Robinson, A. L.: Laboratory investigation of photochemical oxidation of organic aerosol from wood fires 2: analysis of aerosol mass spectrometer data, Atmos. Chem. Phys., 9, 2227-2240, 10.5194/acp-9-2227-2009, 2009.

Guenther, A., Karl, T., Harley, P., Wiedinmyer, C., Palmer, P. I., and Geron, C.: Estimates of global terrestrial isoprene emissions using MEGAN (Model of Emissions of Gases and Aerosols from Nature), Atmos Chem Phys, 6, 3181-3210, 2006.

Guo, H., Xu, L., Bougiatioti, A., Cerully, K. M., Capps, S. L., Hite Jr, J. R., Carlton, A. G., Lee, S. H., Bergin, M. H., Ng, N. L., Nenes, A., and Weber, R. J.: ~~Particle~~Fine-particle water and pH in the southeastern United States, Atmos. Chem. Phys~~. Discuss., 14, 27143-27193~~., 15, 5211-5228, 10.5194/~~acpd-14-27143-2014, 2014~~acp-15-5211-2015, 2015.

Hansen, D. A., Edgerton, E. S., Hartsell, B. E., Jansen, J. J., Kandasamy, N., Hidy, G. M., and Blanchard, C. L.: The southeastern aerosol research and characterization study: Part 1-overview, J Air Waste Manage, 53, 1460-1471, 2003.

Hao, L. Q., Kortelainen, A., Romakkaniemi, S., Portin, H., Jaatinen, A., Leskinen, A., Komppula, M., Miettinen, P., Sueper, D., Pajunoja, A., Smith, J. N., Lehtinen, K. E. J., Worsnop, D. R., Laaksonen, A., and Virtanen, A.: Atmospheric submicron aerosol composition and particulate organic nitrate formation in a boreal forestland–urban mixed region, Atmos. Chem. Phys., 14, 13483-13495, 10.5194/acp-14-13483-2014, 2014.

Hayes, P. L., Ortega, A. M., Cubison, M. J., Froyd, K. D., Zhao, Y., Cliff, S. S., Hu, W. W., Toohey, D. W., Flynn, J. H., Lefer, B. L., Grossberg, N., Alvarez, S., Rappenglueck, B., Taylor, J. W., Allan, J. D., Holloway, J. S., Gilman, J. B., Kuster, W. C., De Gouw, J. A., Massoli, P., Zhang, X., Liu, J., Weber, R. J., Corrigan, A. L., Russell, L. M., Isaacman, G., Worton, D. R., Kreisberg, N. M., Goldstein, A. H., Thalman, R., Waxman, E. M., Volkamer, R., Lin, Y. H., Surratt, J. D., Kleindienst, T. E., Offenberg, J. H., Dusanter, S., Griffith, S., Stevens, P. S., Brioude, J., Angevine, W. M., and Jimenez, J. L.: Organic aerosol composition and sources in Pasadena, California, during the 2010 CalNex campaign, J Geophys Res-Atmos, 118, 9233-9257, Doi 10.1002/Jgrd.50530, 2013.

Hecobian, A., Zhang, X., Zheng, M., Frank, N., Edgerton, E. S., and Weber, R. J.: Water-Soluble Organic Aerosol material and the light-absorption characteristics of aqueous extracts measured over the Southeastern United States, Atmos. Chem. Phys., 10, 5965-5977, 10.5194/acp-10-5965-2010, 2010.

Hennigan, C. J., Sullivan, A. P., Fountoukis, C. I., Nenes, A., Hecobian, A., Vargas, O., Peltier, R. E., Case Hanks, A. T., Huey, L. G., Lefer, B. L., Russell, A. G., and Weber, R. J.: On the volatility and production mechanisms of newly formed nitrate and water soluble organic aerosol in Mexico City, Atmos. Chem. Phys., 8, 3761-3768, 10.5194/acp-8-3761-2008, 2008.

Hennigan, C. J., Bergin, M. H., Russell, A. G., Nenes, A., and Weber, R. J.: Gas/particle partitioning of water-soluble organic aerosol in Atlanta, Atmos Chem Phys, 9, 3613-3628, 2009.

Hennigan, C. J., Miracolo, M. A., Engelhart, G. J., May, A. A., Presto, A. A., Lee, T., Sullivan, A. P., McMeeking, G. R., Coe, H., Wold, C. E., Hao, W. M., Gilman, J. B., Kuster, W. C., de Gouw, J., Schichtel, B. A., Collett Jr, J. L., Kreidenweis, S. M., and Robinson, A. L.: Chemical and physical transformations of organic aerosol from the photo-oxidation of open biomass burning emissions in an environmental chamber, Atmos. Chem. Phys., 11, 7669-7686, 10.5194/acp-11-7669-2011, 2011.

Heringa, M. F., DeCarlo, P. F., Chirico, R., Tritscher, T., Dommen, J., Weingartner, E., Richter, R., Wehrle, G., Prévôt, A. S. H., and Baltensperger, U.: Investigations of primary and secondary particulate matter of different wood combustion appliances with a high-resolution time-of-flight aerosol mass spectrometer, Atmos. Chem. Phys., 11, 5945-5957, 10.5194/acp-11-5945-2011, 2011.

Hidy, G. M., Blanchard, C. L., Baumann, K., Edgerton, E., Tanenbaum, S., Shaw, S., Knipping, E., Tombach, I., Jansen, J., and Walters, J.: Chemical climatology of the southeastern United States, 1999–2013, Atmos. Chem. Phys., 14, 11893-11914, 10.5194/acp-14-11893-2014, 2014.

Hildebrandt, L., Engelhart, G. J., Mohr, C., Kostenidou, E., Lanz, V. A., Bougiatioti, A., DeCarlo, P. F., Prevot, A. S. H., Baltensperger, U., Mihalopoulos, N., Donahue, N. M., and Pandis, S. N.: Aged organic aerosol in the Eastern Mediterranean: the Finokalia Aerosol

Measurement Experiment-2008, Atmos Chem Phys, 10, 4167-4186, DOI 10.5194/acp-10-4167-2010, 2010.

Huang, X. F., He, L. Y., Hu, M., Canagaratna, M. R., Sun, Y., Zhang, Q., Zhu, T., Xue, L., Zeng, L. W., Liu, X. G., Zhang, Y. H., Jayne, J. T., Ng, N. L., and Worsnop, D. R.: Highly time-resolved chemical characterization of atmospheric submicron particles during 2008 Beijing Olympic Games using an Aerodyne High-Resolution Aerosol Mass Spectrometer, Atmos Chem Phys, 10, 8933-8945, DOI 10.5194/acp-10-8933-2010, 2010.

Huffman, J. A., Docherty, K. S., Aiken, A. C., Cubison, M. J., Ulbrich, I. M., DeCarlo, P. F., Sueper, D., Jayne, J. T., Worsnop, D. R., Ziemann, P. J., and Jimenez, J. L.: Chemically-resolved aerosol volatility measurements from two megacity field studies, Atmos Chem Phys, 9, 7161-7182, 2009.

Isaacman, G., Kreisberg, N. M., Yee, L. D., Worton, D. R., Chan, A. W. H., Moss, J. A., Hering, S. V., and Goldstein, A. H.: Online derivatization for hourly measurements of gas- and particle-phase semi-volatile oxygenated organic compounds by thermal desorption aerosol gas chromatography (SV-TAG), Atmos. Meas. Tech., 7, 4417-4429, 10.5194/amt-7-4417-2014, 2014.

Jacobs, M. I., Burke, W. J., and Elrod, M. J.: Kinetics of the reactions of isoprene-derived hydroxynitrates: gas phase epoxide formation and solution phase hydrolysis, Atmos. Chem. Phys., 14, 8933-8946, 10.5194/acp-14-8933-2014, 2014.

Jaeckels, J. M., Bae, M.-S., and Schauer, J. J.: Positive Matrix Factorization (PMF) Analysis of Molecular Marker Measurements to Quantify the Sources of Organic Aerosols, Environ Sci Technol, 41, 5763-5769, 10.1021/es062536b, 2007.

Janssen, R. H. H., Vilà-Guerau de Arellano, J., Jimenez, J. L., Ganzeveld, L. N., Robinson, N. H., Allan, J. D., Coe, H., and Pugh, T. A. M.: Influence of boundary layer dynamics and isoprene chemistry on the organic aerosol budget in a tropical forest, Journal of Geophysical Research: Atmospheres, 118, 9351-9366, 10.1002/jgrd.50672, 2013.

Jathar, S. H., Gordon, T. D., Hennigan, C. J., Pye, H. O. T., Pouliot, G., Adams, P. J., Donahue, N. M., and Robinson, A. L.: Unspeciated organic emissions from combustion sources and their influence on the secondary organic aerosol budget in the United States, P Natl Acad Sci USA, 111, 10473-10478, DOI 10.1073/pnas.1323740111, 2014.

Jayne, J. T., Leard, D. C., Zhang, X. F., Davidovits, P., Smith, K. A., Kolb, C. E., and Worsnop, D. R.: Development of an aerosol mass spectrometer for size and composition analysis of submicron particles, Aerosol Sci Tech, 33, 49-70, Doi 10.1080/027868200410840, 2000.

Jimenez, J. L., Canagaratna, M. R., Donahue, N. M., Prevot, A. S. H., Zhang, Q., Kroll, J. H., DeCarlo, P. F., Allan, J. D., Coe, H., Ng, N. L., Aiken, A. C., Docherty, K. S., Ulbrich, I. M., Grieshop, A. P., Robinson, A. L., Duplissy, J., Smith, J. D., Wilson, K. R., Lanz, V. A., Hueglin, C., Sun, Y. L., Tian, J., Laaksonen, A., Raatikainen, T., Rautiainen, J., Vaattovaara, P., Ehn, M., Kulmala, M., Tomlinson, J. M., Collins, D. R., Cubison, M. J., Dunlea, E. J., Huffman, J. A., Onasch, T. B., Alfarra, M. R., Williams, P. I., Bower, K., Kondo, Y., Schneider, J., Drewnick, F., Borrmann, S., Weimer, S., Demerjian, K., Salcedo, D., Cottrell, L., Griffin, R., Takami, A., Miyoshi, T., Hatakeyama, S., Shimono, A., Sun, J. Y., Zhang, Y. M., Dzepina, K., Kimmel, J. R., Sueper, D., Jayne, J. T., Herndon, S. C., Trimborn, A. M., Williams, L. R., Wood, E. C., Middlebrook, A. M., Kolb, C. E., Baltensperger, U., and Worsnop, D. R.: Evolution of Organic Aerosols in the Atmosphere, Science, 326, 1525-1529, DOI 10.1126/science.1180353, 2009.

Kroll, J. H., Ng, N. L., Murphy, S. M., Flagan, R. C., and Seinfeld, J. H.: Secondary organic aerosol formation from isoprene photooxidation, Environ Sci Technol, 40, 1869-1877, Doi 10.1021/Es0524301, 2006.

Kroll, J. H., Donahue, N. M., Jimenez, J. L., Kessler, S. H., Canagaratna, M. R., Wilson, K. R., Altieri, K. E., Mazzoleni, L. R., Wozniak, A. S., Bluhm, H., Mysak, E. R., Smith, J. D., Kolb, C. E., and Worsnop, D. R.: Carbon oxidation state as a metric for describing the chemistry of atmospheric organic aerosol, Nat Chem, 3, 133-139, Doi 10.1038/Nchem.948, 2011.

Lack, D. A., Bahreini, R., Langridge, J. M., Gilman, J. B., and Middlebrook, A. M.: Brown carbon absorption linked to organic mass tracers in biomass burning particles, Atmos. Chem. Phys., 13, 2415-2422, 10.5194/acp-13-2415-2013, 2013.

Lanz, V. A., Alfarra, M. R., Baltensperger, U., Buchmann, B., Hueglin, C., and Prevot, A. S. H.: Source apportionment of submicron organic aerosols at an urban site by factor analytical modelling of aerosol mass spectra, Atmos Chem Phys, 7, 1503-1522, 2007.

Li, Y. J., Lee, B. P., Su, L., Fung, J. C. H., and Chan, C. K.: Seasonal characteristics of fine particulate matter (PM) based on high-resolution time-of-flight aerosol mass spectrometric (HR-ToF-AMS) measurements at the HKUST Supersite in Hong Kong, Atmos. Chem. Phys., 15, 37-53, 10.5194/acp-15-37-2015, 2015.

Lim, H.-J., and Turpin, B. J.: Origins of Primary and Secondary Organic Aerosol in Atlanta: Results of Time-Resolved Measurements during the Atlanta Supersite Experiment, Environ Sci Technol, 36, 4489-4496, 10.1021/es0206487, 2002.

Lin, Y.-H., Budisulistiorini, S. H., Chu, K., Siejack, R. A., Zhang, H., Riva, M., Zhang, Z., Gold, A., Kautzman, K. E., and Surratt, J. D.: Light-Absorbing Oligomer Formation in Secondary

Organic Aerosol from Reactive Uptake of Isoprene Epoxydiols, Environ Sci Technol, 48, 12012-12021, 10.1021/es503142b, 2014.

Lin, Y. H., Zhang, Z. F., Docherty, K. S., Zhang, H. F., Budisulistiorini, S. H., Rubitschun, C. L., Shaw, S. L., Knipping, E. M., Edgerton, E. S., Kleindienst, T. E., Gold, A., and Surratt, J. D.: Isoprene Epoxydiols as Precursors to Secondary Organic Aerosol Formation: Acid-Catalyzed Reactive Uptake Studies with Authentic Compounds, Environ Sci Technol, 46, 250-258, Doi 10.1021/Es202554c, 2012.

Liu, J., Scheuer, E., Dibb, J., Ziemba, L. D., Thornhill, K. L., Anderson, B. E., Wisthaler, A., Mikoviny, T., Devi, J. J., Bergin, M., and Weber, R. J.: Brown carbon in the continental troposphere, Geophysical Research Letters, 41, 2013GL058976, 10.1002/2013GL058976, 2014.

Liu, S., Day, D. A., Shields, J. E., and Russell, L. M.: Ozone-driven daytime formation of secondary organic aerosol containing carboxylic acid groups and alkane groups, Atmos Chem Phys, 11, 8321-8341, DOI 10.5194/acp-11-8321-2011, 2011.

Liu, Y., Kuwata, M., Strick, B. F., Geiger, F. M., Thomson, R. J., McKinney, K. A., and Martin, S. T.: Uptake of Epoxydiol Isomers Accounts for Half of the Particle-Phase Material Produced from Isoprene Photooxidation via the HO2 Pathway, Environ Sci Technol, 49, 250-258, 10.1021/es5034298, 2015.

Mao, J., Ren, X., Zhang, L., Van Duin, D. M., Cohen, R. C., Park, J. H., Goldstein, A. H., Paulot, F., Beaver, M. R., Crounse, J. D., Wennberg, P. O., DiGangi, J. P., Henry, S. B., Keutsch, F. N., Park, C., Schade, G. W., Wolfe, G. M., Thornton, J. A., and Brune, W. H.: Insights into hydroxyl measurements and atmospheric oxidation in a California forest, Atmos. Chem. Phys., 12, 8009-8020, 10.5194/acp-12-8009-2012, 2012.

Matthew, B. M., Middlebrook, A. M., and Onasch, T. B.: Collection efficiencies in an Aerodyne Aerosol Mass Spectrometer as a function of particle phase for laboratory generated aerosols, Aerosol Sci~~. Technol.,~~ Tech, 42, 884-898, Doi 10.1080/02786820802356797, 2008.

May, A. A., Saleh, R., Hennigan, C. J., Donahue, N. M., and Robinson, A. L.: Volatility of Organic Molecular Markers Used for Source Apportionment Analysis: Measurements and Implications for Atmospheric Lifetime, Environ Sci Technol, 46, 12435-12444, 10.1021/es302276t, 2012.

Middlebrook, A. M., Bahreini, R., Jimenez, J. L., and Canagaratna, M. R.: Evaluation of Composition-Dependent Collection Efficiencies for the Aerodyne Aerosol Mass Spectrometer using Field Data, Aerosol Sci~~. Technol.,~~ Tech, 46, 258-271, Doi 10.1080/02786826.2011.620041, 2012.

Mohr, C., Huffman, J. A., Cubison, M. J., Aiken, A. C., Docherty, K. S., Kimmel, J. R., Ulbrich, I. M., Hannigan, M., and Jimenez, J. L.: Characterization of Primary Organic Aerosol Emissions from Meat Cooking, Trash Burning, and Motor Vehicles with High-Resolution Aerosol Mass Spectrometry and Comparison with Ambient and Chamber Observations, Environ Sci Technol, 43, 2443-2449, 10.1021/es8011518, 2009.

Mohr, C., DeCarlo, P. F., Heringa, M. F., Chirico, R., Slowik, J. G., Richter, R., Reche, C., Alastuey, A., Querol, X., Seco, R., Peñuelas, J., Jiménez, J. L., Crippa, M., Zimmermann, R., Baltensperger, U., and Prévôt, A. S. H.: Identification and quantification of organic aerosol from cooking and other sources in Barcelona using aerosol mass spectrometer data, Atmos. Chem. Phys., 12, 1649-1665, 10.5194/acp-12-1649-2012, 2012.

Ng, N. L., Canagaratna, M. R., Zhang, Q., Jimenez, J. L., Tian, J., Ulbrich, I. M., Kroll, J. H., Docherty, K. S., Chhabra, P. S., Bahreini, R., Murphy, S. M., Seinfeld, J. H., Hildebrandt, L., Donahue, N. M., DeCarlo, P. F., Lanz, V. A., Prevot, A. S. H., Dinar, E., Rudich, Y., and Worsnop, D. R.: Organic aerosol components observed in Northern Hemispheric datasets from Aerosol Mass Spectrometry, Atmos Chem Phys, 10, 4625-4641, DOI 10.5194/acp-10-4625-2010, 2010.

Ng, N. L., Herndon, S. C., Trimborn, A., Canagaratna, M. R., Croteau, P. L., Onasch, T. B., Sueper, D., Worsnop, D. R., Zhang, Q., Sun, Y. L., and Jayne, J. T.: An Aerosol Chemical Speciation Monitor (ACSM) for Routine Monitoring of the Composition and Mass Concentrations of Ambient Aerosol, Aerosol Sci Tech, 45, 780-794, Pii 934555189 Doi 10.1080/02786826.2011.560211, 2011.

Nguyen, T. B., Coggon, M. M., Bates, K. H., Zhang, X., Schwantes, R. H., Schilling, K. A., Loza, C. L., Flagan, R. C., Wennberg, P. O., and Seinfeld, J. H.: Organic aerosol formation from the reactive uptake of isoprene epoxydiols (IEPOX) onto non-acidified inorganic seeds, Atmos. Chem. Phys., 14, 3497-3510, 10.5194/acp-14-3497-2014, 2014.

Nordin, E. Z., Eriksson, A. C., Roldin, P., Nilsson, P. T., Carlsson, J. E., Kajos, M. K., Hellén, H., Wittbom, C., Rissler, J., Löndahl, J., Swietlicki, E., Svenningsson, B., Bohgard, M., Kulmala, M., Hallquist, M., and Pagels, J. H.: Secondary organic aerosol formation from idling gasoline passenger vehicle emissions investigated in a smog chamber, Atmos. Chem. Phys., 13, 6101-6116, 10.5194/acp-13-6101-2013, 2013.

Orsini, D. A., Ma, Y. L., Sullivan, A., Sierau, B., Baumann, K., and Weber, R. J.: Refinements to the particle-into-liquid sampler (PILS) for ground and airborne measurements of water soluble aerosol composition, Atmospheric Environment, 37, 1243-1259, Doi 10.1016/S1352-2310(02)01015-4, 2003.

Paatero, P., and Tapper, U.: Positive Matrix Factorization - a Nonnegative Factor Model with Optimal Utilization of Error-Estimates of Data Values, Environmetrics, 5, 111-126, DOI 10.1002/env.3170050203, 1994.

Paatero, P.: A weighted non-negative least squares algorithm for three-way 'PARAFAC' factor analysis, Chemometr Intell Lab, 38, 223-242, Doi 10.1016/S0169-7439(97)00031-2, 1997.

Paglione, M., Kiendler-Scharr, A., Mensah, A. A., Finessi, E., Giulianelli, L., Sandrini, S., Facchini, M. C., Fuzzi, S., Schlag, P., Piazzalunga, A., Tagliavini, E., Henzing, J. S., and Decesari, S.: Identification of humic-like substances (HULIS) in oxygenated organic aerosols using NMR and AMS factor analyses and liquid chromatographic techniques, Atmos. Chem. Phys., 14, 25-45, 10.5194/acp-14-25-2014, 2014.

Paulot, F., Crounse, J. D., Kjaergaard, H. G., Kurten, A., St Clair, J. M., Seinfeld, J. H., and Wennberg, P. O.: Unexpected Epoxide Formation in the Gas-Phase Photooxidation of Isoprene, Science, 325, 730-733, DOI 10.1126/science.1172910, 2009.

Perring, A. E., Pusede, S. E., and Cohen, R. C.: An Observational Perspective on the Atmospheric Impacts of Alkyl and Multifunctional Nitrates on Ozone and Secondary Organic Aerosol, Chem Rev, 113, 5848-5870, Doi 10.1021/Cr300520x, 2013.

Piletic, I. R., Edney, E. O., and Bartolotti, L. J.: A computational study of acid catalyzed aerosol reactions of atmospherically relevant epoxides, Phys Chem Chem Phys, 15, 18065-18076, 10.1039/C3CP52851K, 2013.

Platt, S. M., El Haddad, I., Zardini, A. A., Clairotte, M., Astorga, C., Wolf, R., Slowik, J. G., Temime-Roussel, B., Marchand, N., Jezek, I., Drinovec, L., Mocnik, G., Mohler, O., Richter, R., Barmet, P., Bianchi, F., Baltensperger, U., and Prevot, A. S. H.: Secondary organic aerosol formation from gasoline vehicle emissions in a new mobile environmental reaction chamber, Atmos Chem Phys, 13, 9141-9158, DOI 10.5194/acp-13-9141-2013, 2013.

Presto, A. A., Gordon, T. D., and Robinson, A. L.: Primary to secondary organic aerosol: evolution of organic emissions from mobile combustion sources, Atmos. Chem. Phys., 14, 5015-5036, 10.5194/acp-14-5015-2014, 2014.

Raatikainen, T., Vaattovaara, P., Tiitta, P., Miettinen, P., Rautiainen, J., Ehn, M., Kulmala, M., Laaksonen, A., and Worsnop, D. R.: Physicochemical properties and origin of organic groups detected in boreal forest using an aerosol mass spectrometer, Atmos. Chem. Phys., 10, 2063-2077, 10.5194/acp-10-2063-2010, 2010.

Robinson, A. L., Donahue, N. M., Shrivastava, M. K., Weitkamp, E. A., Sage, A. M., Grieshop, A. P., Lane, T. E., Pierce, J. R., and Pandis, S. N.: Rethinking organic aerosols: Semivolatile emissions and photochemical aging, Science, 315, 1259-1262, DOI 10.1126/science.1133061, 2007.

Robinson, N. H., Hamilton, J. F., Allan, J. D., Langford, B., Oram, D. E., Chen, Q., Docherty, K., Farmer, D. K., Jimenez, J. L., Ward, M. W., Hewitt, C. N., Barley, M. H., Jenkin, M. E., Rickard, A. R., Martin, S. T., McFiggans, G., and Coe, H.: Evidence for a significant proportion of Secondary Organic Aerosol from isoprene above a maritime tropical forest, Atmos Chem Phys, 11, 1039-1050, DOI 10.5194/acp-11-1039-2011, 2011a.

Robinson, N. H., Newton, H. M., Allan, J. D., Irwin, M., Hamilton, J. F., Flynn, M., Bower, K. N., Williams, P. I., Mills, G., Reeves, C. E., McFiggans, G., and Coe, H.: Source attribution of Bornean air masses by back trajectory analysis during the OP3 project, Atmos. Chem. Phys., 11, 9605-9630, 10.5194/acp-11-9605-2011, 2011b.

Rollins, A. W., Fry, J. L., Hunter, J. F., Kroll, J. H., Worsnop, D. R., Singaram, S. W., and Cohen, R. C.: Elemental analysis of aerosol organic nitrates with electron ionization high-resolution mass spectrometry, Atmos Meas Tech, 3, 301-310, 2010.

Rollins, A. W., Browne, E. C., Min, K.-E., Pusede, S. E., Wooldridge, P. J., Gentner, D. R., Goldstein, A. H., Liu, S., Day, D. A., Russell, L. M., and Cohen, R. C.: Evidence for NOx Control over Nighttime SOA Formation, Science, 337, 1210-1212, 10.1126/science.1221520, 2012.

Russell, A., Holmes, H., Friberg, M., Ivey, C., Hu, Y., Balachandran, S., Mulholland, J., Tolbert, P., Sarnat, J., Sarnat, S., Strickland, M., Chang, H., and Liu, Y.: Use of Air Quality Modeling Results in Health Effects Research, in: Air Pollution Modeling and its Application XXIII, edited by: Steyn, D., and Mathur, R., Springer Proceedings in Complexity, Springer International Publishing, 1-5, 2014.

Sato, K., Takami, A., Isozaki, T., Hikida, T., Shimono, A., and Imamura, T.: Mass spectrometric study of secondary organic aerosol formed from the photo-oxidation of aromatic hydrocarbons, Atmospheric Environment, 44, 1080-1087, ~~http://dx.doi.org/10.1016/j.atmosenv.2009.12.013,~~dx.doi.org/10.1016/j.atmosenv.2009.12.013, 2010.

Schichtel, B. A., Malm, W. C., Bench, G., Fallon, S., McDade, C. E., Chow, J. C., and Watson, J. G.: Fossil and contemporary fine particulate carbon fractions at 12 rural and urban sites in the United States, Journal of Geophysical Research: Atmospheres, 113, D02311, 10.1029/2007JD008605, 2008.

Schneider, J., Weimer, S., Drewnick, F., Borrmann, S., Helas, G., Gwaze, P., Schmid, O., Andreae, M. O., and Kirchner, U.: Mass spectrometric analysis and aerodynamic properties of various types of combustion-related aerosol particles, Int J Mass Spectrom, 258, 37-49, ~~http://dx.doi.org/10.1016/j.ijms.2006.07.008,~~dx.doi.org/10.1016/j.ijms.2006.07.008, 2006.

Setyan, A., Zhang, Q., Merkel, M., Knighton, W. B., Sun, Y., Song, C., Shilling, J. E., Onasch, T. B., Herndon, S. C., Worsnop, D. R., Fast, J. D., Zaveri, R. A., Berg, L. K., Wiedensohler, A., Flowers, B. A., Dubey, M. K., and Subramanian, R.: Characterization of submicron particles influenced by mixed biogenic and anthropogenic emissions using high-resolution aerosol mass spectrometry: results from CARES, Atmos Chem Phys, 12, 8131-8156, DOI 10.5194/acp-12-8131-2012, 2012.

Slowik, J. G., Vlasenko, A., McGuire, M., Evans, G. J., and Abbatt, J. P. D.: Simultaneous factor analysis of organic particle and gas mass spectra: AMS and PTR-MS measurements at an urban site, Atmos Chem Phys, 10, 1969-1988, 2010.

Slowik, J. G., Brook, J., Chang, R. Y. W., Evans, G. J., Hayden, K., Jeong, C. H., Li, S. M., Liggio, J., Liu, P. S. K., McGuire, M., Mihele, C., Sjostedt, S., Vlasenko, A., and Abbatt, J. P. D.: Photochemical processing of organic aerosol at nearby continental sites: contrast between urban plumes and regional aerosol, Atmos Chem Phys, 11, 2991-3006, DOI 10.5194/acp-11-2991-2011, 2011.

Sun, Y. L., Zhang, Q., Schwab, J. J., Chen, W. N., Bae, M. S., Hung, H. M., Lin, Y. C., Ng, N. L., Jayne, J., Massoli, P., Williams, L. R., and Demerjian, K. L.: Characterization of near-highway submicron aerosols in New York City with a high-resolution aerosol mass spectrometer, Atmos. Chem. Phys., 12, 2215-2227, 10.5194/acp-12-2215-2012, 2012a.

Sun, Y. L., Zhang, Q., Schwab, J. J., Yang, T., Ng, N. L., and Demerjian, K. L.: Factor analysis of combined organic and inorganic aerosol mass spectra from high resolution aerosol mass spectrometer measurements, Atmos. Chem. Phys., 12, 8537-8551, 10.5194/acp-12-8537-2012, 2012b.

Surratt, J. D., Lewandowski, M., Offenberg, J. H., Jaoui, M., Kleindienst, T. E., Edney, E. O., and Seinfeld, J. H.: Effect of acidity on secondary organic aerosol formation from isoprene, Environ Sci Technol, 41, 5363-5369, Doi 10.1021/Es0704176, 2007.

Tsigaridis, K., Daskalakis, N., Kanakidou, M., Adams, P. J., Artaxo, P., Bahadur, R., Balkanski, Y., Bauer, S. E., Bellouin, N., Benedetti, A., Bergman, T., Berntsen, T. K., Beukes, J. P., Bian, H., Carslaw, K. S., Chin, M., Curci, G., Diehl, T., Easter, R. C., Ghan, S. J., Gong, S. L., Hodzic, A., Hoyle, C. R., Iversen, T., Jathar, S., Jimenez, J. L., Kaiser, J. W., Kirkevåg, A., Koch, D., Kokkola, H., Lee, Y. H., Lin, G., Liu, X., Luo, G., Ma, X., Mann, G. W., Mihalopoulos, N., Morcrette, J. J., Müller, J. F., Myhre, G., Myriokefalitakis, S., Ng, N. L., O'Donnell, D., Penner, J. E., Pozzoli, L., Pringle, K. J., Russell, L. M., Schulz, M., Sciare, J., Seland, Ø., Shindell, D. T., Sillman, S., Skeie, R. B., Spracklen, D., Stavrakou, T., Steenrod, S. D., Takemura, T., Tiitta, P., Tilmes, S., Tost, H., van Noije, T., van Zyl, P. G., von Salzen, K., Yu, F., Wang, Z., Wang, Z., Zaveri, R. A., Zhang, H., Zhang, K., Zhang, Q., and Zhang, X.: The AeroCom evaluation and intercomparison of organic aerosol in global models, Atmos. Chem. Phys., 14, 10845-10895, 10.5194/acp-14-10845-2014, 2014.

Ulbrich, I. M., Canagaratna, M. R., Zhang, Q., Worsnop, D. R., and Jimenez, J. L.: Interpretation of organic components from Positive Matrix Factorization of aerosol mass spectrometric data, Atmos. Chem. Phys., 9, 2891-2918, 10.5194/acp-9-2891-2009, 2009.

Verma, V., Fang, T., Guo, H., King, L., Bates, J. T., Peltier, R. E., Edgerton, E., Russell, A. G., and Weber, R. J.: Reactive oxygen species associated with water-soluble PM2.5 in the southeastern United States: spatiotemporal trends and source apportionment, Atmos. Chem. Phys., 14, 12915-12930, 10.5194/acp-14-12915-2014, 2014.

Verma, V., Fang, T., Xu, L., Peltier, R. E., Russell, A. G., Ng, N. L., and Weber, R. J.: Organic Aerosols Associated with the Generation of Reactive Oxygen Species (ROS) by Water-Soluble PM2.5, Environ Sci Technol, 10.1021/es505577w, 2015.

Virkkula, A., Mäkelä, T., Hillamo, R., Yli-Tuomi, T., Hirsikko, A., Hämeri, K., and Koponen, I. K.: A Simple Procedure for Correcting Loading Effects of Aethalometer Data, J Air Waste Manage, 57, 1214-1222, 10.3155/1047-3289.57.10.1214, 2007.

Visser, S., Slowik, J. G., Furger, M., Zotter, P., Bukowiecki, N., Canonaco, F., Flechsig, U., Appel, K., Green, D. C., Tremper, A. H., Young, D. E., Williams, P. I., Allan, J. D., Coe, H., Williams, L. R., Mohr, C., Xu, L., Ng, N. L., Nemitz, E., Barlow, J. F., Halios, C. H., Fleming, Z. L., Baltensperger, U., and Prévôt, A. S. H.: Advanced source apportionment of size-resolved trace elements at multiple sites in London during winter, Atmos. Chem. Phys. Discuss., 15, 14733-14781, 10.5194/acpd-15-14733-2015, 2015.

Washenfelder, R. A., Attwood, A. R., Brock, C. A., Guo, H., Xu, L., Weber, R. J., Ng, N. L., Allen, H. M., Ayres, B. R., Baumann, K., Cohen, R. C., Draper, D. C., Duffey, K. C., Edgerton, E., Fry, J. L., Hu, W. W., Jimenez, J. L., Palm, B. B., Romer, P., Stone, E. A., Wooldridge, P. J., and Brown, S. S.: Biomass burning dominates brown carbon absorption in the rural southeastern United States, Geophysical Research Letters, 2014GL062444, 10.1002/2014GL062444, 2015.

Weber, R.: Short-Term Temporal Variation in PM2.5 Mass and Chemical Composition during the Atlanta Supersite Experiment, 1999, J Air Waste Manage, 53, 84-91, 10.1080/10473289.2003.10466123, 2003.

Weber, R., Orsini, D., Duan, Y., Baumann, K., Kiang, C. S., Chameides, W., Lee, Y. N., Brechtel, F., Klotz, P., Jongejan, P., ten Brink, H., Slanina, J., Boring, C. B., Genfa, Z., Dasgupta, P., Hering, S., Stolzenburg, M., Dutcher, D. D., Edgerton, E., Hartsell, B., Solomon, P., and Tanner, R.: Intercomparison of near real time monitors of PM2.5 nitrate and sulfate at the U.S. Environmental Protection Agency Atlanta Supersite, Journal of Geophysical Research: Atmospheres, 108, 8421, 10.1029/2001JD001220, 2003.

Weber, R. J., Orsini, D., Daun, Y., Lee, Y. N., Klotz, P. J., and Brechtel, F.: A particle-into-liquid collector for rapid measurement of aerosol bulk chemical composition, Aerosol Sci Tech, 35, 718-727, Doi 10.1080/02786820152546761, 2001.

Weber, R. J., Sullivan, A. P., Peltier, R. E., Russell, A., Yan, B., Zheng, M., de Gouw, J., Warneke, C., Brock, C., Holloway, J. S., Atlas, E. L., and Edgerton, E.: A study of secondary organic aerosol formation in the anthropogenic-influenced southeastern United States, J Geophys Res-Atmos, 112, Artn D13302 Doi 10.1029/2007jd008408, 2007.

Winquist, A., Kirrane, E., Klein, M., Strickland, M., Darrow, L. A., Sarnat, S. E., Gass, K., Mulholland, J., Russell, A., and Tolbert, P.: Joint Effects of Ambient Air Pollutants on Pediatric Asthma Emergency Department Visits in Atlanta, 1998–2004, Epidemiology, 25, 666-673, 10.1097/ede.0000000000000146, 2014.

Xu, L., Kollman, M. S., Song, C., Shilling, J. E., and Ng, N. L.: Effects of NOx on the Volatility of Secondary Organic Aerosol from Isoprene Photooxidation, Environ Sci Technol, 48, 2253-2262, 10.1021/es404842g, 2014.

Xu, L., Guo, H., Boyd, C. M., Klein, M., Bougiatioti, A., Cerully, K. M., Hite, J. R., Isaacman-VanWertz, G., Kreisberg, N. M., Knote, C., Olson, K., Koss, A., Goldstein, A. H., Hering, S. V., de Gouw, J., Baumann, K., Lee, S.-H., Nenes, A., Weber, R. J., and Ng, N. L.: Effects of anthropogenic emissions on aerosol formation from isoprene and monoterpenes in the southeastern United States, Proceedings of the National Academy of Sciences, 112, 37-42, 10.1073/pnas.1417609112, 2015.

Zhang, Q., Alfarra, M. R., Worsnop, D. R., Allan, J. D., Coe, H., Canagaratna, M. R., and Jimenez, J. L.: Deconvolution and Quantification of Hydrocarbon-like and Oxygenated Organic Aerosols Based on Aerosol Mass Spectrometry, Environ Sci Technol, 39, 4938-4952, 10.1021/es048568l, 2005.

Zhang, Q., Jimenez, J. L., Canagaratna, M. R., Ulbrich, I. M., Ng, N. L., Worsnop, D. R., and Sun, Y. L.: Understanding atmospheric organic aerosols via factor analysis of aerosol mass spectrometry: a review, Anal Bioanal Chem, 401, 3045-3067, DOI 10.1007/s00216-011-5355-y, 2011.

Zhang, X., Hecobian, A., Zheng, M., Frank, N. H., and Weber, R. J.: Biomass burning impact on PM 2.5 over the southeastern US during 2007: integrating chemically speciated FRM filter measurements, MODIS fire counts and PMF analysis, Atmos. Chem. Phys., 10, 6839-6853, 10.5194/acp-10-6839-2010, 2010.

Zhang, X., Liu, Z., Hecobian, A., Zheng, M., Frank, N. H., Edgerton, E. S., and Weber, R. J.: Spatial and seasonal variations of fine particle water-soluble organic carbon (WSOC) over the southeastern United States: implications for secondary organic aerosol formation, Atmos. Chem. Phys., 12, 6593-6607, 10.5194/acp-12-6593-2012, 2012.

Zhao, R., Mungall, E. L., Lee, A. K. Y., Aljawhary, D., and Abbatt, J. P. D.: Aqueous-phase photooxidation of levoglucosan – a mechanistic study using aerosol time-of-flight chemical ionization mass spectrometry (Aerosol ToF-CIMS), Atmos. Chem. Phys., 14, 9695-9706, 10.5194/acp-14-9695-2014, 2014.

Zheng, M., Cass, G. R., Schauer, J. J., and Edgerton, E. S.: Source Apportionment of PM2.5 in the Southeastern United States Using Solvent-Extractable Organic Compounds as Tracers, Environ Sci Technol, 36, 2361-2371, 10.1021/es011275x, 2002.

Zheng, M., Ke, L., Edgerton, E. S., Schauer, J. J., Dong, M., and Russell, A. G.: Spatial distribution of carbonaceous aerosol in the southeastern United States using molecular markers and carbon isotope data, Journal of Geophysical Research: Atmospheres, 111, D10S06, 10.1029/2005JD006777, 2006.

Zotter, P., El-Haddad, I., Zhang, Y., Hayes, P. L., Zhang, X., Lin, Y.-H., Wacker, L., Schnelle-Kreis, J., Abbaszade, G., Zimmermann, R., Surratt, J. D., Weber, R., Jimenez, J. L., Szidat, S., Baltensperger, U., and Prévôt, A. S. H.: Diurnal cycle of fossil and nonfossil carbon using radiocarbon analyses during CalNex, Journal of Geophysical Research: Atmospheres, 119, 2013JD021114, 10.1002/2013JD021114, 2014.

Table Captions

Table 1: Sampling sites and periods for the SCAPE and SOAS studies. Campaign average meteorological conditions, mixing ratios of gas-phase species, and mass concentrations of black carbon and NR-PM_1 species for all datasets. Average ± one standard deviation are reported.

Table 2: A summary of organic nitrates estimation from NO_x^+ ratio method. R_{AN} represents the NO_x^+ ratio ($=NO^+/NO_2^+$) for pure ammonium nitrate (AN). R_{meas} represents the NO_x^+ ratio from observation. $NO_{3,meas}$ represents the total nitrate functionality (from both organic and inorganic nitrates) as measured by the HR-ToF-AMS. $NO_{3,org}$ represents the nitrate functionality from organic nitrates, which is estimated from the NO_x^+ ratio method. ON and OA represent organic nitrate and organic aerosol, respectively.

Table 1.

AMS sampling site		Jefferson Street	Centreville	Yorkville	Georgia Tech	Jefferson Street	Yorkville	Roadside
Sampling period		5/10/2012 - 6/2/2012	6/1/2013- 7/15/2013	6/26/2012 - 7/20/2012	7/20/2012 - 9/4/2012	11/6/2012 - 12/4/2012	12/5/2012 - 1/10/2013	1/26/2013 - 2/28/2013
Abbreviation		JST_May	CTR_June	YRK_July	GT_Aug	JST_Nov	YRK_Dec	RS_Jan
Met[a]	T (°C)[b]	23.0 ± 4.3	24.7 ± 4.3	26.9 ± 4.5	26.1 ± 3.5	11.3 ± 5.0	7.8 ± 5.5	8.1 ± 4.8
	RH(%)	65.8 ± 19.3	82.9 ± 15.3	61.9 ± 18.5	71.2 ± 17.2	64.5 ± 20.6	74.2 ± 20.1	64.6 ± 25.3
	WS ($m\ s^{-1}$)	1.6 ± 1.1	1.9 ± 0.9	2.3 ± 1.1	1.3 ± 0.8	1.3 ± 0.9	3.4 ± 1.7	2.1 ± 1.4
Gas (ppb)	NO	4.1 ± 13.0	0.1 ± 0.2	0.1 ± 0.1	N/A	32.1 ± 60.2	0.3 ± 0.8	N/A
	NO_2	10.3 ± 10.3	0.6 ± 0.6	1.1 ± 0.8	N/A	18.4 ± 12.8	3.0 ± 3.0	N/A
	SO_2	0.4 ± 0.7	0.3 ± 0.7	0.4 ± 0.5	N/A	1.2 ± 1.7	0.6 ± 1.1	N/A
	O_3	39.0 ± 21.9	26.4 ± 12.4	41.1 ± 17.0	N/A	18.8 ± 14.5	28.8 ± 8.3	N/A
$PM_{2.5}$ ($\mu g\ m^{-3}$)	~~BC[b]~~BC[c]	N/A	0.2 ± 0.2	N/A	0.9 ± 0.~~6~~7	0.9 ± 1.0~~.9~~	0.4 ± 0.3	1.3 ± 1.0
$NR\text{-}PM_1$ ($\mu g\ m^{-3}$)	SO_4	3.0 ± 1.5	1.9 ± 1.4	3.5 ± 1.8	4.0 ± 2.1	1.7 ± 0.9	1.4 ± 1.0	1.6 ± 1.2
	NO_3	0.4 ± 0.3	0.1 ± 0.1	0.3 ± 0.2	0.4 ± 0.4	1.2 ± 1.1	0.8 ± 0.8	1.4 ± 1.3
	NH_4	1.1 ± 0.5	0.4 ± 0.3	1.1 ± 0.5	1.2 ± 0.6	0.9 ± 0.6	0.6 ± 0.5	0.9 ± 0.6
	Chl	0.03 ± 0.03	0.01 ± 0.01	0.03 ± 0.03	0.02 ± 0.01	0.06 ± 0.07	0.04 ± 0.07	0.06 ± 0.11
	Org	9.1 ± 4.3	5.0 ± 4.0	11.2 ± 6.4	9.6 ± 4.4	7.9 ± 5.1	3.2 ± 2.3	4.7 ± 3.6

[a] Meteorological data at JST and YRK are recorded by Atmospheric Research & Analysis (ARA). Meteorological data at GT and RS are from JST during the same periods.

~~b~~[b] The numbers reported in the table are campaign-averaged values based on high temporal resolution data (1 - 60min depending on instrument).

[c] Black carbon concentration was measured by a seven-wavelength Aethalometer at GT_Aug and JST_Nov and by a multi-angle absorption photometer (MAAP) at CTR_June, YRK_Dec, and RS_Jan.

Table 2.

Site	R_{AN}[a]	R_{meas}	R with LO-OOA		$NO_{3,org}$ conc. ($\mu g\ m^{-3}$)[d]		$NO_{3,org}/NO_{3,meas}$		ON/OA[e]	
			$NO_{3,meas}$	$NO_{3,org}$[b]	lower	upper	lower	upper	lower	upper
JST_May	1.73	4.47	0.68	0.78	0.19	0.27	0.55	0.76	0.07	0.14
CTR_June[c]	2.93	7.10	0.76	0.84	0.06	0.08	0.80	1.00	0.06	0.10
YRK_July	2.24	5.45	0.66	0.83	0.18	0.28	0.63	1.00	0.05	0.12
GT_Aug	2.26	6.17	0.56	0.70	0.21	0.33	0.64	0.99	0.07	0.16
JST_Nov	1.95	3.12	0.14	0.63	0.23	0.25	0.19	0.21	0.09	0.15
YRK_Dec	2.24	3.16	0.29	0.08	0.09	0.16	0.11	0.21	0.09	0.25
RS_Jan	2.62	2.78	0.46	-0.22	0.13	0.13	0.10	0.10	0.09	0.13

[a] R_{AN} is determined from IE calibrations at each site.

[b] The Pearson's correlation ~~(Pearson'~~ coefficient (R) between LO-OOA and $NO_{3,org}$ are obtained by using R_{ON} = 10 in the NO_x^+ ratio method.

[c] For CTR_June, only 6/24 - 7/15 data are reported in order to compare with results from AMS-IC method where a PM_1 cyclone was used.

[d] For CTR_June and YRK_July, the NO_x^+ ratio method with R_{ON} = 10 and PMF method define the lower and upper bound for $NO_{3,org}$, respectively; for JST_Nov, YRK_Dec, the PMF method and NO_x^+ ratio method with R_{ON} = 10 define the lower and upper bound, respectively; for RS_Jan, the PMF method defines both the lower and upper bound; for JST_May and GT_Aug, the NO_x^+ ratio method with R_{ON} = 10 and 5 defines the lower and upper bound, respectively.

[e] The lower and upper bounds correspond to an assumed MW of organic nitrates of 200 and 300 g mol^{-1}.

Figure Captions

Figure 1: Sampling sites ~~of~~for SCAPE and SOAS studies. The gray circled region represents urban Atlanta.

Figure 2: ~~The~~Mass concentrations (a) and mass fractions (b) of non-refractory PM$_1$ (NR-PM$_1$) species measured by HR-ToF-AMS.~~ The campaign average concentrations (μg m^{-3}) with one standard deviation of total NR-PM$_1$ are listed at the top of the bar charts.~~

Figure 3: ~~The diurnal~~Diurnal profiles of non-refractory PM$_1$ (NR-PM$_1$) species measured by HR-ToF-AMS. Panel (d) shows the diurnal profiles of NR-PM$_1$ species after multiplying by the boundary layer height for the Centreville ~~site.~~ (CTR) site. The solid lines indicate the median concentration and the error bars indicate the standard error.

Figure 4: (a) *f44* vs. *f43* for total OA and OA factors resolved from PMF analysis. (b) The oxidation state of OA factors.

Figure 5: ~~(a) The compaign average mass concentrations of OA factors resolved from PMF analysis. (b) The mass fractions of OA factors resolved from PMF analysis. The campaign average concentrations (μg m^{-3}) with one standard deviation of total OA are listed at the top of the bar charts~~Diurnal~~. SOA is the sum of Isoprene-OA, MO-OOA, and LO-OOA. POA is the sum of HOA, COA, and BBOA.~~

~~Figure 6: The diurnal~~ profiles of OA factors resolved from PMF analysis on organic mass spectra. Panel (d) shows the diurnal profiles of OA factors after multiplying by the boundary layer height for the Centreville ~~site~~(CTR) site. The solid lines indicate the median concentration and the error bars indicate the standard error.

Figure 6: (a) Campaign-averaged mass concentrations of OA factors resolved from PMF analysis on organic mass spectra. (b) Campaign-averaged mass fractions of OA factors resolved from PMF analysis on organic mass spectra. SOA is the sum of Isoprene-OA, MO-OOA, and LO-OOA. POA is the sum of HOA, COA, and BBOA.

Figure 7: ~~The scatter~~Scatter plot (left panel) and the time series (right panel) of BBOA and brown carbon light absorption for the datasets where a BBOA factor ~~is~~was resolved.

Figure 8: ~~The scatter~~Scatter plot (left panel) and the time series (right panel) of MO-OOA and ozone.

Figure 9: ~~The scatter~~Scatter plot of LO-OOA vs. the total measured nitrates (i.e., NO$_{3,meas}$) and LO-OOA vs. estimated concentration of “nitrate funcionality from organic nitrates” (i.e., NO$_{3,org}$) by using R$_{ON}$ = 10 in the NO$_x^+$ ratio metod.

Figure 10. (a) ~~The concentrations~~Concentrations of total measured NO$_3$ (i.e., NO$_{3,meas}$), estimated “nitrate ~~functional group~~functionality from organic nitrates” (i.e., NO$_{3,org}$) by the NO$_x^+$ ratio method and the PMF method. (b) The contribution of NO$_{3,org}$ to NO$_{3,meas}$ (i.e., NO$_{3,org}$/NO$_{3,meas}$)

from the NO_x^+ ratio method and the PMF method. Also shown are the estimated contribution of organic nitrates to total OA from the "best estimate" range of $NO_{3,org}$ and by assuming a MW of 200 and 300 g mol^{-1} ~~of~~for organic nitrates.

Figure 11. ~~The comparion~~Comparion of estimated concentration of "nitrate functionality from organic nitrates" (i.e., $NO_{3,org}$) at the Centreville (CTR) site between the AMS-IC method and NO_x^+ ratio method with R_{ON} values of 5 and 10. The intercept and slope are obtained by orthogonal fit, which considers ~~the~~ measurement errors in both dependent and independent variables. The correlation coefficient R is obtained by linear least-squares fit. ~~The intercepts~~Intercepts are within ~~to~~ the detection limit of PILS-IC nitrate (i.e., 0.03 µg m^{-3}). The 1:1 line is offset by the ~~dection~~detection limit of PILS-IC nitrate (i.e., -0.03 µg m^{-3}) for visual clarity. The uncertainty of PILS-IC measurements is about 10% according to Weber et al. (2001).

~~Figure 12. The correlations~~Figure 12. Diurnal variation of $NO_{3,meas}$, $NO_{3,org}$, and $NO_{3,inorg}$ for all datasets. $NO_{3,org}$, and $NO_{3,inorg}$ are estimated by the NO_x^+ ratio method with an R_{ON} value of 10. The solid lines indicate the median concentration and the error bars indicate the standard error.

Figure 13. Correlation coefficients for NR-PM_1 species between ACSM measurements (stationary at the Georgia Tech site) and HR-ToF-AMS measuremens (rotating among different sites). ~~The~~Values are plotted vs. the relevant distance of the measurement site from the GT site, where the dotted lines represent the sampling sites where the HR-ToF-AMS measurements were made.

~~Figure 13.~~Figure 14. Diurnal variation of boundary layer height for CTR_June. The solid line indicates the median concentration and the error bars indicate the standard error.

Figure 15. Mean seasonal concentrations of organic carbon at the Jefferson Street ~~site~~(JST) and the Yorkville ~~site~~(YRK) sites. Summer: June – August. Winter: December – Februry.

Figure ~~14~~16. The seasonality of the correlation between organic carbon and sulfate at the Jefferson Street~~,~~ (JST), Yorkville~~,~~ (YRK), and Centreville ~~site~~(CTR) sites. Seasons are by grouped by calendar months (Spring: March–May, Summer: June–August, Fall: September–November, and Winter: December–February).

Fig. 1.

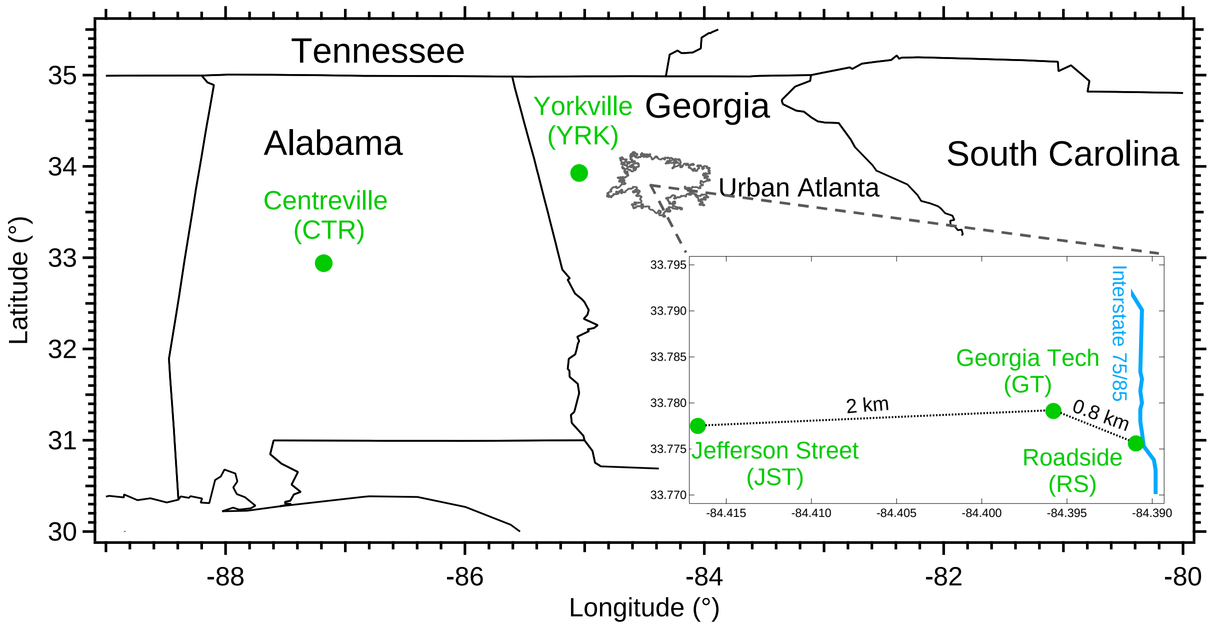
Tennessee
Alabama
Georgia
South Carolina
Yorkville
(YRK)
Centreville
(CTR)
Urban Atlanta
Latitude (°)
Longitude (°)
35
34
33
32
31
30
-88
-86
-84
-82
-80
33.795
33.790
33.785
33.780
33.775
33.770
-84.415
-84.410
-84.405
-84.400
-84.395
-84.390
Interstate 75/85
Georgia Tech
(GT)
2 km
0.8 km
Jefferson Street
(JST)
Roadside
(RS)

Fig. 2.

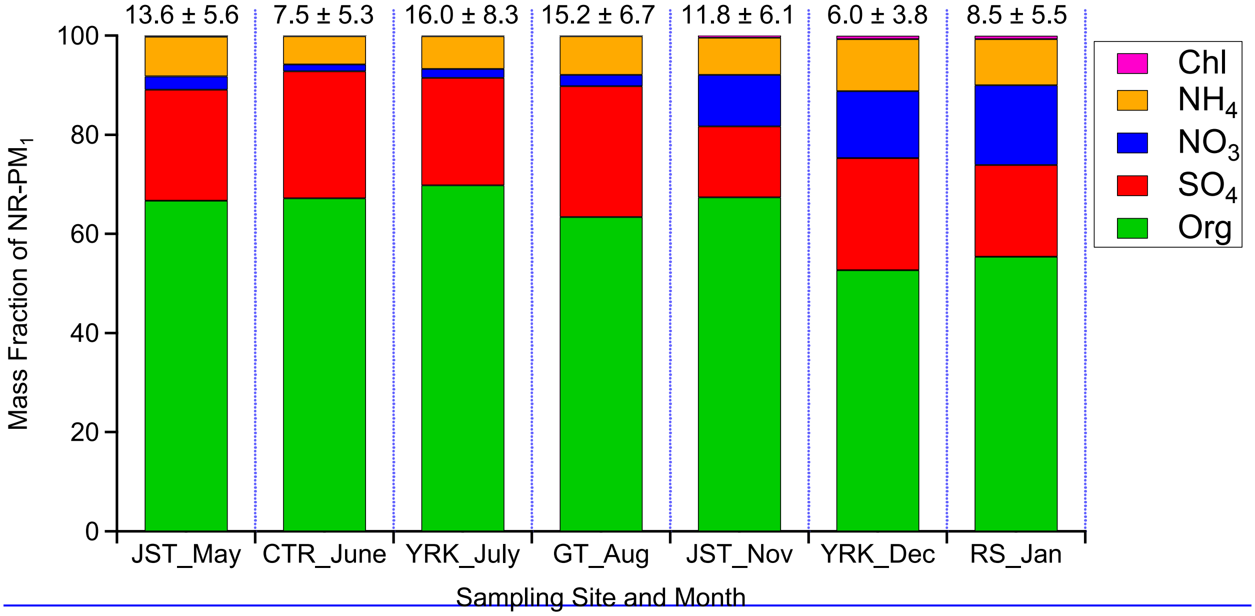
13.6 ± 5.6
7.5 ± 5.3
16.0 ± 8.3
15.2 ± 6.7
11.8 ± 6.1
6.0 ± 3.8
8.5 ± 5.5
100
80
60
40
20
0
Mass Fraction of NR-PM$_1$
JST_May
CTR_June
YRK_July
GT_Aug
JST_Nov
YRK_Dec
RS_Jan
Sampling Site and Month
Chl
NH$_4$
NO$_3$
SO$_4$
Org

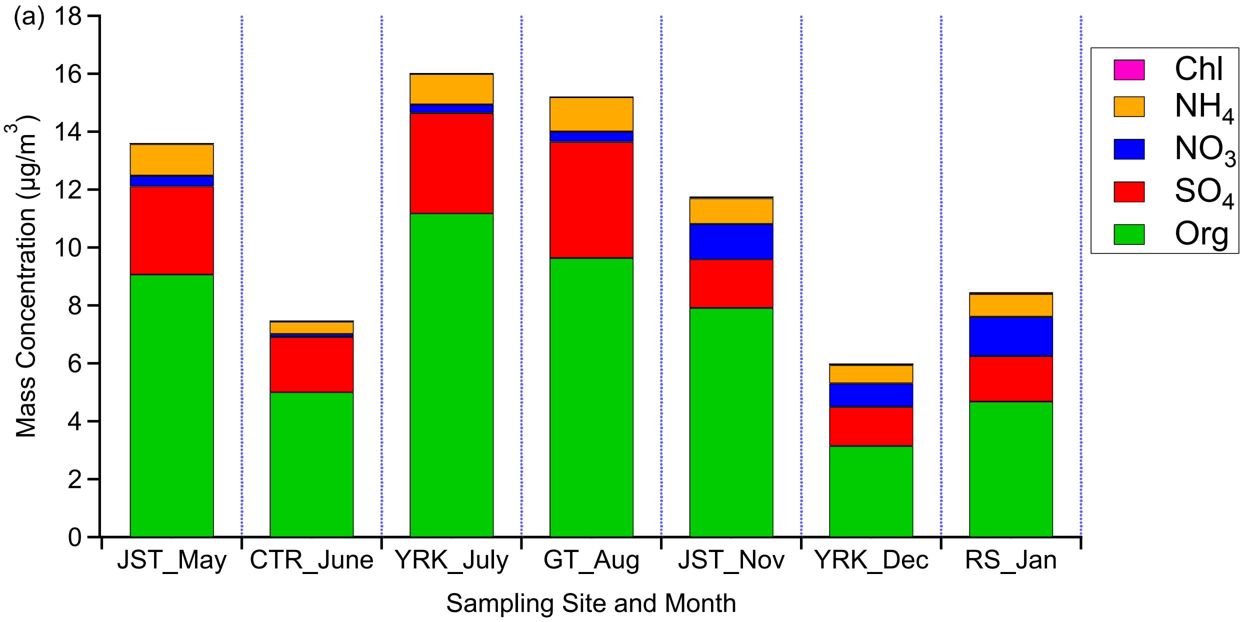
(a)
Mass Concentration (µg/m^3)
0
2
4
6
8
10
12
14
16
18
JST_May
CTR_June
YRK_July
GT_Aug
JST_Nov
YRK_Dec
RS_Jan
Sampling Site and Month
Chl
NH$_4$
NO$_3$
SO$_4$
Org

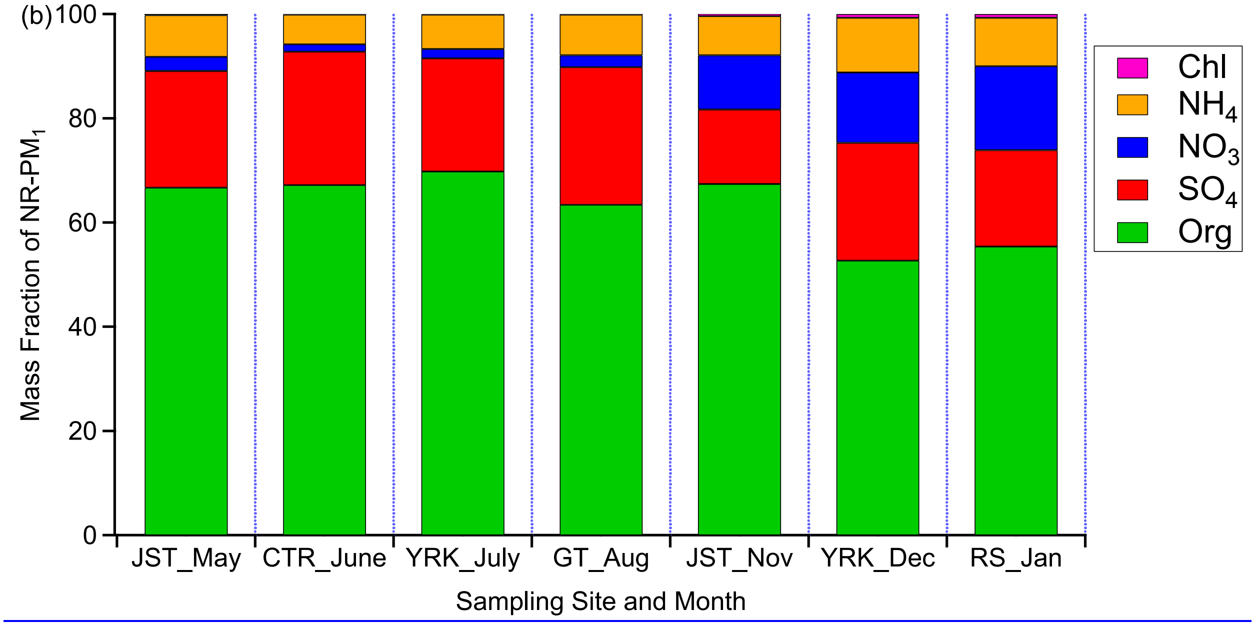
(b)
Mass Fraction of NR-PM$_1$
0
20
40
60
80
100
JST_May
CTR_June
YRK_July
GT_Aug
JST_Nov
YRK_Dec
RS_Jan
Sampling Site and Month
Chl
NH$_4$
NO$_3$
SO$_4$
Org

Fig. 3.

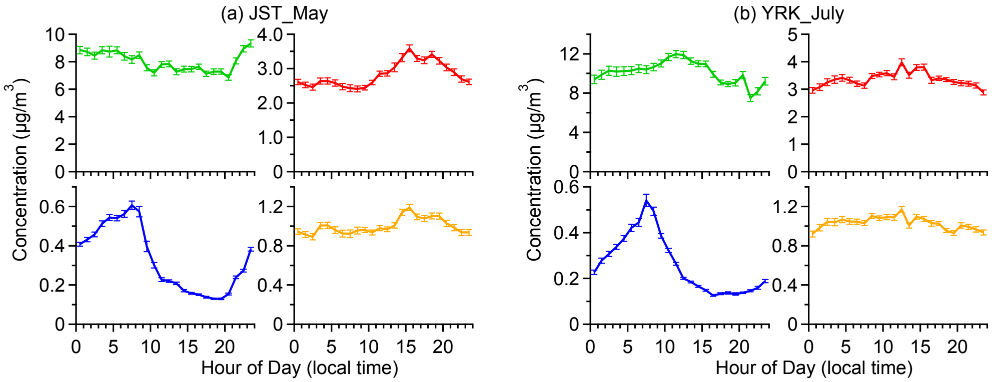
(a) JST_May
(b) YRK_July
Concentration (μg/m³)
Hour of Day (local time)
0
5
10
15
20

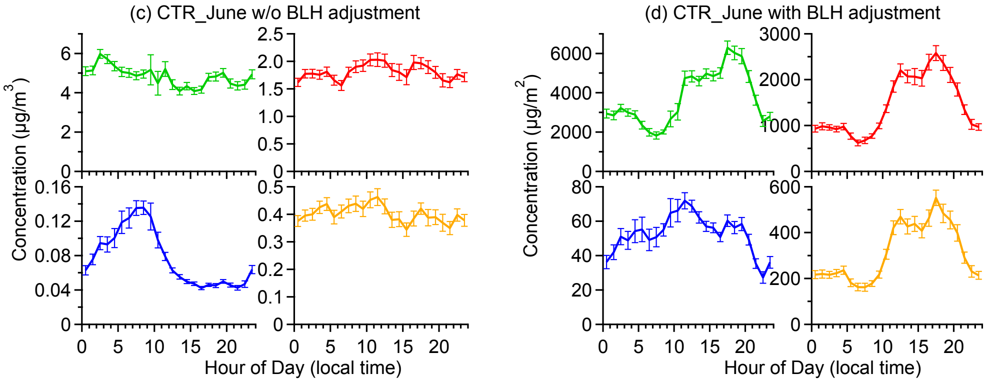
(c) CTR_June w/o BLH adjustment
(d) CTR_June with BLH adjustment
Concentration (μg/m³)
Concentration (μg/m²)
Hour of Day (local time)
0
5
10
15
20

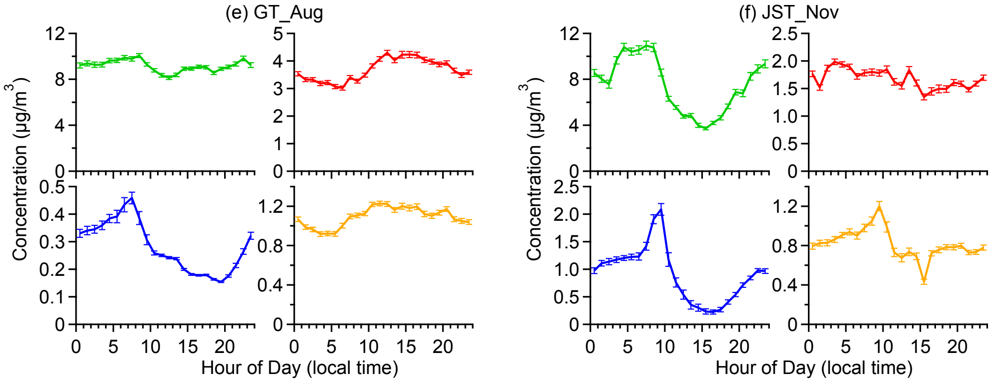
(e) GT_Aug
(f) JST_Nov
Concentration (μg/m³)
Hour of Day (local time)
0
5
10
15
20

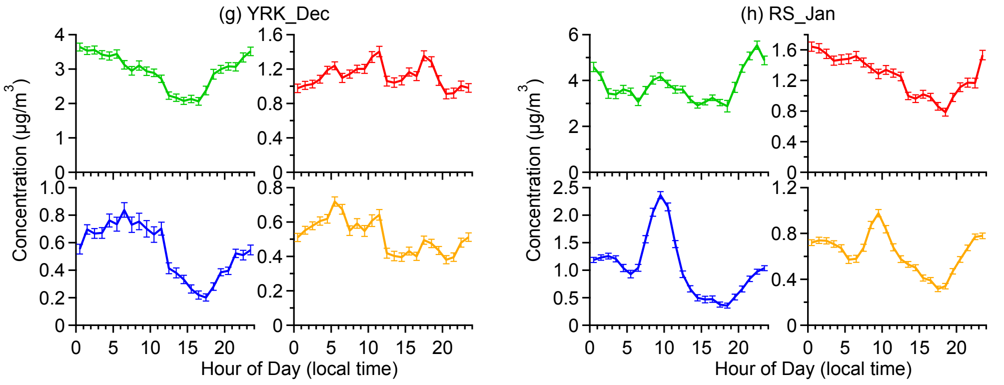
(g) YRK_Dec
(h) RS_Jan
Concentration (μg/m3)
Hour of Day (local time)
0
5
10
15
20
4
3
2
1
1.6
1.2
0.8
0.4
1.0
0.6
0.2
6
2.5
2.0
1.5
0.5

Fig. 4.

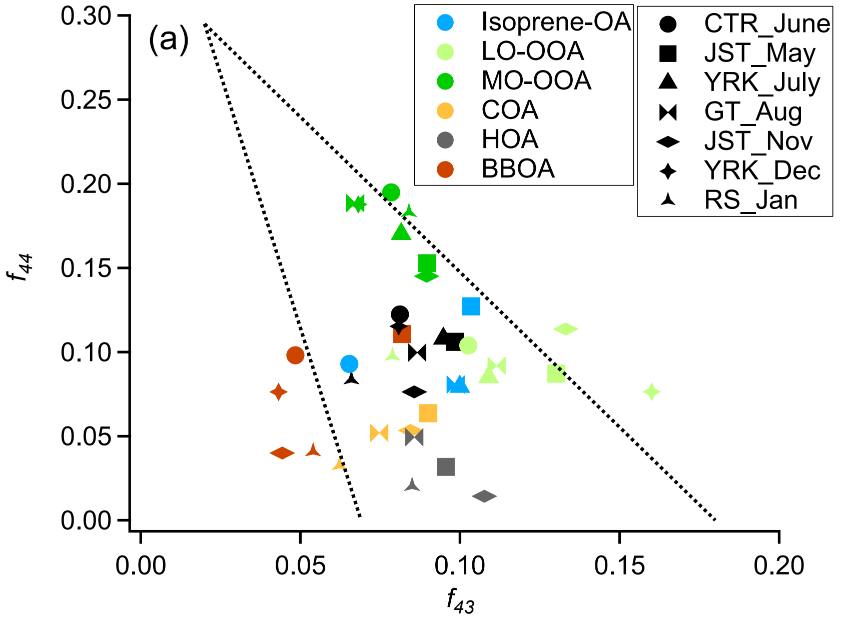
(a)
Isoprene-OA
LO-OOA
MO-OOA
COA
HOA
BBOA
CTR_June
JST_May
YRK_July
GT_Aug
JST_Nov
YRK_Dec
RS_Jan
f44
f43
0.30
0.25
0.20
0.15
0.10
0.05
0.00
0.00
0.05
0.10
0.15
0.20

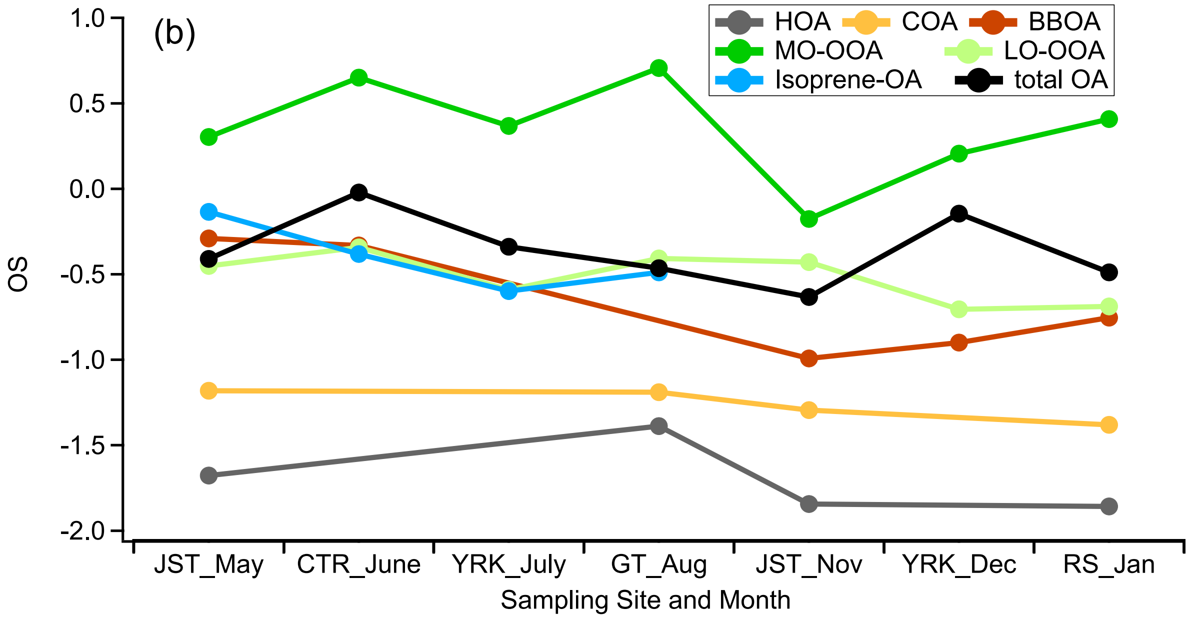

Fig. 5.

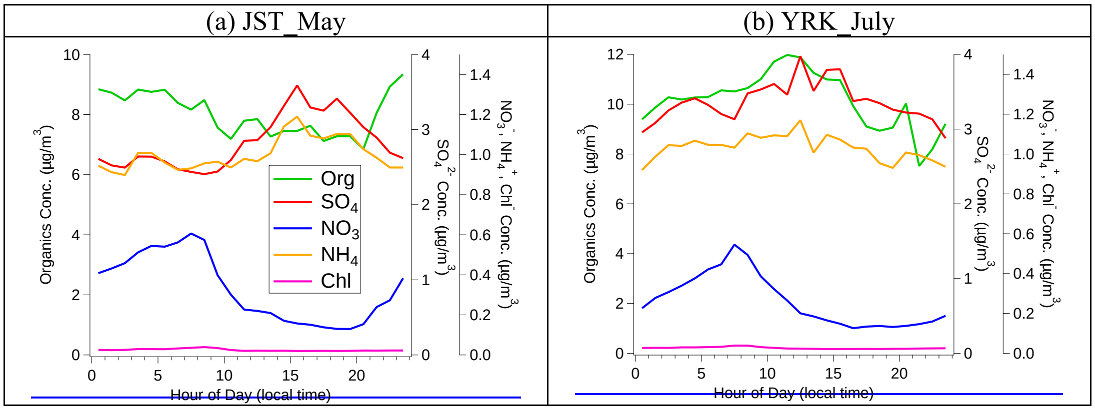
(a) JST_May

(b) YRK_July

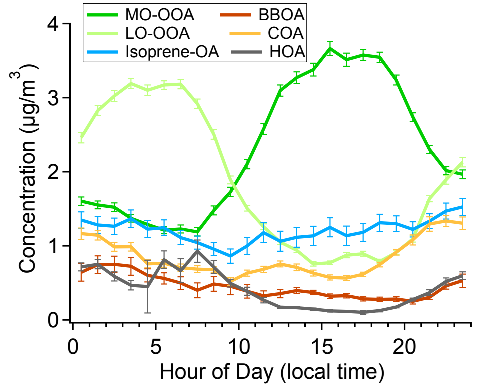

(c) CTR_June w/o BLH adjustment

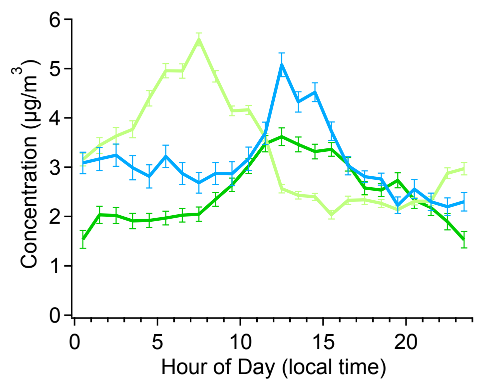

(d) CTR_June with BLH adjustment

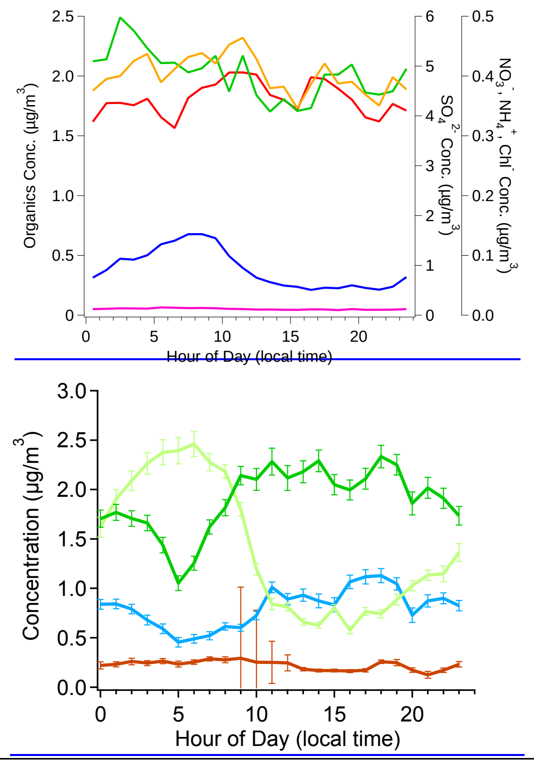

~~(e) GT_Aug~~

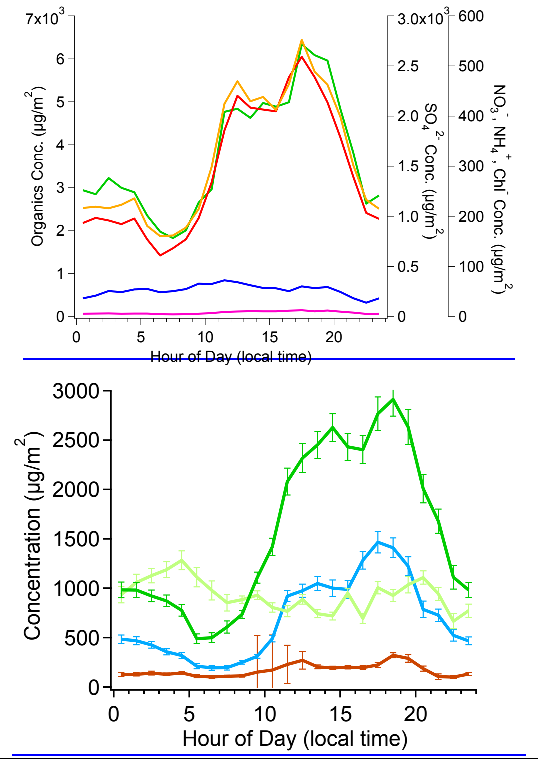

~~(f) JST_Nov~~

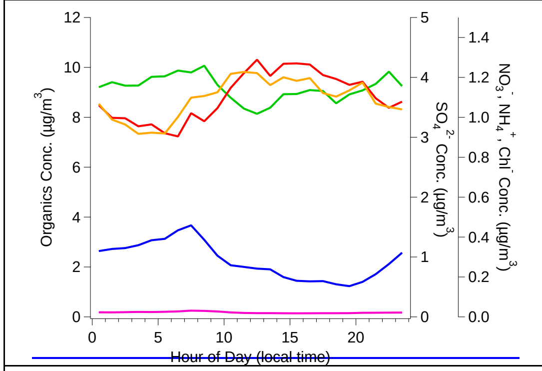

~~(g) YRK_Dec~~

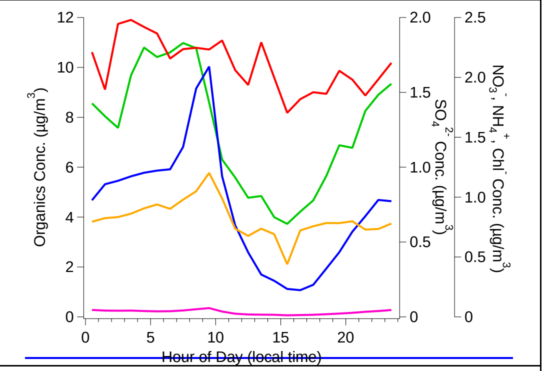

~~(h) RS_Jan~~

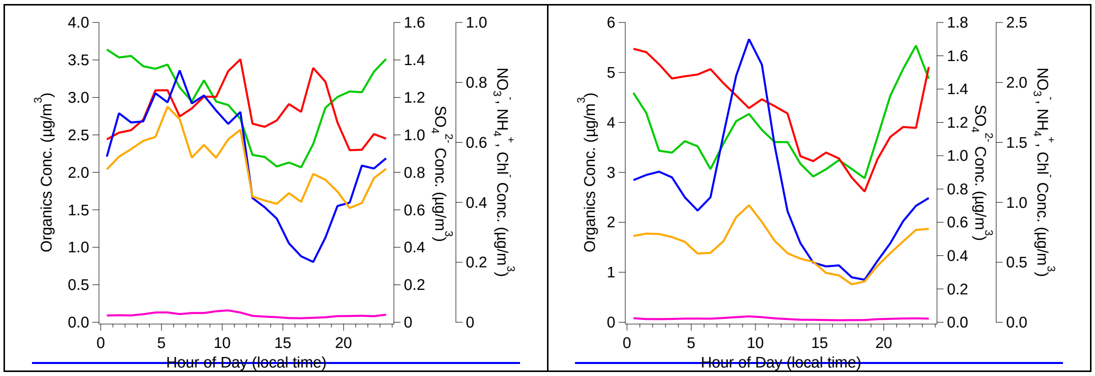

Organics Conc. (µg/m³)
SO₄²⁻ Conc. (µg/m³)
NO₃⁻, NH₄⁺, Chl⁻ Conc. (µg/m³)
Hour of Day (local time)
4.0
3.5
3.0
2.5
2.0
1.5
1.0
0.5
0.0
1.6
1.4
1.2
1.0
0.8
0.6
0.4
0.2
0
1.0
0.8
0.6
0.4
0.2
0
0
5
10
15
20
6
5
4
3
2
1
0
1.8
1.6
1.4
1.2
1.0
0.8
0.6
0.4
0.2
0.0
2.5
2.0
1.5
1.0
0.5
0.0

~~Fig. 4.~~

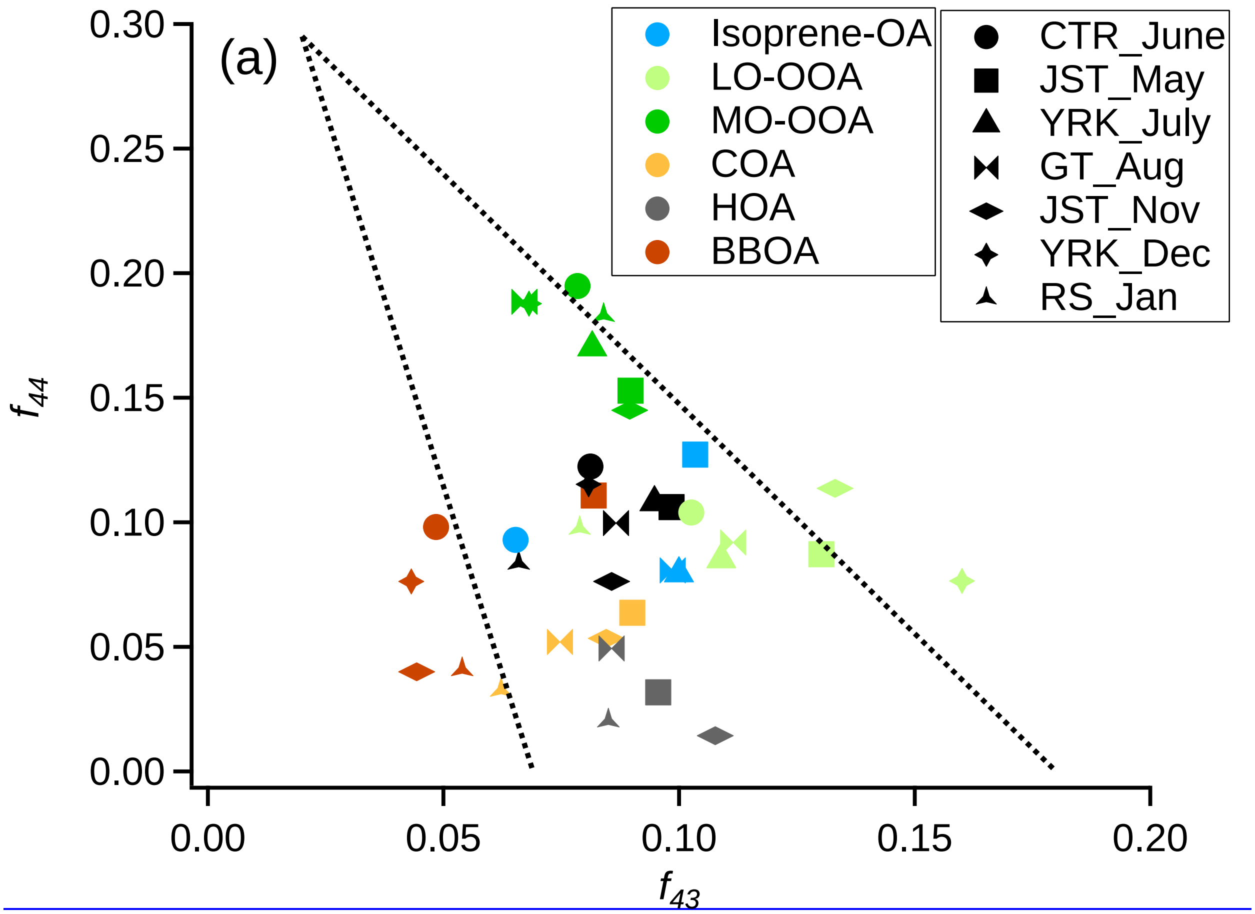

(a)
f44
f43
0.30
0.25
0.20
0.15
0.10
0.05
0.00
0.00
0.05
0.10
0.15
0.20
Isoprene-OA
LO-OOA
MO-OOA
COA
HOA
BBOA
CTR_June
JST_May
YRK_July
GT_Aug
JST_Nov
YRK_Dec
RS_Jan

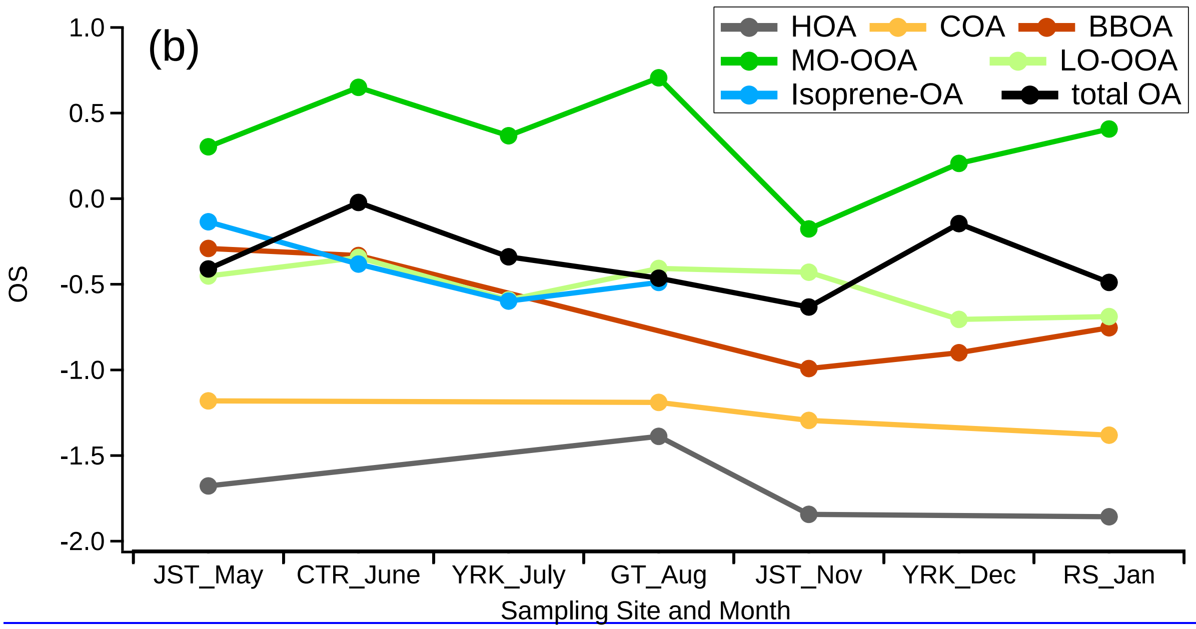
(b)
OS
1.0
0.5
0.0
-0.5
-1.0
-1.5
-2.0
HOA
COA
BBOA
MO-OOA
LO-OOA
Isoprene-OA
total OA
JST_May
CTR_June
YRK_July
GT_Aug
JST_Nov
YRK_Dec
RS_Jan
Sampling Site and Month

~~Fig. 5.~~

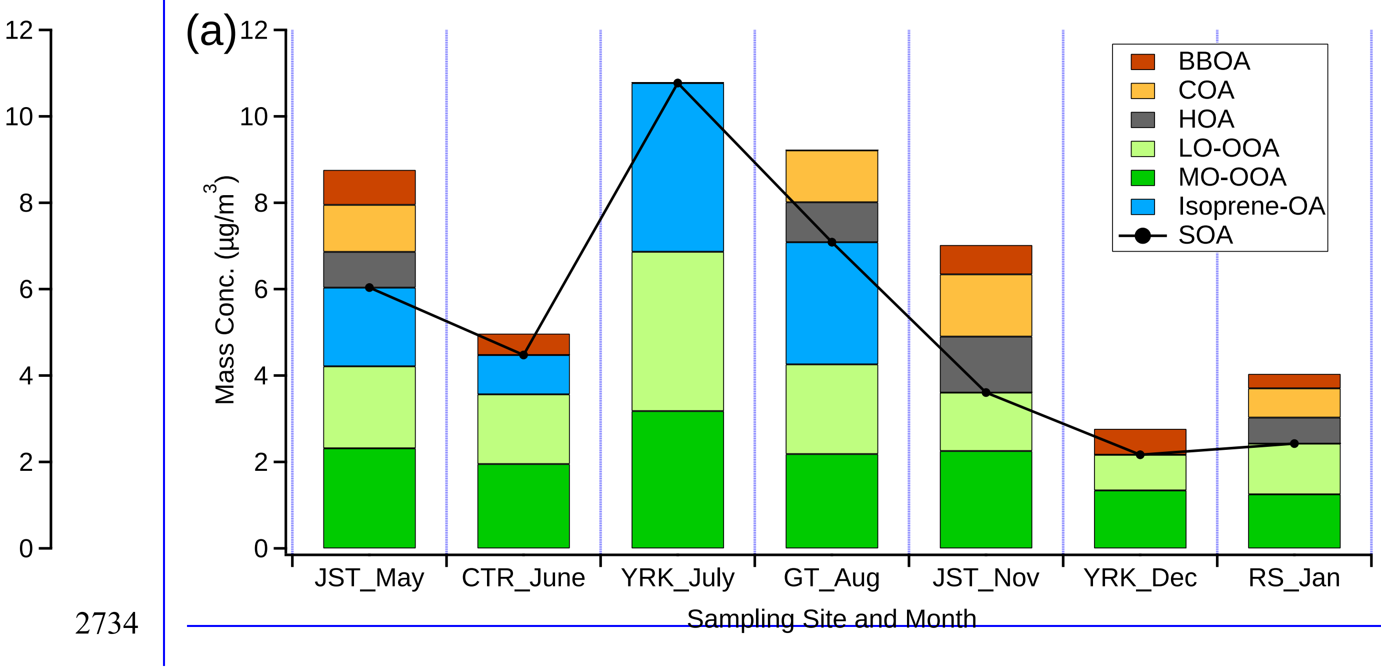
(a)
12
10
8
6
4
2
0
Mass Conc. (µg/m3)
BBOA
COA
HOA
LO-OOA
MO-OOA
Isoprene-OA
SOA
JST_May
CTR_June
YRK_July
GT_Aug
JST_Nov
YRK_Dec
RS_Jan
Sampling Site and Month

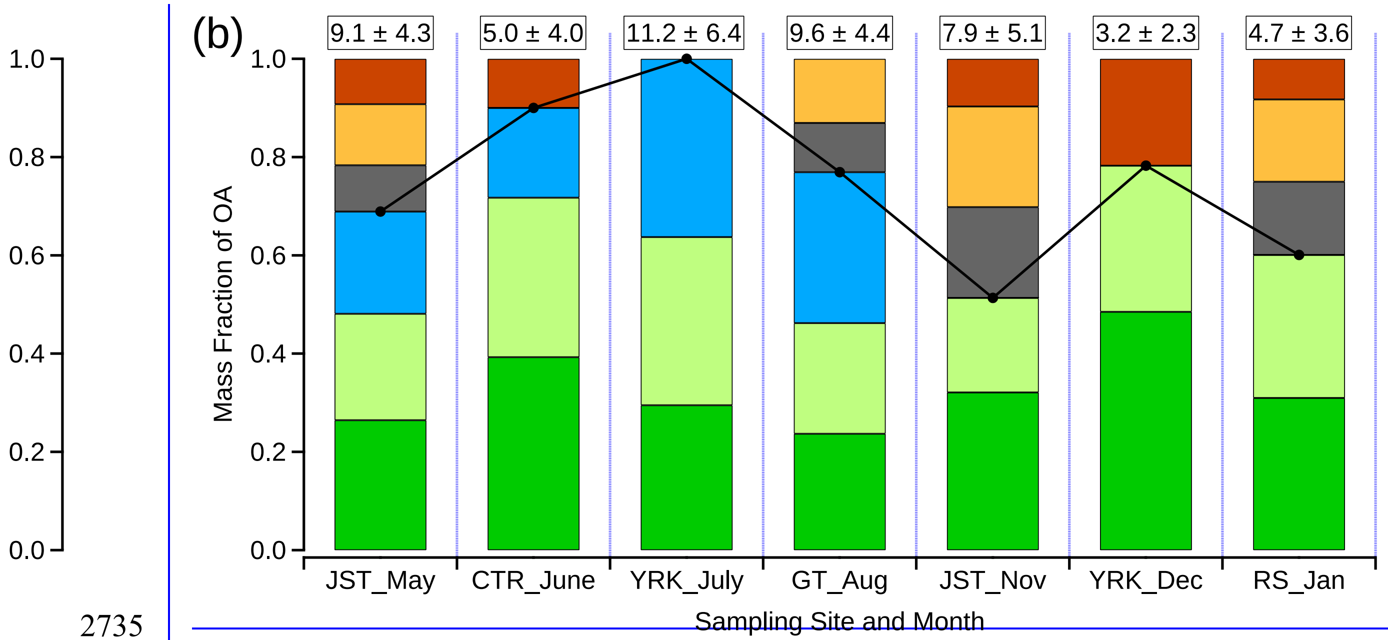

~~Fig. 6.~~

~~(a) JST_May~~	~~(b) YRK_July~~
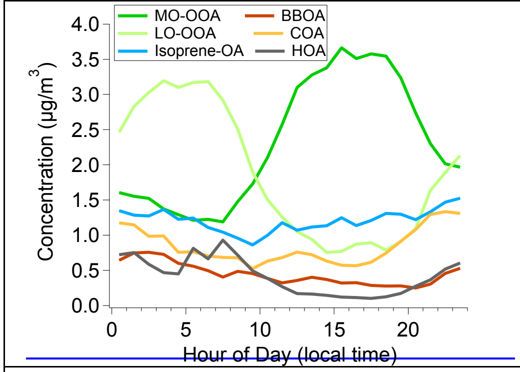	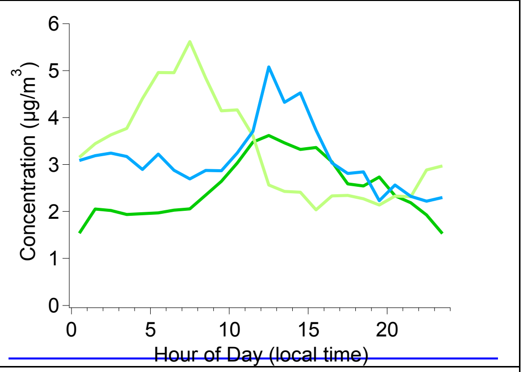
~~(c) CTR_June w/o BLH~~	~~(d) CTR_June with BLH adjustment~~

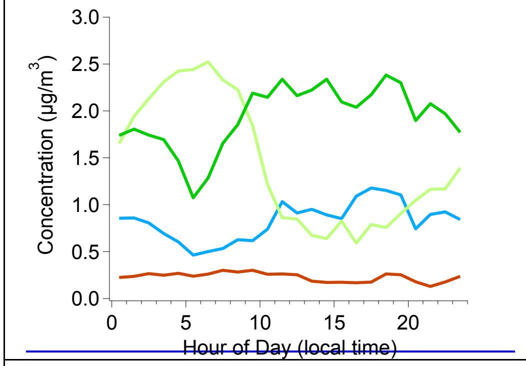

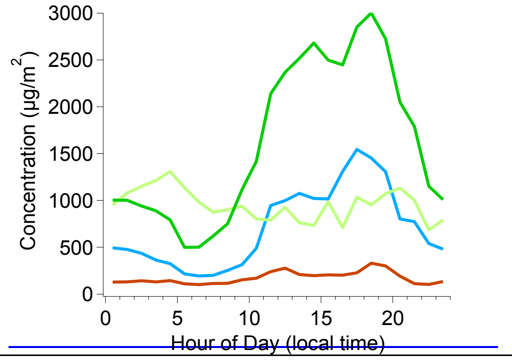

(e) GT_Aug

(f) JST_Nov

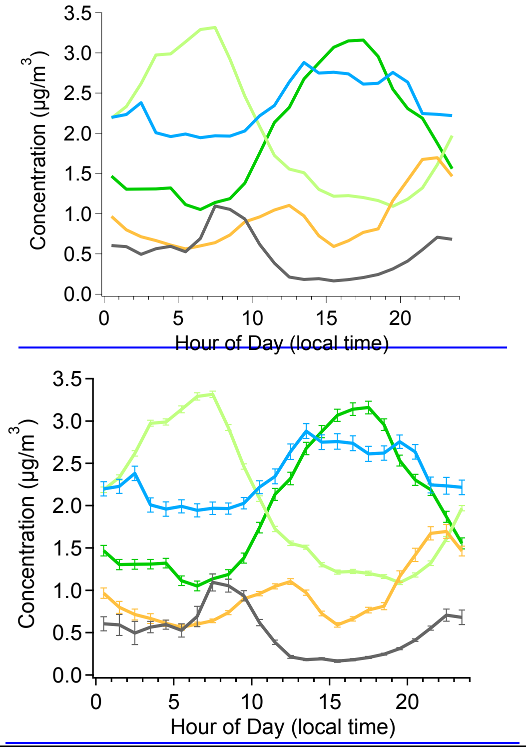

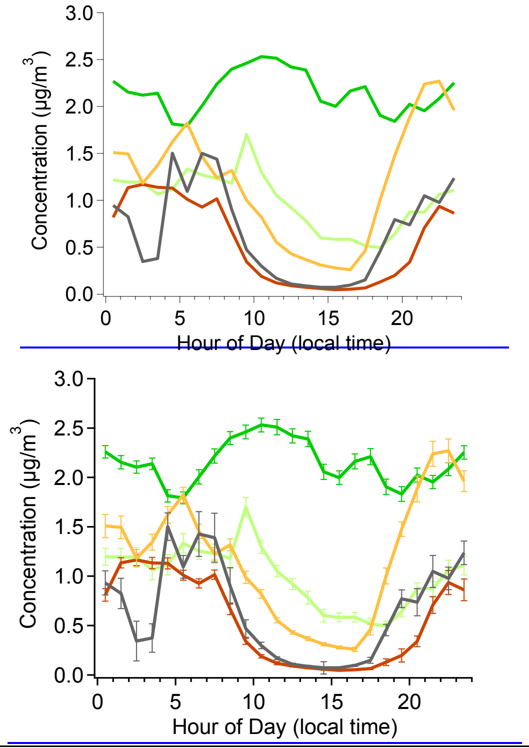

(g) YRK_Dec

(h) RS_Jan

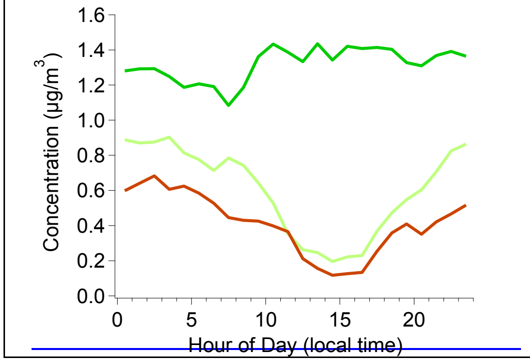

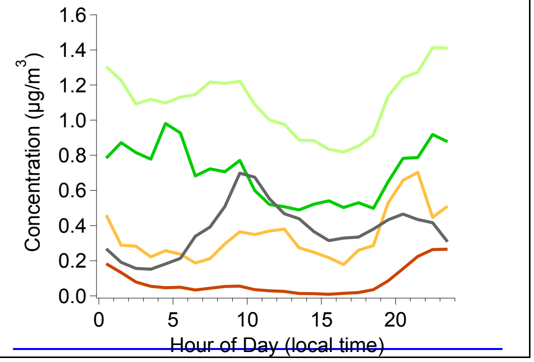

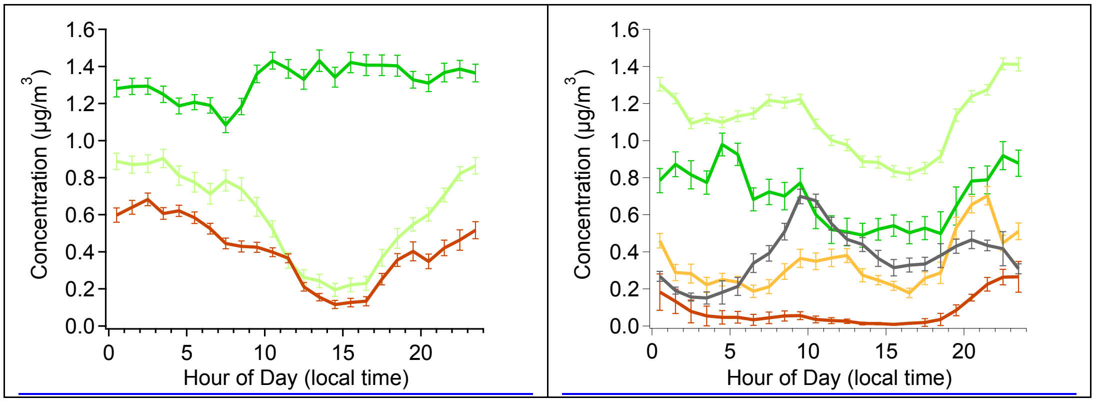
Concentration (µg/m³)
1.6
1.4
1.2
1.0
0.8
0.6
0.4
0.2
0.0
0
5
10
15
20
Hour of Day (local time)
Concentration (µg/m³)
1.6
1.4
1.2
1.0
0.8
0.6
0.4
0.2
0.0
0
5
10
15
20
Hour of Day (local time)

Fig. 6.

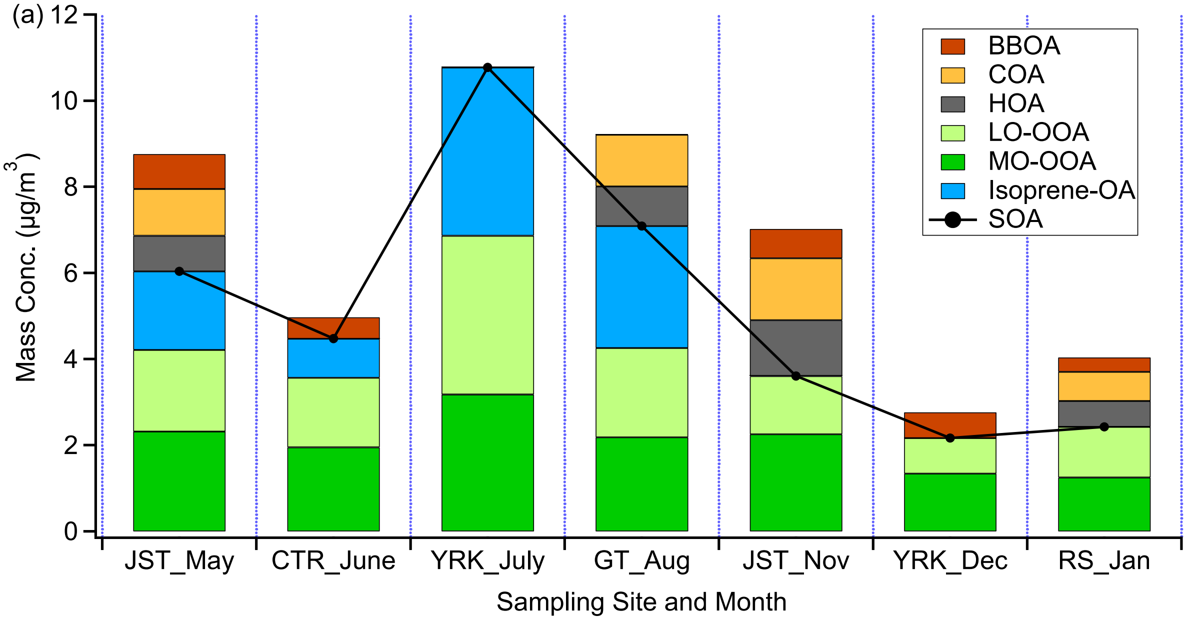
(a)
Mass Conc. (µg/m³)
12
10
8
6
4
2
0
JST_May
CTR_June
YRK_July
GT_Aug
JST_Nov
YRK_Dec
RS_Jan
Sampling Site and Month
BBOA
COA
HOA
LO-OOA
MO-OOA
Isoprene-OA
SOA

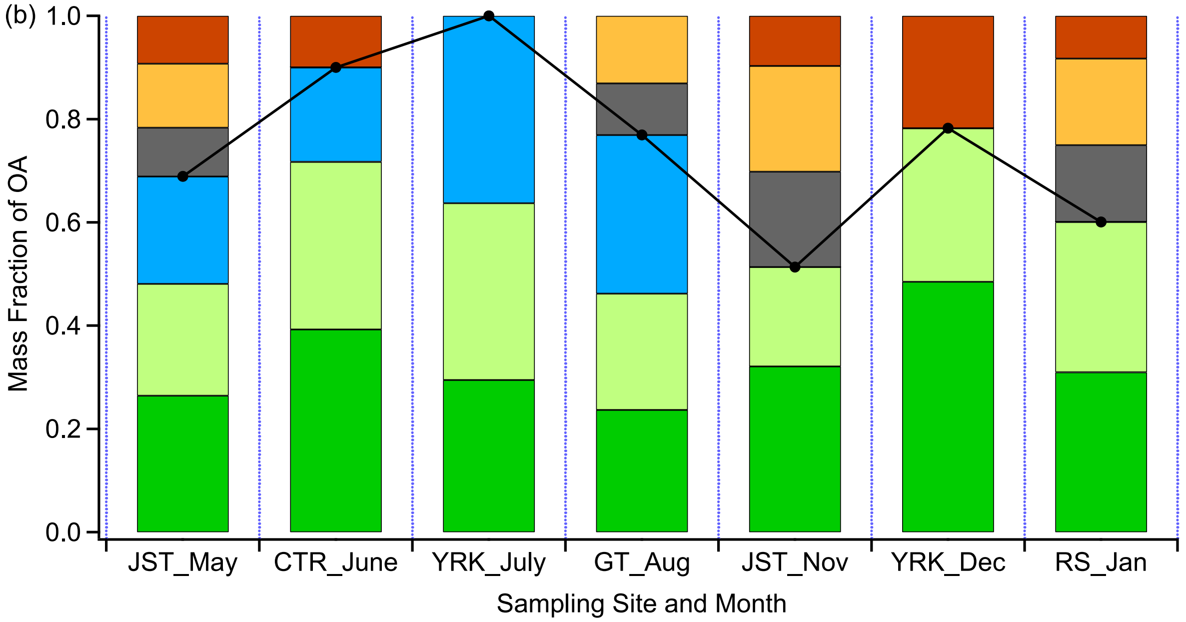
(b)
Mass Fraction of OA
0.0
0.2
0.4
0.6
0.8
1.0
JST_May
CTR_June
YRK_July
GT_Aug
JST_Nov
YRK_Dec
RS_Jan
Sampling Site and Month

Fig. 7.

JST_May	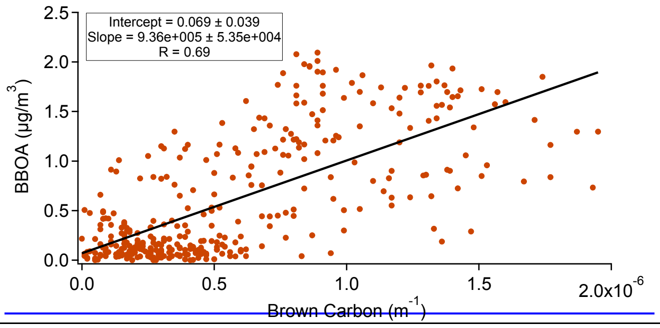Intercept = 0.069 ± 0.039 Slope = 9.36e+005 ± 5.35e+004 R = 0.69 BBOA (µg/m^3) Brown Carbon (m^{-1}) 0.0 0.5 1.0 1.5 2.0 2.5 2.0x10^{-6}	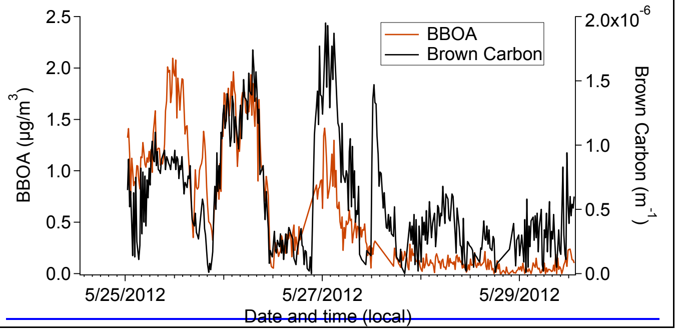BBOA Brown Carbon BBOA (µg/m^3) Brown Carbon (m^{-1}) 2.0x10^{-6} 5/25/2012 5/27/2012 5/29/2012 Date and time (local)

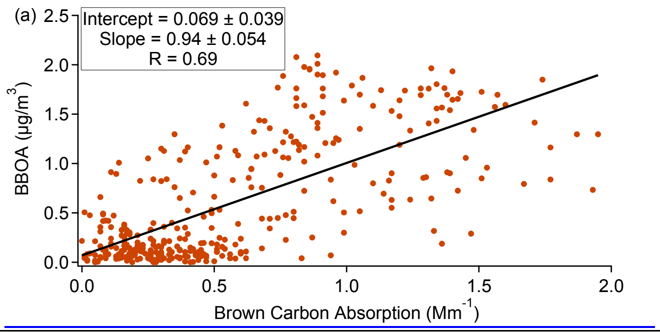

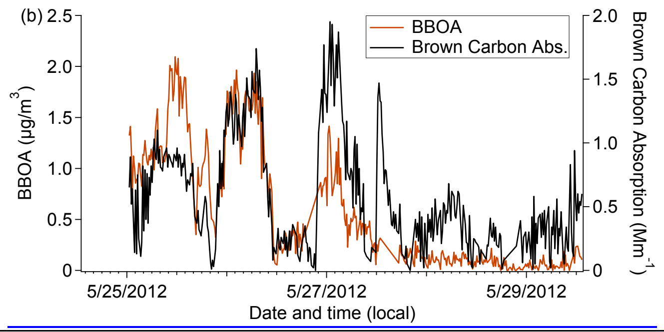

CTR_June

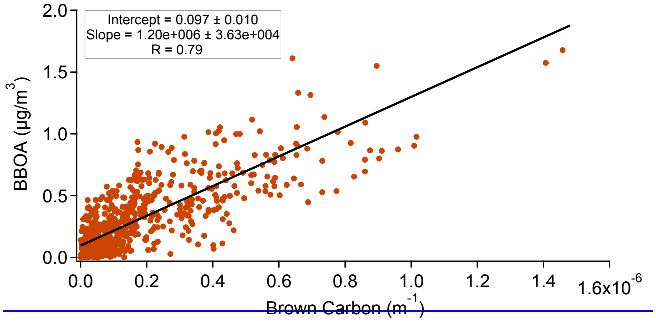

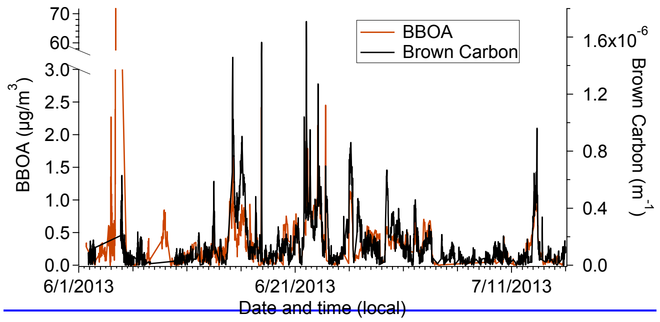

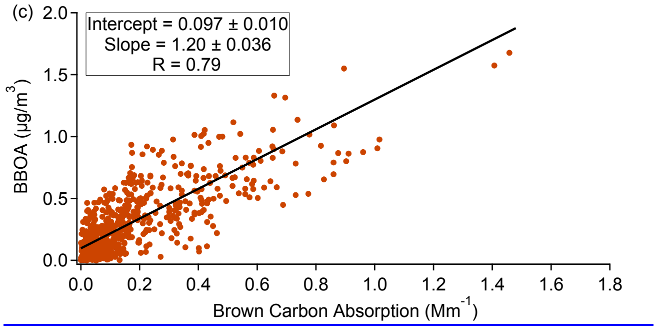

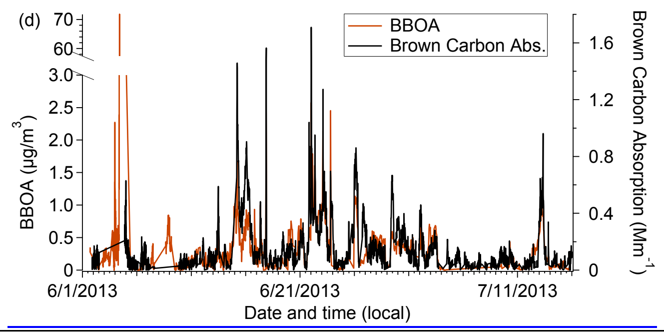

JST_Nov

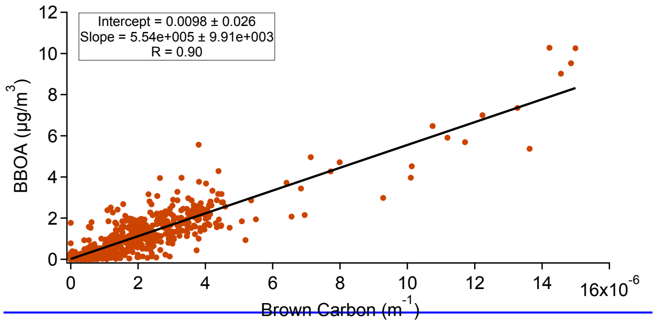

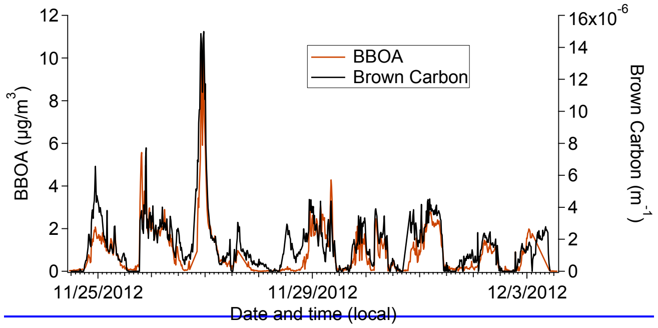

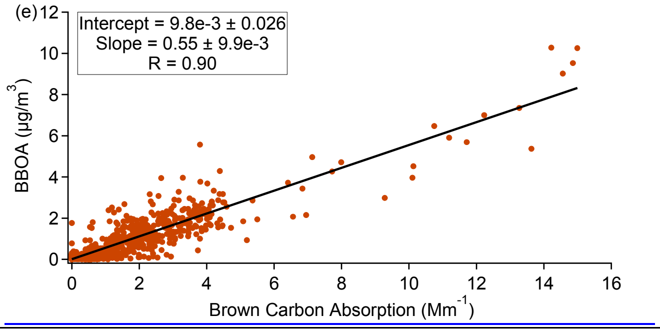

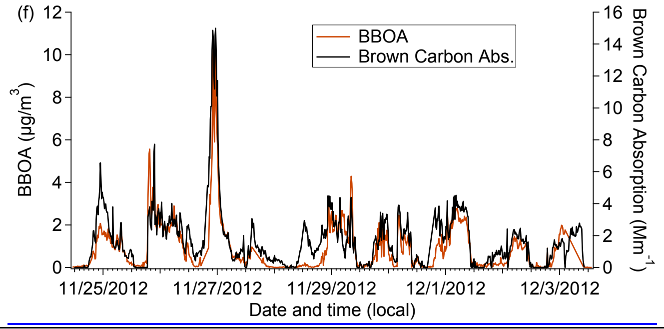

YRK_Dec

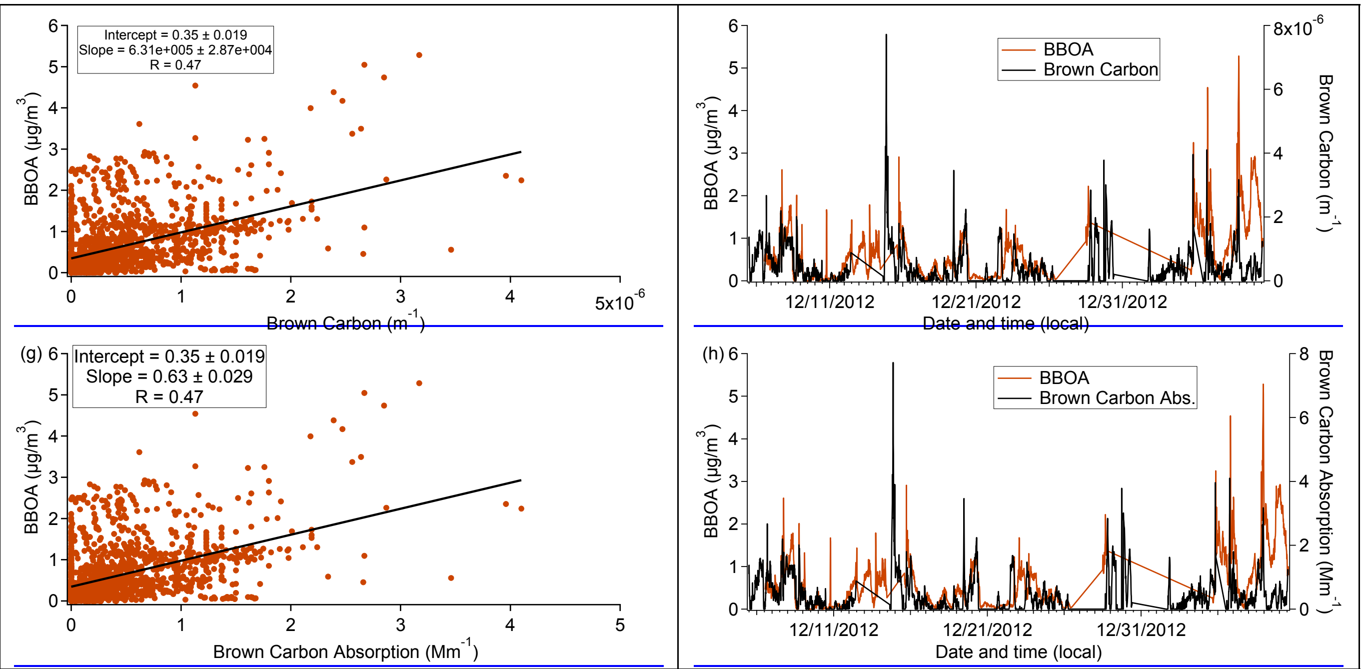

RS_Jan

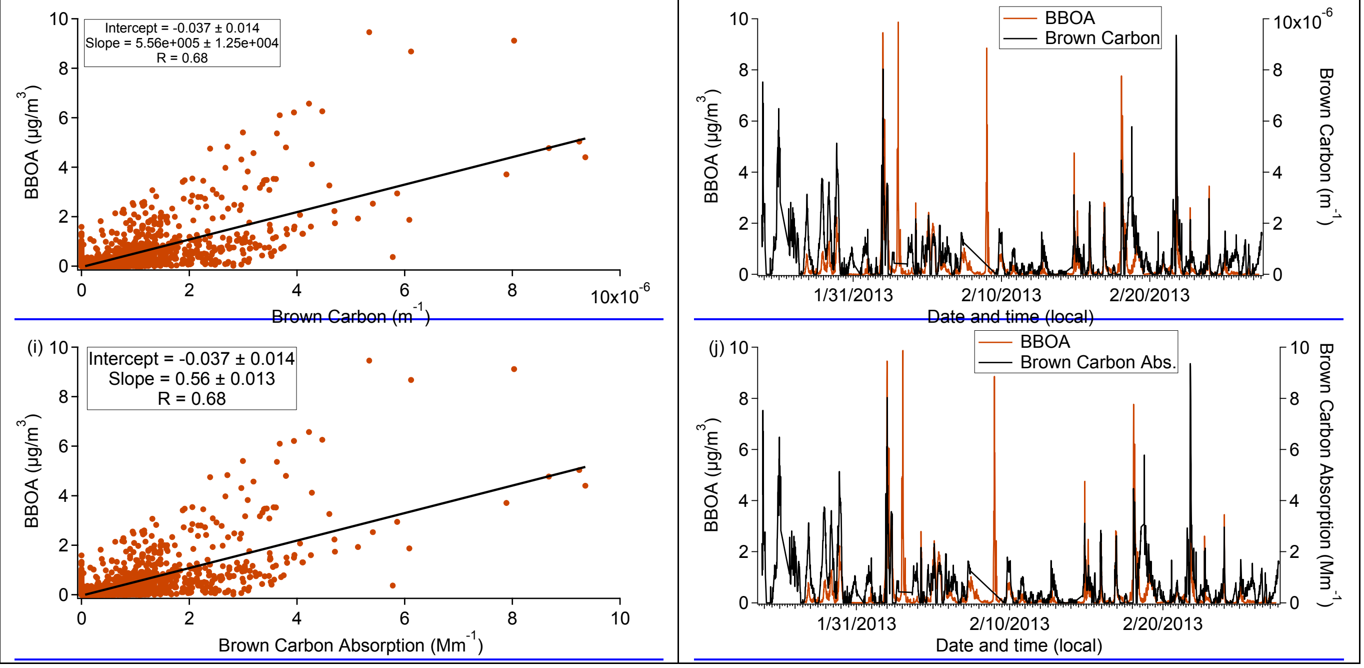

Fig. 8.

JST_May

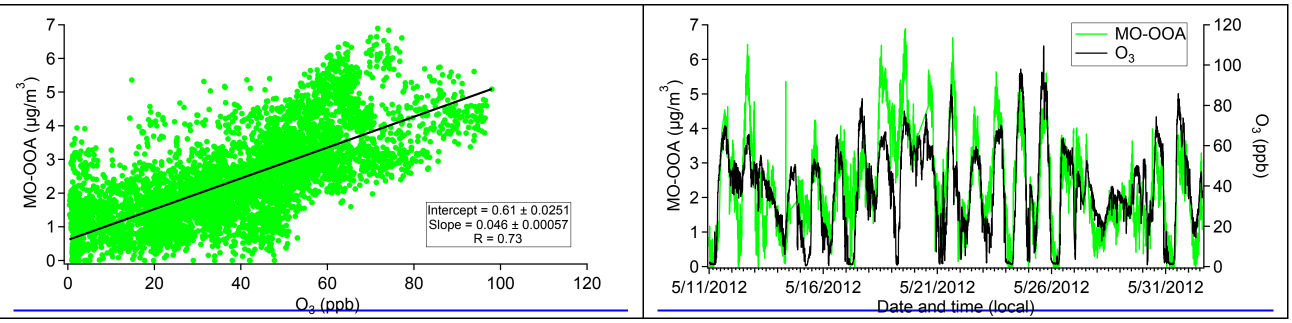

	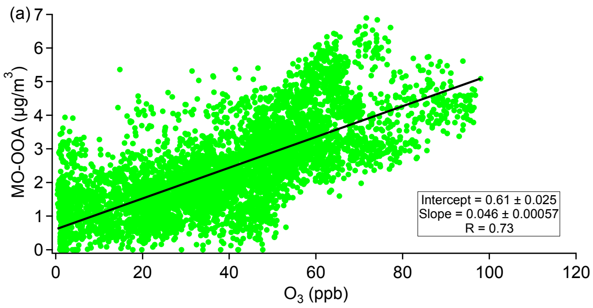	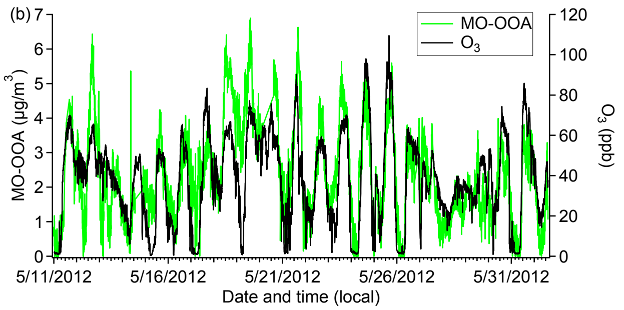
YRK_July	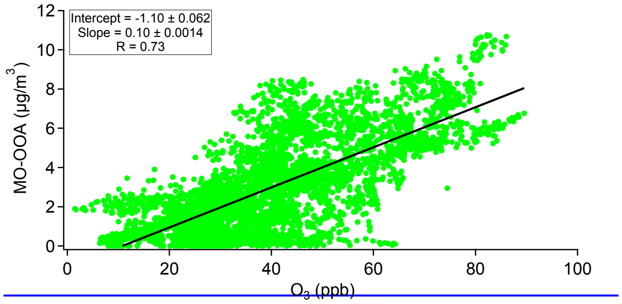	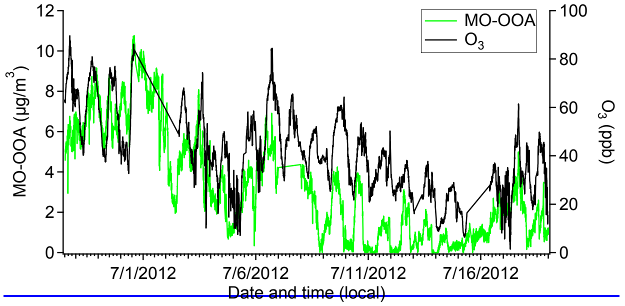
	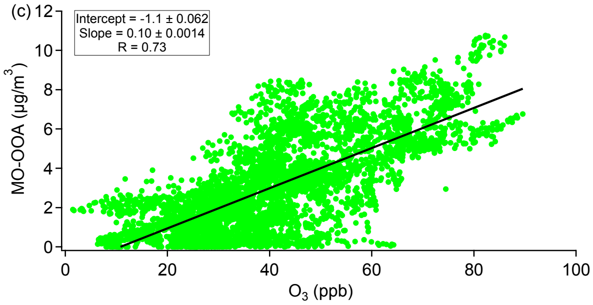	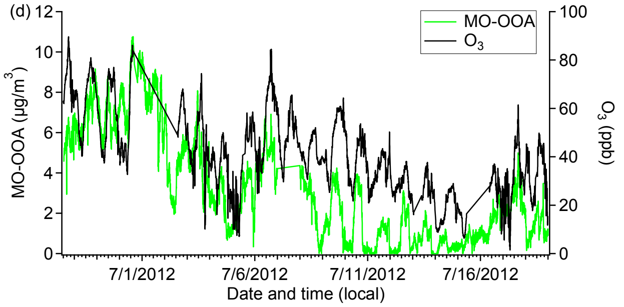
JST_Nov	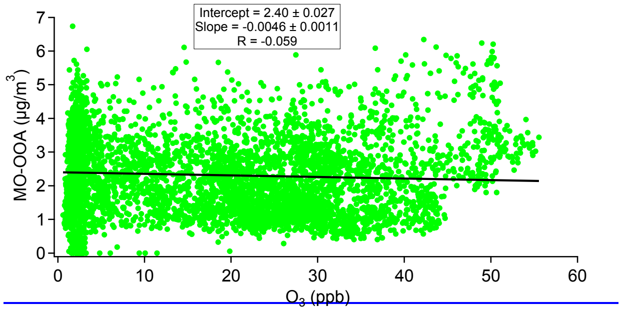	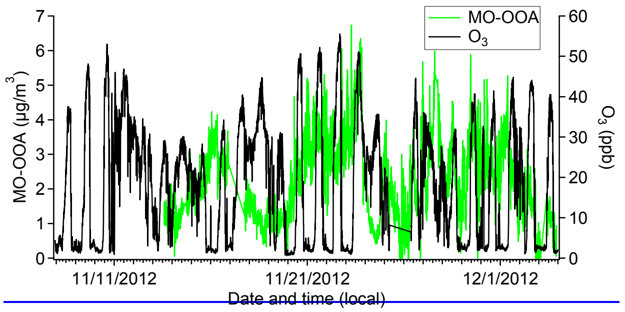
	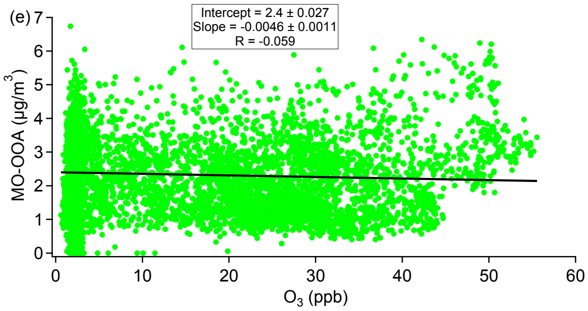	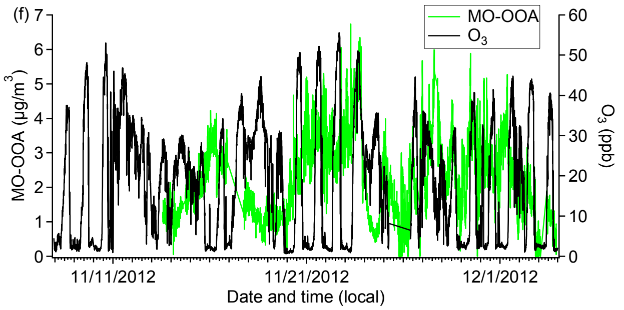

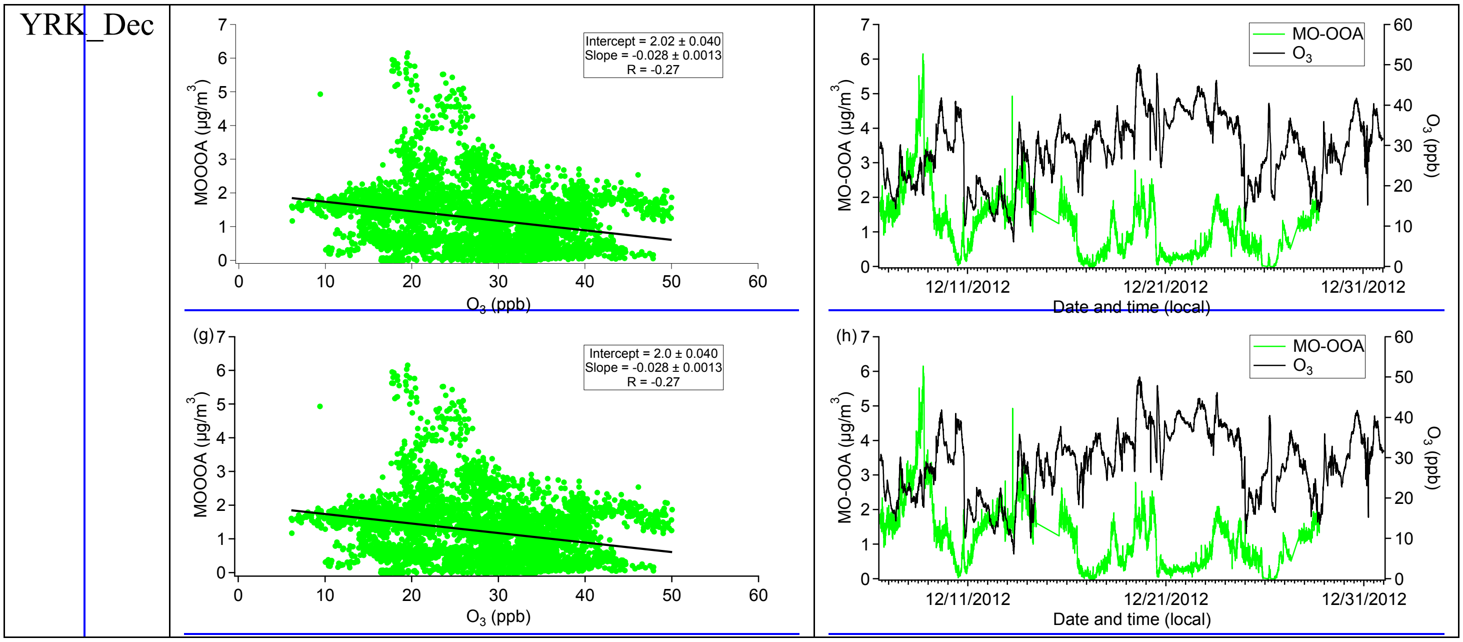
YRK_Dec
Intercept = 2.02 ± 0.040
Slope = -0.028 ± 0.0013
R = -0.27
MOOOA (µg/m3)
O3 (ppb)
MO-OOA
O3
MO-OOA (µg/m3)
O3 (ppb)
12/11/2012
12/21/2012
12/31/2012
Date and time (local)
(g)
Intercept = 2.0 ± 0.040
Slope = -0.028 ± 0.0013
R = -0.27
MOOOA (µg/m3)
O3 (ppb)
(h)
MO-OOA
O3
MO-OOA (µg/m3)
O3 (ppb)
12/11/2012
12/21/2012
12/31/2012
Date and time (local)

Fig. 9.

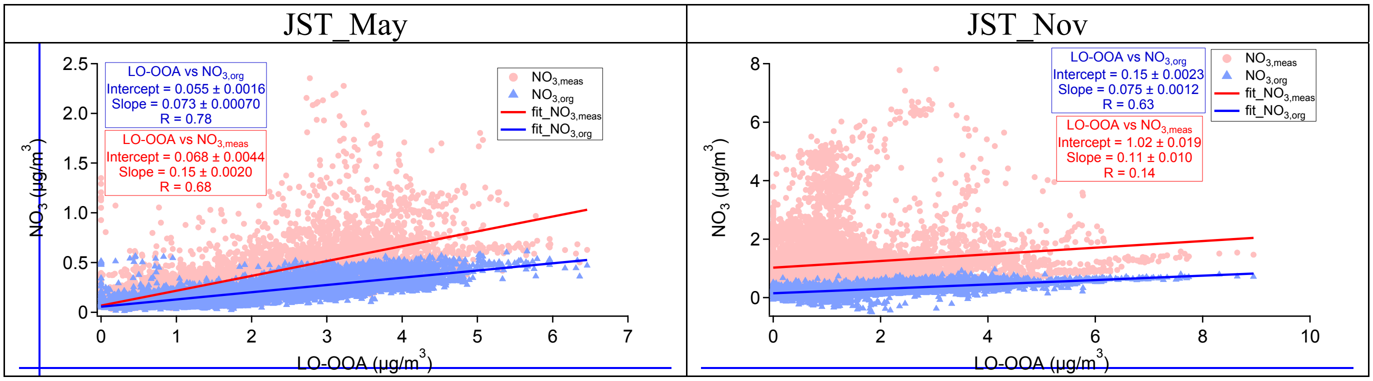
JST_May
LO-OOA vs NO3,org
Intercept = 0.055 ± 0.0016
Slope = 0.073 ± 0.00070
R = 0.78
LO-OOA vs NO3,meas
Intercept = 0.068 ± 0.0044
Slope = 0.15 ± 0.0020
R = 0.68
NO3,meas
NO3,org
fit_NO3,meas
fit_NO3,org
NO3 (µg/m3)
LO-OOA (µg/m3)
JST_Nov
LO-OOA vs NO3,org
Intercept = 0.15 ± 0.0023
Slope = 0.075 ± 0.0012
R = 0.63
LO-OOA vs NO3,meas
Intercept = 1.02 ± 0.019
Slope = 0.11 ± 0.010
R = 0.14
NO3,meas
NO3,org
fit_NO3,meas
fit_NO3,org
NO3 (µg/m3)
LO-OOA (µg/m3)

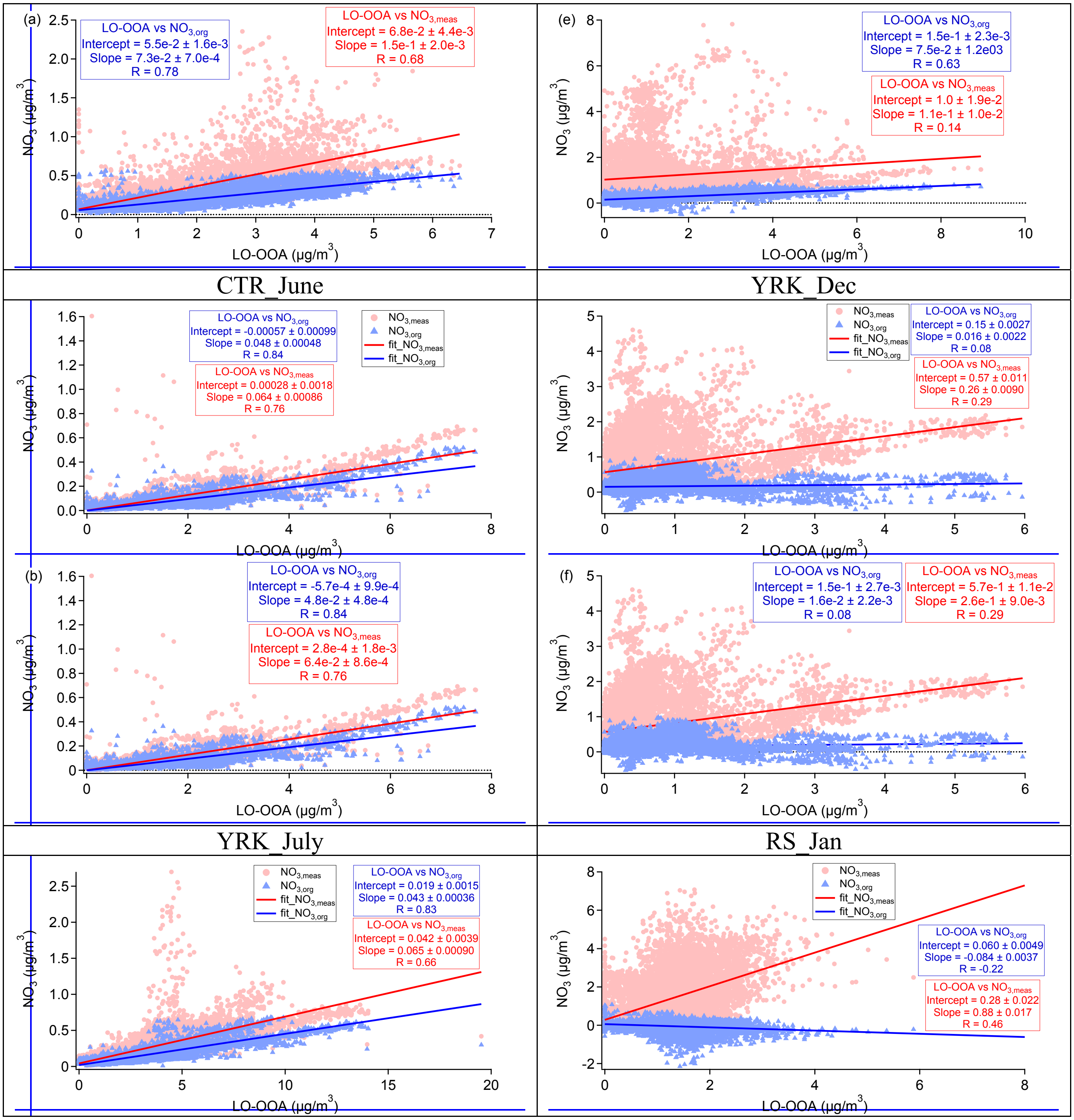
(a)
LO-OOA vs NO3,org
Intercept = 5.5e-2 ± 1.6e-3
Slope = 7.3e-2 ± 7.0e-4
R = 0.78
LO-OOA vs NO3,meas
Intercept = 6.8e-2 ± 4.4e-3
Slope = 1.5e-1 ± 2.0e-3
R = 0.68
NO3 (µg/m3)
LO-OOA (µg/m3)
(e)
LO-OOA vs NO3,org
Intercept = 1.5e-1 ± 2.3e-3
Slope = 7.5e-2 ± 1.2e03
R = 0.63
LO-OOA vs NO3,meas
Intercept = 1.0 ± 1.9e-2
Slope = 1.1e-1 ± 1.0e-2
R = 0.14
CTR_June
YRK_Dec
LO-OOA vs NO3,org
Intercept = -0.00057 ± 0.00099
Slope = 0.048 ± 0.00048
R = 0.84
LO-OOA vs NO3,meas
Intercept = 0.00028 ± 0.0018
Slope = 0.064 ± 0.00086
R = 0.76
NO3,meas
NO3,org
fit_NO3,meas
fit_NO3,org
LO-OOA vs NO3,org
Intercept = 0.15 ± 0.0027
Slope = 0.016 ± 0.0022
R = 0.08
LO-OOA vs NO3,meas
Intercept = 0.57 ± 0.011
Slope = 0.26 ± 0.0090
R = 0.29
(b)
LO-OOA vs NO3,org
Intercept = -5.7e-4 ± 9.9e-4
Slope = 4.8e-2 ± 4.8e-4
R = 0.84
LO-OOA vs NO3,meas
Intercept = 2.8e-4 ± 1.8e-3
Slope = 6.4e-2 ± 8.6e-4
R = 0.76
(f)
LO-OOA vs NO3,org
Intercept = 1.5e-1 ± 2.7e-3
Slope = 1.6e-2 ± 2.2e-3
R = 0.08
LO-OOA vs NO3,meas
Intercept = 5.7e-1 ± 1.1e-2
Slope = 2.6e-1 ± 9.0e-3
R = 0.29
YRK_July
RS_Jan
LO-OOA vs NO3,org
Intercept = 0.019 ± 0.0015
Slope = 0.043 ± 0.00036
R = 0.83
LO-OOA vs NO3,meas
Intercept = 0.042 ± 0.0039
Slope = 0.065 ± 0.00090
R = 0.66
LO-OOA vs NO3,org
Intercept = 0.060 ± 0.0049
Slope = -0.084 ± 0.0037
R = -0.22
LO-OOA vs NO3,meas
Intercept = 0.28 ± 0.022
Slope = 0.88 ± 0.017
R = 0.46

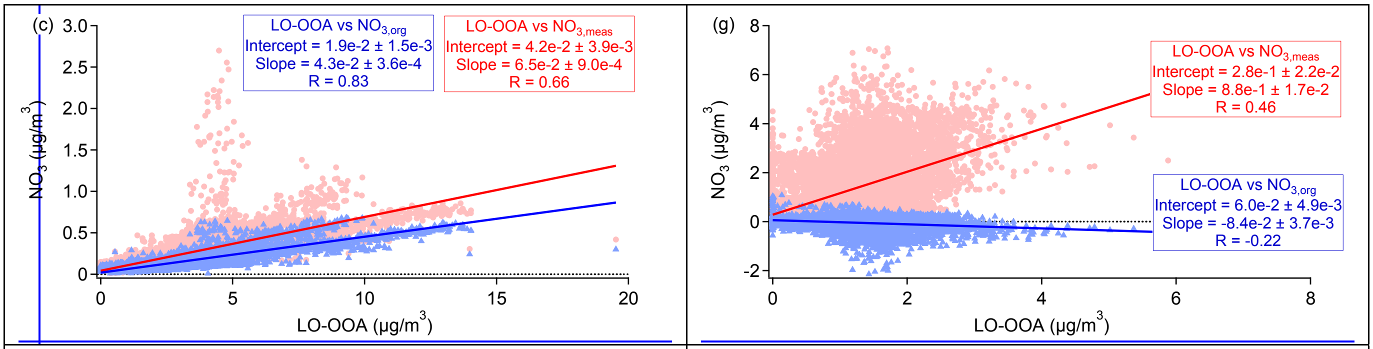
(c)
LO-OOA vs $NO_{3,org}$
Intercept = 1.9e-2 ± 1.5e-3
Slope = 4.3e-2 ± 3.6e-4
R = 0.83
LO-OOA vs $NO_{3,meas}$
Intercept = 4.2e-2 ± 3.9e-3
Slope = 6.5e-2 ± 9.0e-4
R = 0.66
NO_3 ($\mu g/m^3$)
LO-OOA ($\mu g/m^3$)
(g)
LO-OOA vs $NO_{3,meas}$
Intercept = 2.8e-1 ± 2.2e-2
Slope = 8.8e-1 ± 1.7e-2
R = 0.46
LO-OOA vs $NO_{3,org}$
Intercept = 6.0e-2 ± 4.9e-3
Slope = -8.4e-2 ± 3.7e-3
R = -0.22
NO_3 ($\mu g/m^3$)
LO-OOA ($\mu g/m^3$)

GT_Aug

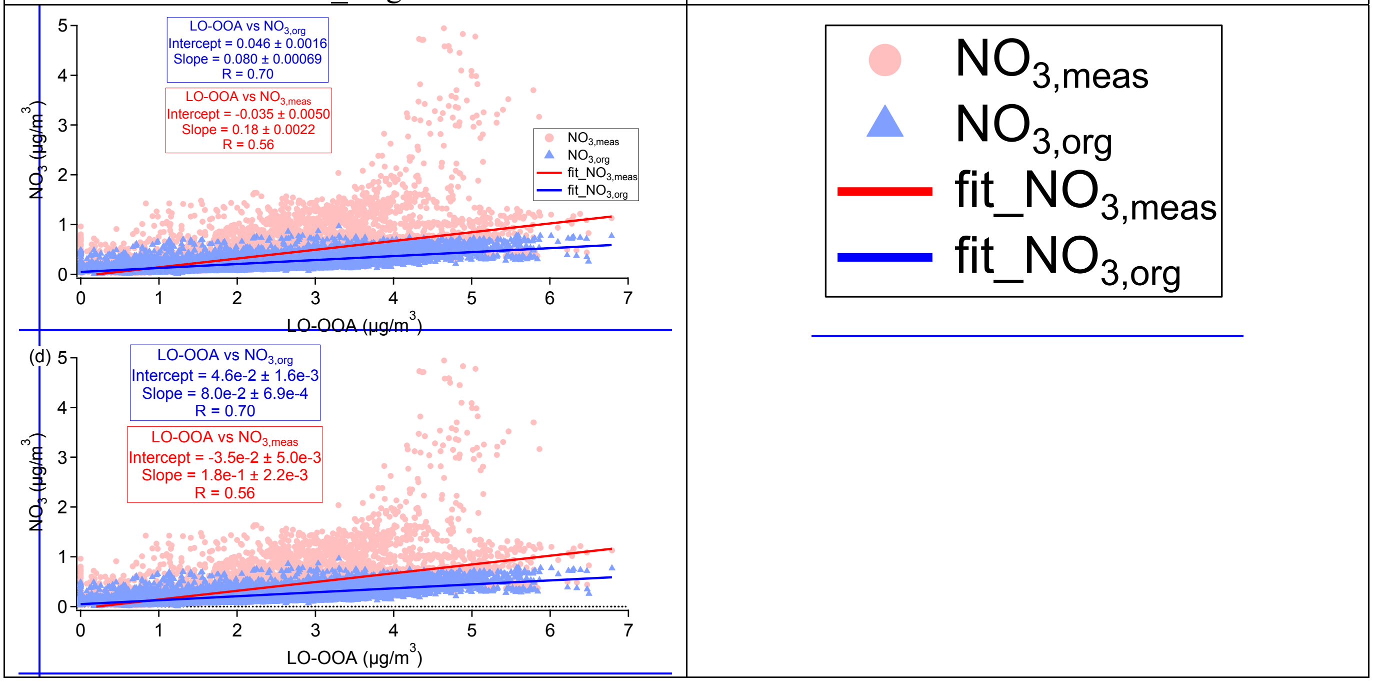
LO-OOA vs $NO_{3,org}$
Intercept = 0.046 ± 0.0016
Slope = 0.080 ± 0.00069
R = 0.70
LO-OOA vs $NO_{3,meas}$
Intercept = -0.035 ± 0.0050
Slope = 0.18 ± 0.0022
R = 0.56
$NO_{3,meas}$
$NO_{3,org}$
fit_$NO_{3,meas}$
fit_$NO_{3,org}$
NO_3 ($\mu g/m^3$)
LO-OOA ($\mu g/m^3$)
(d)
LO-OOA vs $NO_{3,org}$
Intercept = 4.6e-2 ± 1.6e-3
Slope = 8.0e-2 ± 6.9e-4
R = 0.70
LO-OOA vs $NO_{3,meas}$
Intercept = -3.5e-2 ± 5.0e-3
Slope = 1.8e-1 ± 2.2e-3
R = 0.56
NO_3 ($\mu g/m^3$)
LO-OOA ($\mu g/m^3$)
$NO_{3,meas}$
$NO_{3,org}$
fit_$NO_{3,meas}$
fit_$NO_{3,org}$

Fig. 10.

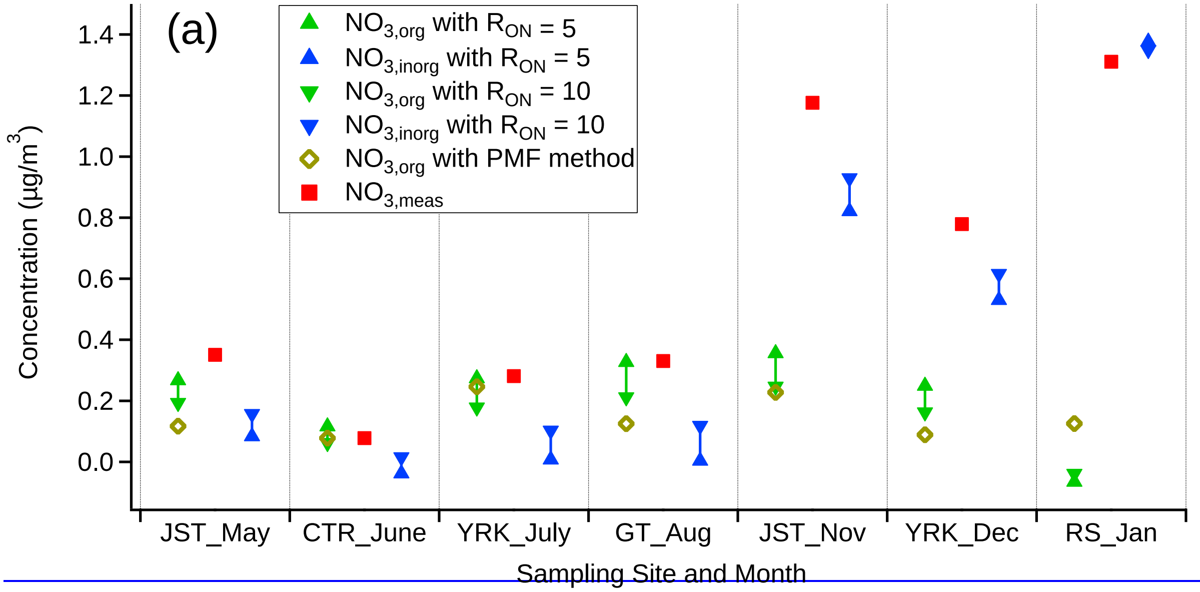
(a)
$NO_{3,org}$ with R_{ON} = 5
$NO_{3,inorg}$ with R_{ON} = 5
$NO_{3,org}$ with R_{ON} = 10
$NO_{3,inorg}$ with R_{ON} = 10
$NO_{3,org}$ with PMF method
$NO_{3,meas}$
Concentration (µg/m^3)
1.4
1.2
1.0
0.8
0.6
0.4
0.2
0.0
JST_May
CTR_June
YRK_July
GT_Aug
JST_Nov
YRK_Dec
RS_Jan
Sampling Site and Month

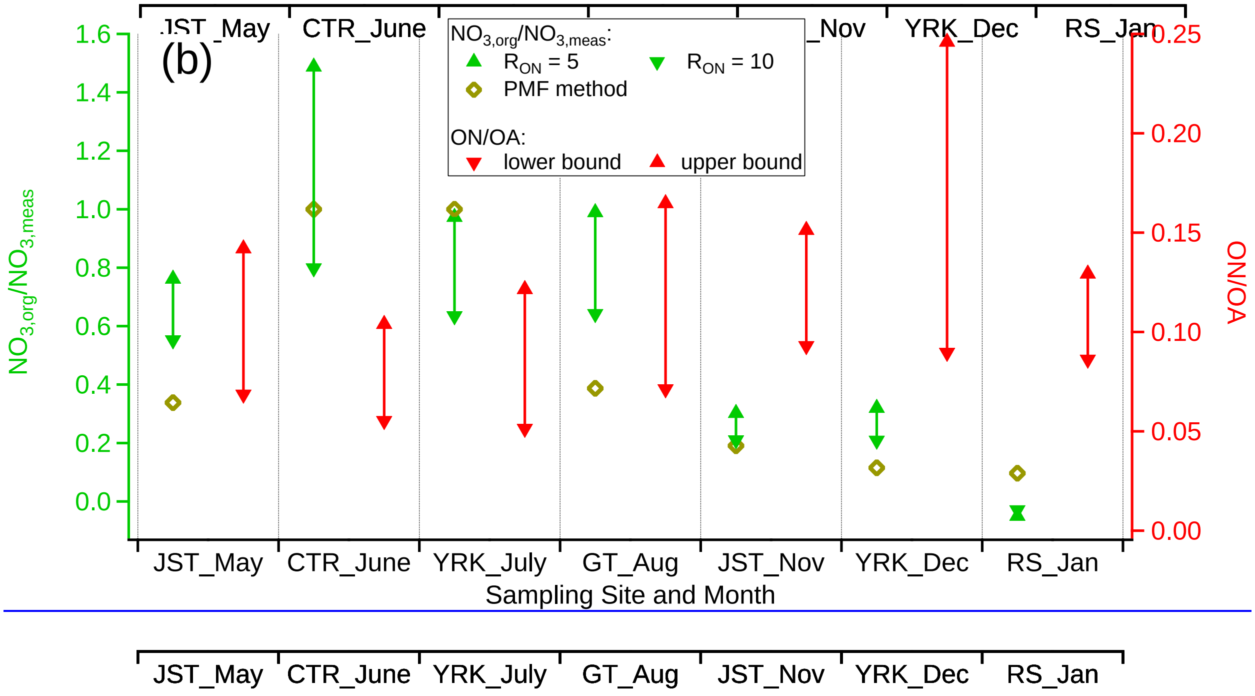
(b)
$NO_{3,org}/NO_{3,meas}$:
R_{ON} = 5
R_{ON} = 10
PMF method
ON/OA:
lower bound
upper bound
$NO_{3,org}/NO_{3,meas}$
1.6
1.4
1.2
1.0
0.8
0.6
0.4
0.2
0.0
ON/OA
0.25
0.20
0.15
0.10
0.05
0.00
JST_May
CTR_June
YRK_July
GT_Aug
JST_Nov
YRK_Dec
RS_Jan
Sampling Site and Month

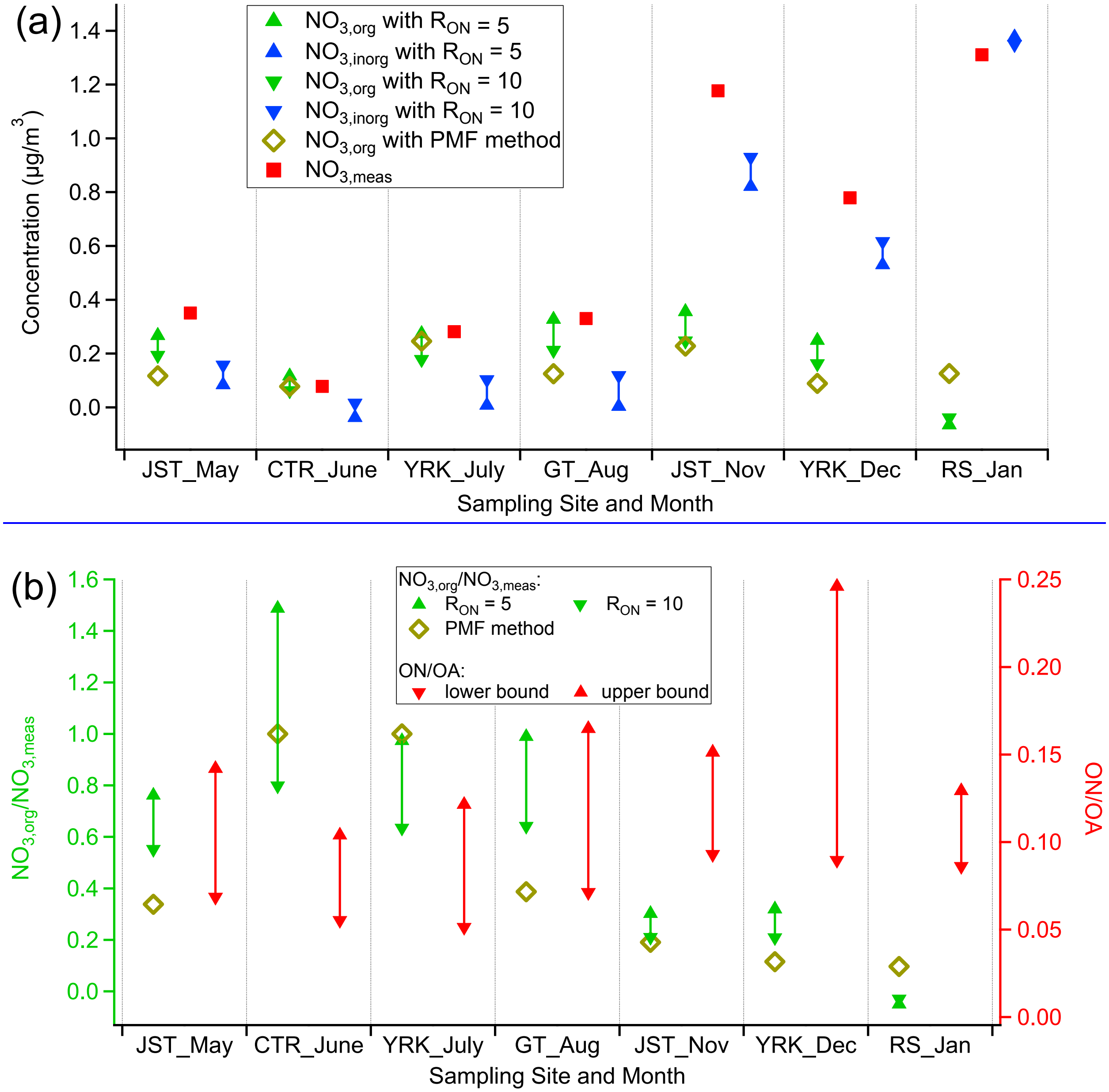
(a)
NO3,org with RON = 5
NO3,inorg with RON = 5
NO3,org with RON = 10
NO3,inorg with RON = 10
NO3,org with PMF method
NO3,meas
Concentration (µg/m3)
1.4
1.2
1.0
0.8
0.6
0.4
0.2
0.0
JST_May
CTR_June
YRK_July
GT_Aug
JST_Nov
YRK_Dec
RS_Jan
Sampling Site and Month
(b)
NO3,org/NO3,meas:
RON = 5
RON = 10
PMF method
ON/OA:
lower bound
upper bound
NO3,org/NO3,meas
1.6
1.4
1.2
1.0
0.8
0.6
0.4
0.2
0.0
ON/OA
0.25
0.20
0.15
0.10
0.05
0.00
JST_May
CTR_June
YRK_July
GT_Aug
JST_Nov
YRK_Dec
RS_Jan
Sampling Site and Month

Fig. 11.

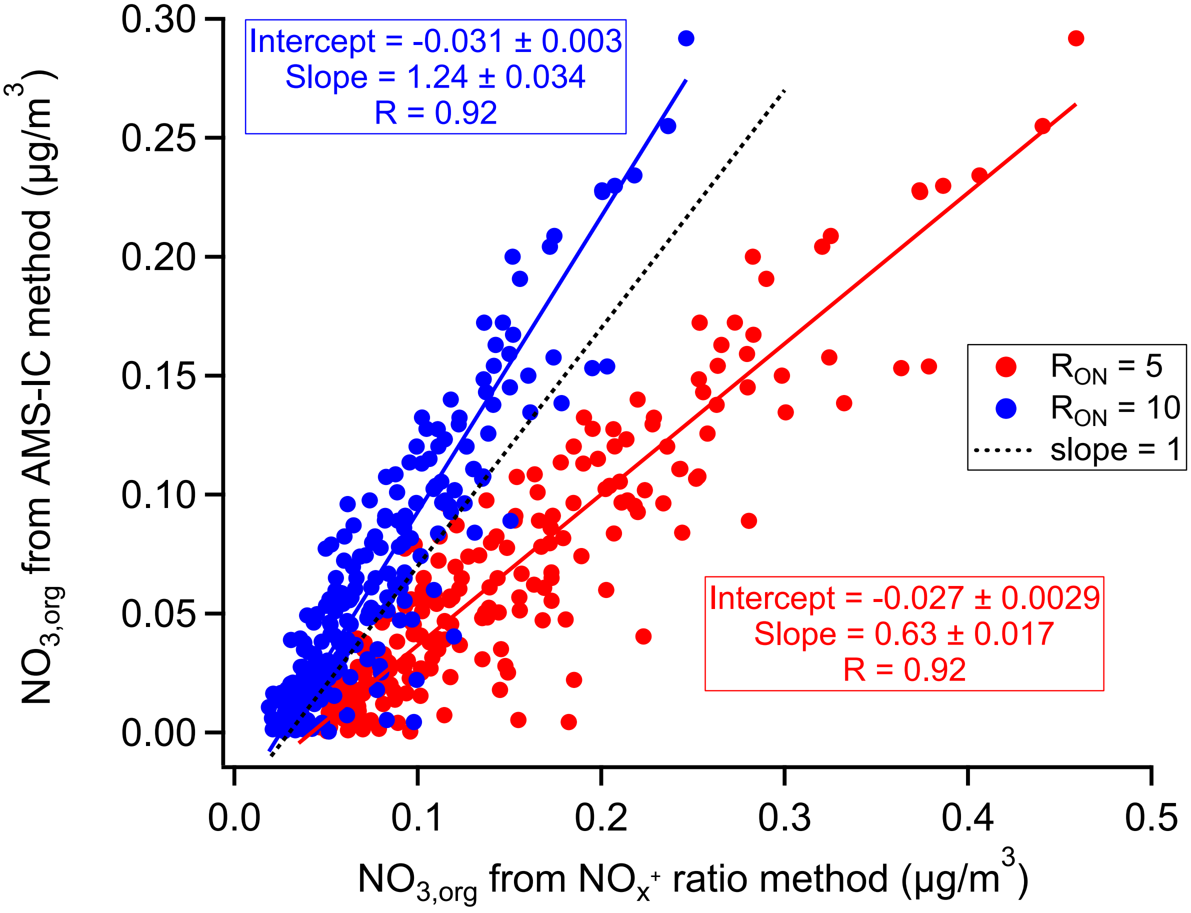
Intercept = -0.031 ± 0.003
Slope = 1.24 ± 0.034
R = 0.92
Intercept = -0.027 ± 0.0029
Slope = 0.63 ± 0.017
R = 0.92
● R_{ON} = 5
● R_{ON} = 10
slope = 1
0.30
0.25
0.20
0.15
0.10
0.05
0.00
0.0
0.1
0.2
0.3
0.4
0.5
$NO_{3,org}$ from AMS-IC method ($\mu g/m^3$)
$NO_{3,org}$ from NO_x^+ ratio method ($\mu g/m^3$)

Fig. 12.

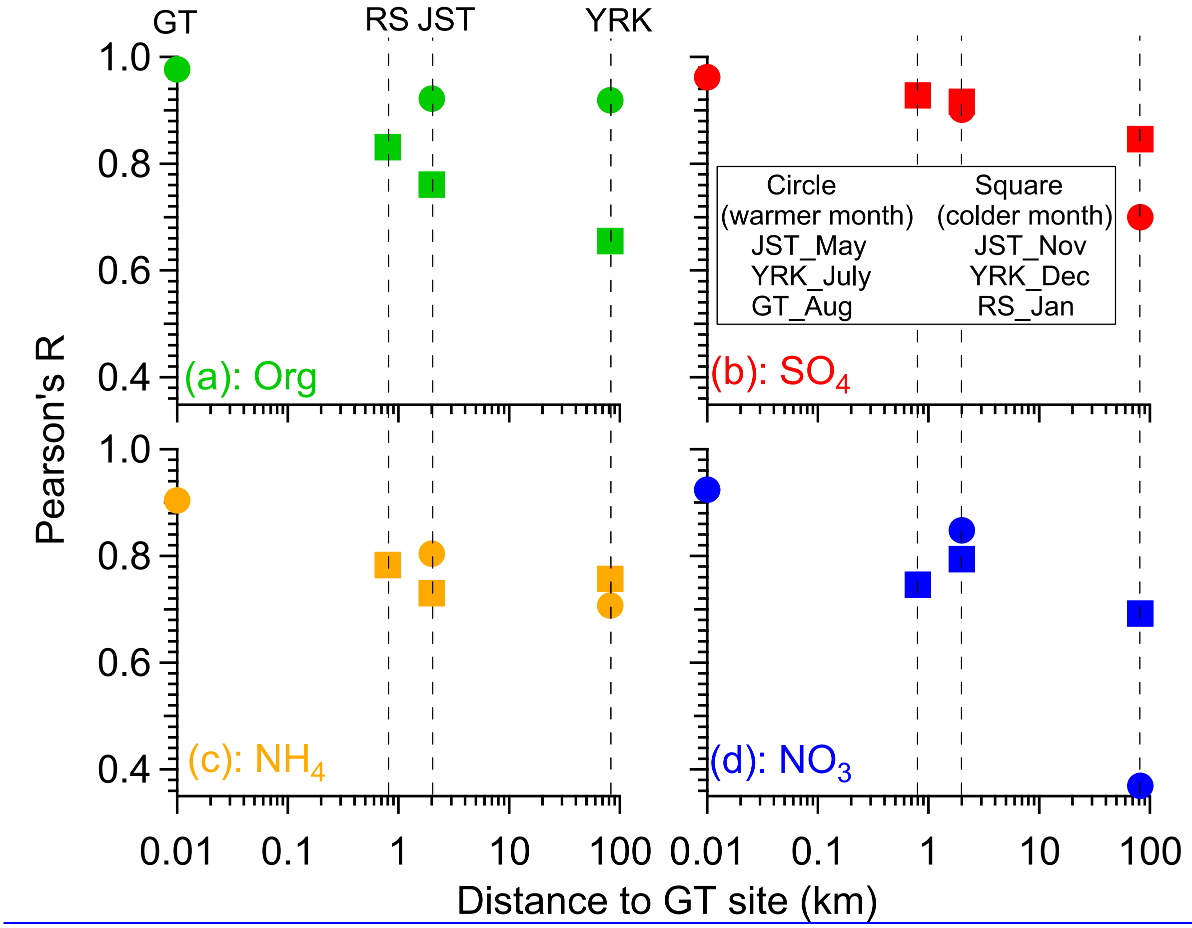
GT
RS JST
YRK
Pearson's R
1.0
0.8
0.6
0.4
(a): Org
(b): SO$_4$
(c): NH$_4$
(d): NO$_3$
Circle (warmer month)
JST_May
YRK_July
GT_Aug
Square (colder month)
JST_Nov
YRK_Dec
RS_Jan
0.01
0.1
1
10
100
Distance to GT site (km)

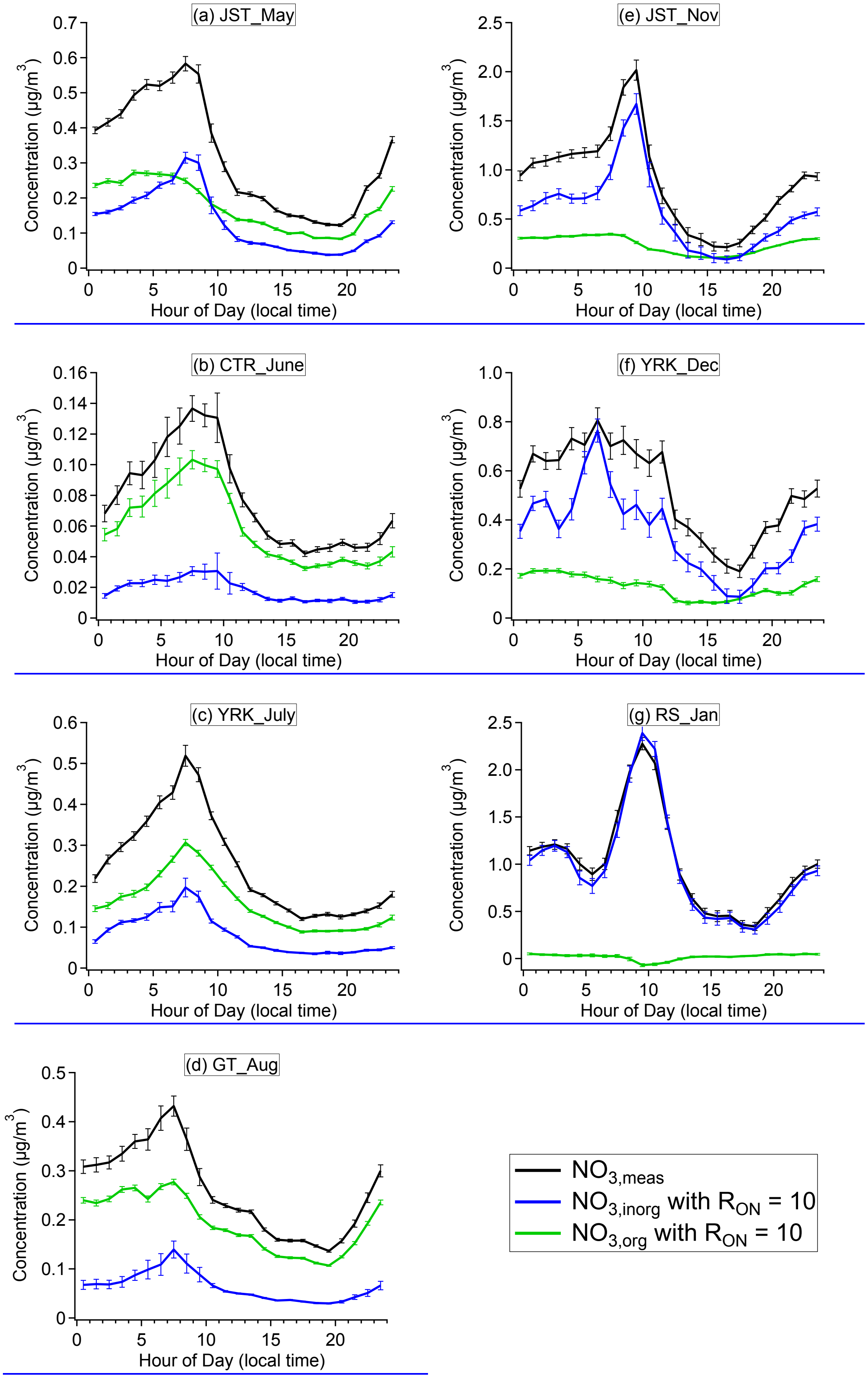
(a) JST_May
(b) CTR_June
(c) YRK_July
(d) GT_Aug
(e) JST_Nov
(f) YRK_Dec
(g) RS_Jan
Concentration (µg/m^3)
Hour of Day (local time)
0
5
10
15
20
$NO_{3,meas}$
$NO_{3,inorg}$ with R_{ON} = 10
$NO_{3,org}$ with R_{ON} = 10

Fig. 13.

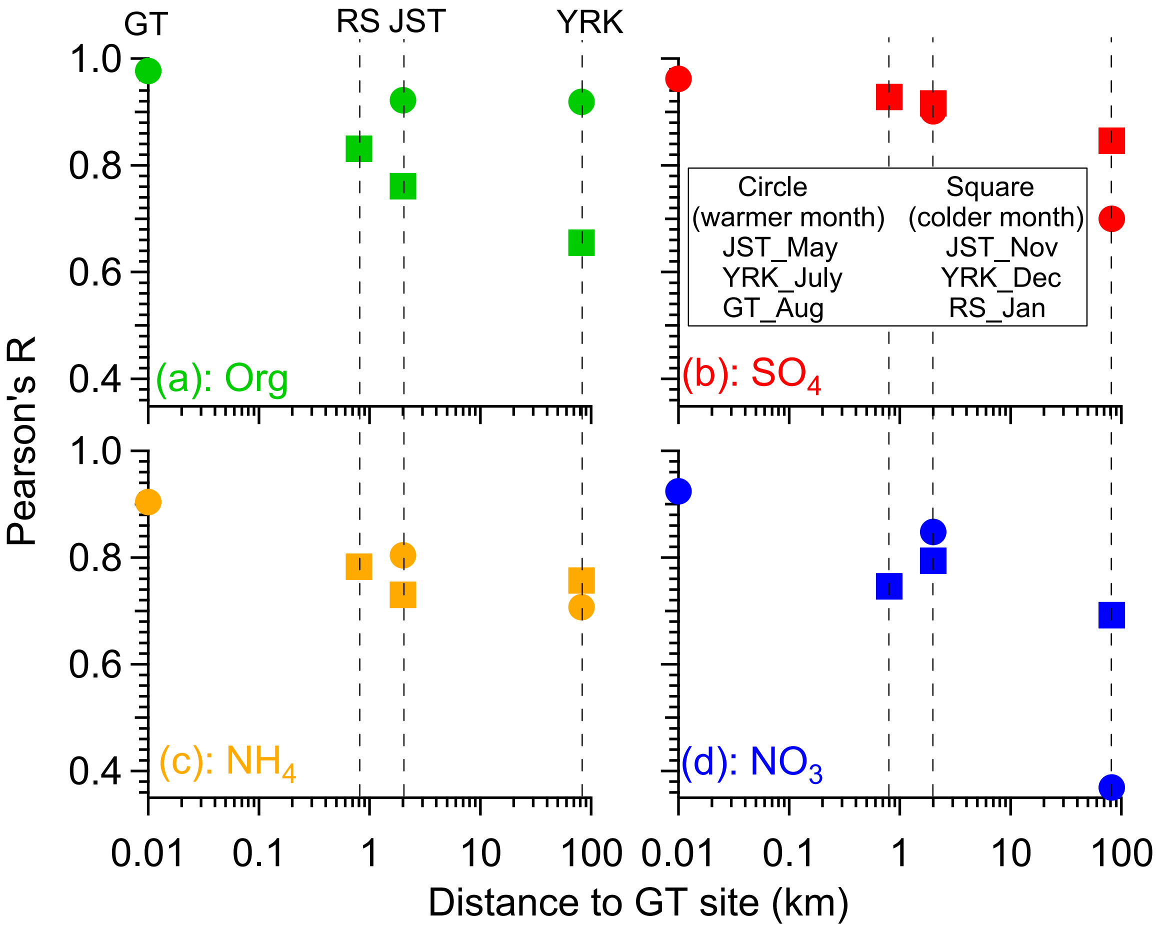
GT
RS JST
YRK
Pearson's R
1.0
0.8
0.6
0.4
(a): Org
(b): SO_4
(c): NH_4
(d): NO_3
Circle
(warmer month)
JST_May
YRK_July
GT_Aug
Square
(colder month)
JST_Nov
YRK_Dec
RS_Jan
0.01
0.1
1
10
100
Distance to GT site (km)

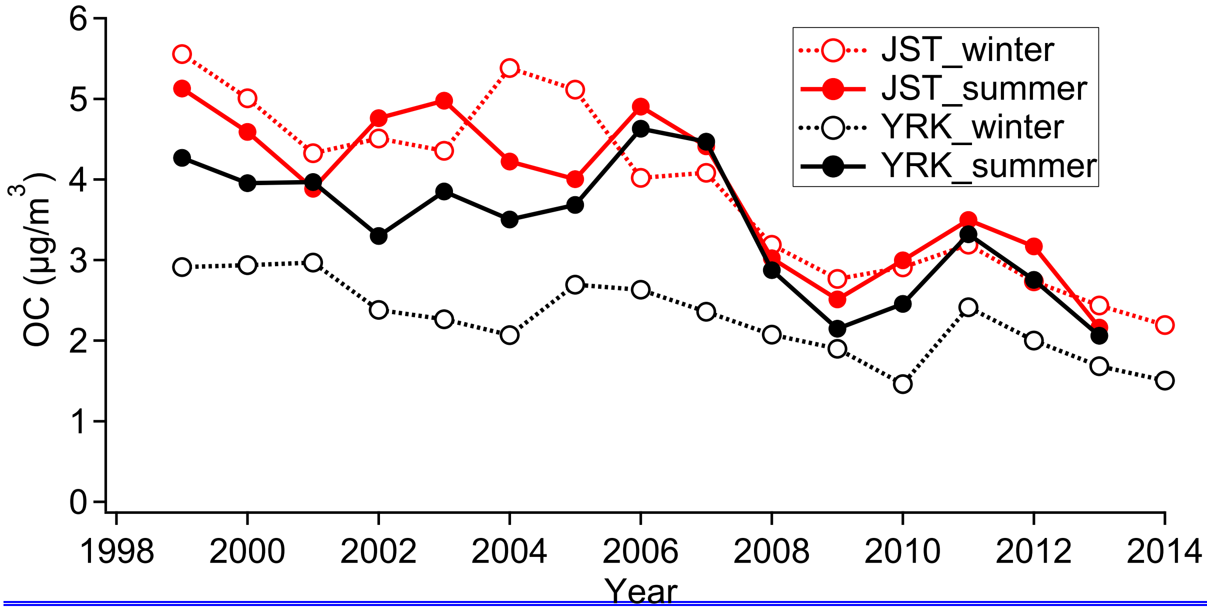
JST_winter
JST_summer
YRK_winter
YRK_summer
OC (μg/m^3)
0
1
2
3
4
5
6
1998
2000
2002
2004
2006
2008
2010
2012
2014
Year

Fig. 14.

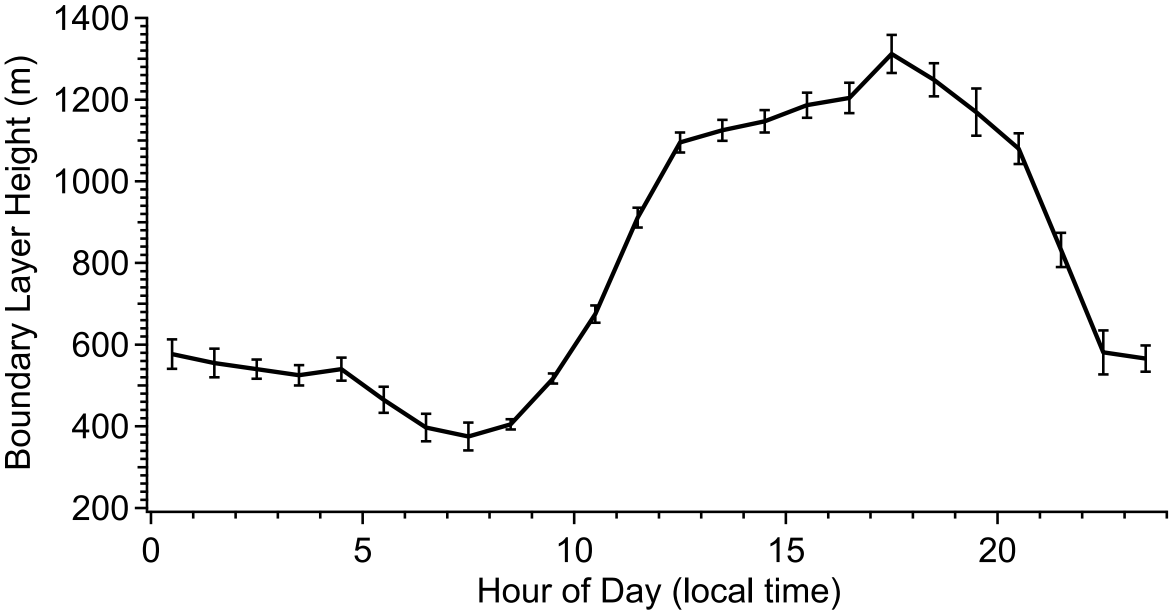
Boundary Layer Height (m)
1400
1200
1000
800
600
400
200
0
5
10
15
20
Hour of Day (local time)

Fig.15.

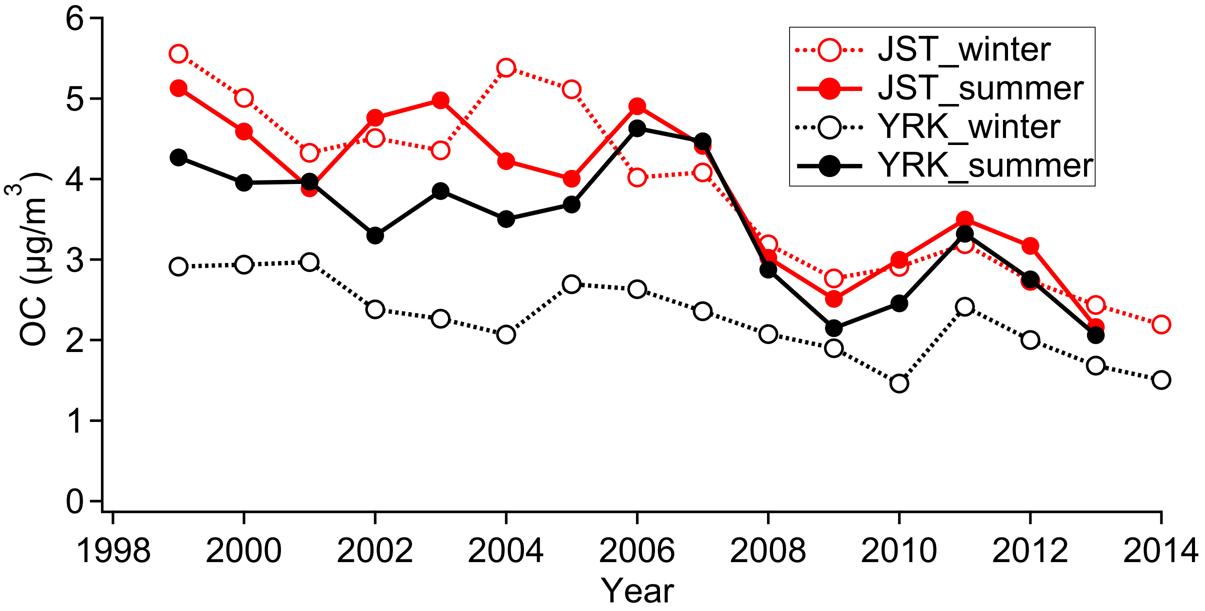
JST_winter
JST_summer
YRK_winter
YRK_summer
OC (μg/m^3)
0
1
2
3
4
5
6
1998
2000
2002
2004
2006
2008
2010
2012
2014
Year

Fig.16.

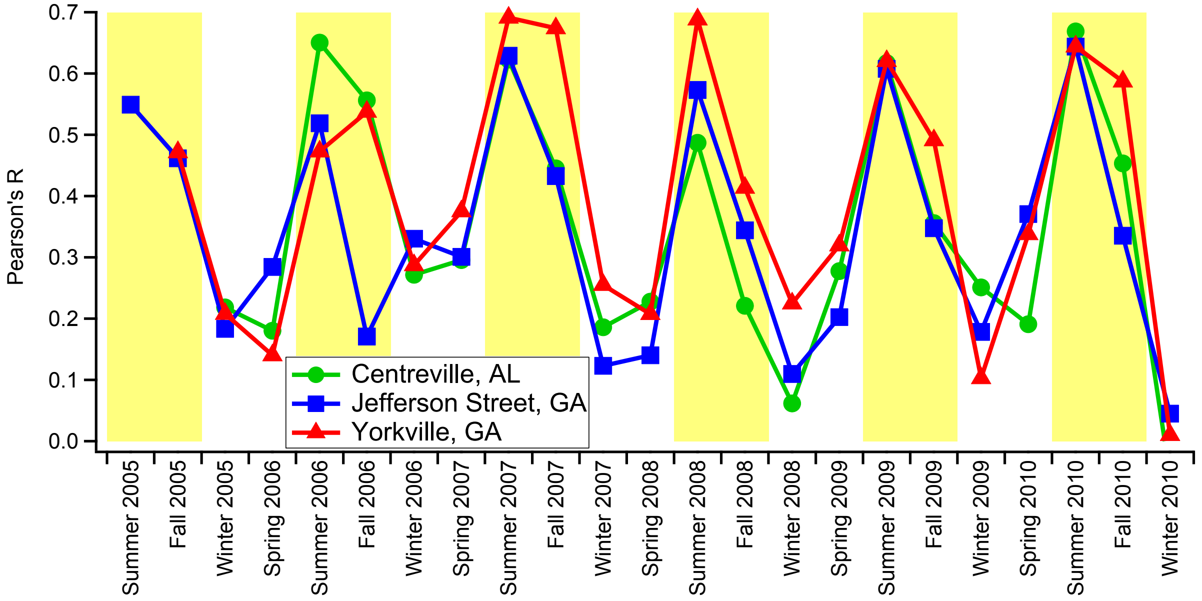
0.7
0.6
0.5
0.4
0.3
0.2
0.1
0.0
Pearson's R
Centreville, AL
Jefferson Street, GA
Yorkville, GA
Summer 2005
Fall 2005
Winter 2005
Spring 2006
Summer 2006
Fall 2006
Winter 2006
Spring 2007
Summer 2007
Fall 2007
Winter 2007
Spring 2008
Summer 2008
Fall 2008
Winter 2008
Spring 2009
Summer 2009
Fall 2009
Winter 2009
Spring 2010
Summer 2010
Fall 2010
Winter 2010